AD_____

Award Number: W81XWH-09-1-0487

TITLE: Developing a Drosophila Model of Schwannomatosis

PRINCIPAL INVESTIGATOR: James A. Walker, Ph.D.

CONTRACTING ORGANIZATION: Massachusetts General Hospital
Boston, MA 02114-2696

REPORT DATE: February 2013

TYPE OF REPORT: Final

PREPARED FOR: U.S. Army Medical Research and Materiel Command
Fort Detrick, Maryland 21702-5012

REPORT DOCUMENTATION PAGE

Form Approved
OMB No. 0704-0188

1. REPORT DATE	2. REPORT TYPE	3. DATES COVERED
February 2013	Final	15 July 2009 – 14 January 2013

4. TITLE AND SUBTITLE

Developing a Drosophila Model of Schwannomatosis

5a. CONTRACT NUMBER

5b. GRANT NUMBER
W81XWH-09-1-0487

5c. PROGRAM ELEMENT NUMBER

6. AUTHOR(S)

James A. Walker

E-Mail: jwalker@helix.mgh.harvard.edu

5d. PROJECT NUMBER

5e. TASK NUMBER

5f. WORK UNIT NUMBER

7. PERFORMING ORGANIZATION NAME(S) AND ADDRESS(ES)

Massachusetts General Hospital
Boston, MA 02114-2696

8. PERFORMING ORGANIZATION REPORT NUMBER

9. SPONSORING / MONITORING AGENCY NAME(S) AND ADDRESS(ES)
U.S. Army Medical Research and Materiel Command
Fort Detrick, Maryland 21702-5012

10. SPONSOR/MONITOR'S ACRONYM(S)

11. SPONSOR/MONITOR'S REPORT NUMBER(S)

12. DISTRIBUTION / AVAILABILITY STATEMENT
Approved for Public Release; Distribution Unlimited

13. SUPPLEMENTARY NOTES

14. ABSTRACT

This project examined mutations found in familial cases of schwannomatosis in the tumor suppressor SMARCB1, a component of the SWI/SNF chromatin remodeling complex. Drosophila is was used to investigate the nature of the SMARCB1 mutations and the molecular consequences which give rise to schwannomas. Sensitized in vivo assays for SMARCB1 function using RNAi knockdown of Snr1 (fly ortholog of SMARCB1) revealed missense mutations from patients have varying degrees of residual function suggesting they are hypomorphic. Drosophila genetics identified novel Snr1 interactions, including a potent interaction between Snr1 and the NF2/merlin tumor suppressor gene, which is also involved in schwannomatosis, as well as regulators of Cyclin E and the Hedgehog pathway. The consequences of SMARCB1/Snr1 knockdown on gene expression was examined using microarrays. Purification of wild type and mutant SMARCB1 was performed to examine altered protein interactions that may contribute to schwannomatosis.

15. SUBJECT TERMS
Scwhwannomatosis, chromatin remodeling, epigenetics, genetic interactions

16. SECURITY CLASSIFICATION OF:			17. LIMITATION OF ABSTRACT	18. NUMBER OF PAGES	19a. NAME OF RESPONSIBLE PERSON
a. REPORT	b. ABSTRACT	c. THIS PAGE			USAMRMC
U	U	U	UU	76	19b. TELEPHONE NUMBER *(include area code)*

Table of Contents

Introduction

Schwannomatosis is characterized by multiple spinal, peripheral, and cranial nerve schwannomas in the absence of vestibular nerve schwannomas. Molecular analyses have identified mutations in *NF2* being somatically acquired in schwannomas from patients with schwannomatosis, although linkage studies have excluded *NF2* as a germline transmissible schwannomatosis gene (MacCollin *et al.,* 2003). Recent genetic studies have revealed germline mutations in the tumor-suppressor gene *SMARCB1* in familial schwannomatosis (Hadfield *et al.*, 2008; Hulsebos *et al*., 2007; Boyd *et al*., 2008). A tumor suppressor role for *SMARCB1* was first suggested by frequent loss of function mutations in malignant atypical teratoid rhabdoid tumors (Biegel *et al*., 1999; Versteege *et al*., 1998). SMARCB1 is a component of the SWI/SNF chromatin remodeling complex which consists of 8-11 subunits. By interacting with DNA-binding transcription (co)-factors to recruit histone acetyltransferases and histone deacetylase complexes, the SWI/SNF complex functions to regulate gene expression, DNA replication and repair, and cell division (Euskirchen *et al*., 2012). Intriguingly, however, *SMARCB1* mutations appear to explain only a fraction of familial and sporadic schwannomatosis cases, suggesting the existence of yet another, apparently closely-linked, causative gene on chromosome 22.

We have developed a Drosophila model of schwannomatosis, to help elucidate the specific molecular events that give rise to this disease. Our main objective was to uncover new functions of SMARCB1 and its Drosophila ortholog, Snr1, to help answer the following two fundamental questions: How do germline mutations in *SMARCB1* give rise to two very different tumor predisposition syndromes, namely late-onset familial schwannomatosis and highly malignant pediatric rhabdoid tumors? Why is *SMARCB1* the only human SWI/SNF subunit thus far implicated as a potent tumor suppressor so far? We hypothesized that SMARCB1 may have an important role independent from that of being a core constituent of the SWI/SNF complex. Alternatively, if disease-

causing mutations in SMARCB1 affect the function of this complex, this would suggest that lesions (yet to be described) in genes encoding other SWI/SNF complex components could also contribute to schwannomatosis.

Body

Specific Aim 1. Generating transgenic lines for testing *SMARCB1* disease-causing mutations and for genetic screening.

We asked why seemingly similar *SMARCB1* mutations are implicated in early onset and aggressive AT/RT, and in late onset and more benign schwannomatosis. We hypothesized that AT/RT may result from complete loss-of-function (null) mutations, whereas familial schwannomatosis may result from partial loss-of-function (hypomorphic) alleles. We therefore conducted the following investigations to develop a *Drosophila* model in an attempt to address these issues:

• Generated *Drosophila UAS*-transgenes encoding *SMARCB1*, either wild type or containing disease-causing mutations from patients with familial schwannomatosis.
• Western blots assessed expression levels from *UAS-SMARCB1* transgenes.
• Tested ability of wild type and mutant *UAS-SMARCB1* transgenes to compensate for loss of endogenous *Snr1* in flies.
• Tested ability of of wild type and mutant *UAS-SMARCB1* transgenes to rescue *Snr1* RNAI phenotypes in flies.

• ***Generated Drosophila transgenes encoding SMARCB1 containing disease-causing mutations from patients with familial schwannomatosis.***
In each case, the respective cDNA was placed under the control of the *UAS* promoter, allowing tissue-specific expression using the *UAS/GAL4* system and N-terminal HA-tags were included to allow detection by Western blotting (Figure 1). Transgenes were generated encoding the Drosophila *SMARCB1* ortholog *Snr1* and both alternatively spliced (A and B) variants of human *SMARCB1*. In addition, we made SMARCB1 transgenes harboring schwannomatosis patient missense mutations - P14H and R53L in the N-terminal half (Boyd et al., 2008) and the R374Q mutation in the C-terminus of the protein (Moertel *et al.*, 2009).

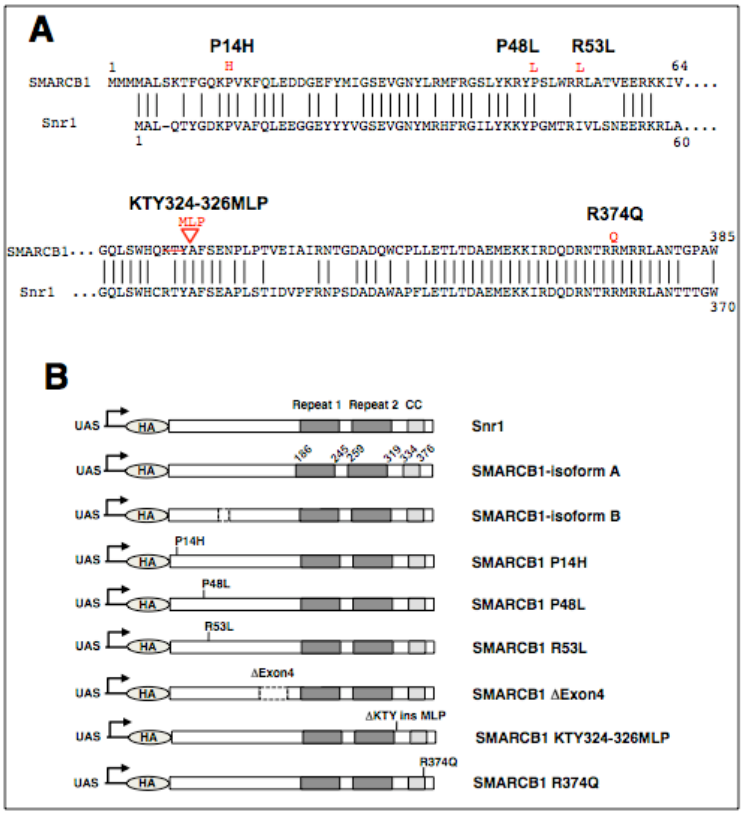

Fig 1. SMARCB1 mutations from schwannomatosis patients used in this study. A. The human (SMARCB1) and Drosophila (Snr1) amino acid sequences are aligned, showing the conservation of the mutated residues (shown in red). B. Schematic of the *Drosophila* transgenes generated. The structure of the SMARCB1 protein (Repeat 1 and 2 and coiled coil domain - CC) as well as the position of the mutations and exon 4 deletion. Each cDNA was subcloned into a vector under the control of UAS elements with an HA-tag at the N-terminus.

We also generated a *SMARCB1* transgene lacking exon 4 (which encodes 46 amino acids), mimicking the in-frame deletion product of a splice site mutant identified in another patient (Smith *et al.,* 2009). We made use of site-specific integration into the Drosophila genome, using phiC31 integrase and the Attp40 landing site, ensuring that transgenes expressed at comparable levels. Each series of transgenes was driven by *actin5C-Gal4* and their expression levels assessed by anti-HA immunoblotting (as in Fig. 2). Subsequently, we have also produced transgenes bearing the more recently described P48L (Christianns *et al*., 2011) and KTY324-326MLP (Rousseau *et al*., 2011) mutations from familial cases of schwannomatosis.

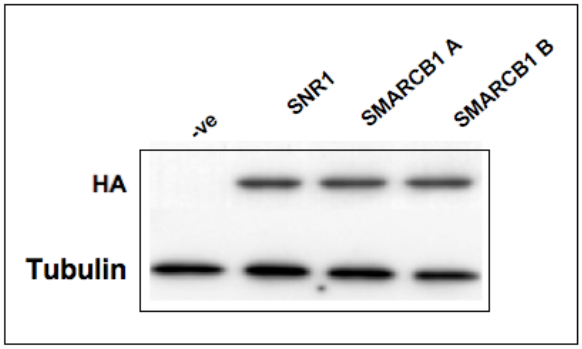

Figure 2. Anti-HA-tag Western analysis of *Act5C-GAL4*-driven *UAS-Snr1* and *UAS-SMARCB1* transgene expression. Two differently spliced isoforms of SMARCB1 were used. The control lane (–ve) refers to lysate from flies not containing a transgene.

• ***Human SMARCB1 can compensate for loss of Drosophila Snr1***

Flies over-expressing either Snr1 or SMARCB1 using the ubiquitous *actin5C-Gal4* driver were viable and showed no obvious defects. When expressed in the $Snr1^{01319}$ null mutant background using the *Act5C-GAL4* driver, several *UAS-Snr1* and *UAS-SMARCB1* (WT) transgenic lines rescued the early lethality to the pupal stage (Annual Report Year 1). One *UAS-SMARCB1-B* transgenic line even allowed the eclosion of viable adults. Western blot analysis showed that transgene expression correlated with rescuing ability. Further experiments using different tissue-specific GAL4 drivers demonstrated that only ubiquitous and potent GAL4 drivers (*Act5C*- and *tubulin*-) rescued, arguing that *Snr1* plays a vital role in multiple tissues during development.

• ***SMARCB1 disease-causing mutations are unable to rescue the lethality of Snr1 mutants.***

Our ability to delay the *Snr1* lethal phase by expressing its human ortholog, *SMARCB1,* set the stage for experiments to determine whether *SMARCB1* transgenes carrying schwannomatosis mutations retained rescuing capacity. The P14H, R53L, R374Q lines were unable to rescue the $Snr1^{01319}$ lethal phase when driven by *actin5C-GAL4*. However, the exon 4 deletion was able to postpone lethality to the pupal stage, demonstrating it retains partial activity. These data argue against our hypothesis that schwannomatosis mutations may retain partial function.

• ***Developing assays to test ability of SMARCB1 to rescue Snr1 RNAi phenotypes***

Since the ability of SMARCB1 mutants to modify the lethal phase of *Snr1* null mutants may have been too stringent a test, we used RNAi mediated tissue-specific knockdown of *Snr1* as a more sensitive system to test residual activity of *SMARCB1* mutants. Tissue-specific knockdown of *Snr1* was performed using *UAS-Snr1 RNAi* lines from the Vienna Drosophila RNAi Center (VDRC) (Dietzl et

al., 2007). Some of the observed phenotypes are illustrated in Figure 3 and many of these are amenable to conducting large-scale genetic modifier screens (see Specific Aim 2).

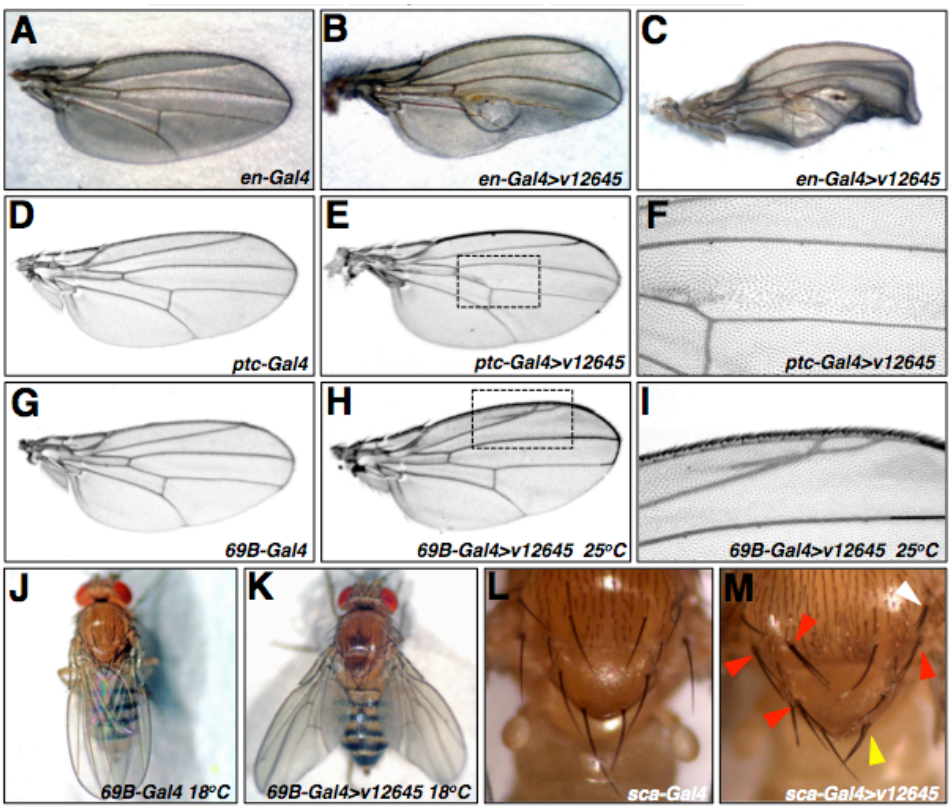

Figure 3. Snr1 RNAi phenotypes observed by driving *UAS-Snr1 RNAi* (*v12645*) line using tissue-specific Gal4 drivers at the indicated temperatures. A-C *engrailed-Gal4* driving RNAi knock down in the posterior half of the wing results in blistering; D-F *ptc-Gal4* driving in a stripe in the middle of the wing causes planar cell polarity defects; G-I *69B-Gal4* driven *Snr1* RNAi results in ectopic vein formation in the anterior of the wings, as well as a held-out wing phenotype (J and K). *Scaborous-Gal4 >UAS-Snr1 RNAi* results in either the duplication or absence of bristles on the thorax. In each case control flies (Gal4 driver alone) is shown – A, D, G, J and L.

Further tests described in the previous Annual Reports showed that the RNAi phenotypes described were due to *Snr1* knockdown, and did not reflect 'off-target' effects. We demonstrated that simultaneous GAL4-mediated induction of human wild type *UAS-SMARCB1* transgenes negated the RNAi-induced phenotypes. Such an experiment was based on the premise that even though Snr1 and SMARCB1 proteins are well conserved as the amino acid level, the nucleotide sequences of their cDNAs are sufficiently distinct so that Snr1 RNAi

would not target transgenic expressed SMARCB1. In contrast, a *UAS-lacZ* transgene in this assay had no effect, demonstrating that rescue using *UAS-SMARCB1* cannot be attributed to reduced RNAi caused by titration of Gal4.

- ***Testing SMARCB1 mutants for ability to rescue Snr1 RNAi phenotypes***

Snr1 RNAi-induced defects enabled us to develop sensitive assays to test for residual functional of our mutant SMARCB1 transgenes. Arguing in favor of our original hypothesis that schwannomatosis mutations are hypomorphic, we observed phenotypic rescue using this more sensitive assay with several of the SMARCB1 transgenes bearing patient mutations. For example, in rescue assays for the extra vein phenotype induced by 69B-Gal4>*UAS-Snr1 RNAi,* the P14H, R374Q and exon 4 deletion are able to significantly rescue (Fig. 4). In contrast, the R53L mutation was unable to rescue in this assay. Since the Brahma complex plays different roles (both repressive and facilitating) in different tissues, we speculated that the differing ability of mutants to rescue may reveal clues to the molecular consequences of these mutations.

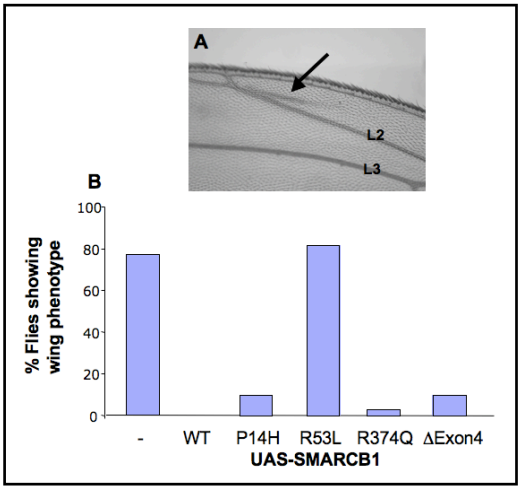

Figure 4. Assay of SMARCB1 mutants for ability to rescue extra vein phenotype induced by 69B-Gal4>*UAS-Snr1 RNAi*. A. Extra vein phenotype in anterior part of wing at 25ºC when 69B-Gal4 drives the *UAS-Snr1-RNAi* (*v12645*) line. B. Graph showing % of flies displaying extra vein phenotype when expressing SMARCB1 WT (100% rescue) or the SMARCB1 mutants.

Consistent with this idea, the schwannomatosis-causing point mutations differ in their relative abilities to rescue RNAi phenotypes in other tissues (in different parts of the wing, eye and bristles). These results are currently being prepared for publication.

Specific Aim 2: To identify dominant genetic modifiers of Snr1 function.

- Developed lines of flies suitable for conducting genetic screens using knockdown of *Snr1* by RNA interference (RNAi).
- Conducted pilot screen using *UAS-shRNA-Snr1* with known modifiers of *Snr1*.
- Candidate screen identified genetic interaction between *Snr1* and *NF2/Merlin*
- Deficiency modifier screen of RNAi knockdown of *Snr1* in eye identified *dacapo* (*dap*) and *second wave mitotic* (*swm*) as novel *Snr1* interactors

• ***Using Snr1 transgenic RNAi to screen for genetic interactions***

As described above, we identified a number of potential phenotypes that are amenable to performing genetic screens. We generated fly stocks with a *UAS-Snr1-shRNA* transgene, and either *en-Gal4* or *ey-Gal4*, along with a *Gal80* balancer chromosome, as described in detail in Annual Report Year 1. Previously identified interactors of *Snr1* were tested in a small candidate modifier screen (*mor*, *osa* and *brm* all enhanced *Snr1* RNAi phenotypes*)*.

• ***Snr1 interacts with NF2/Merlin in Drosophila***

We found that alleles of *expanded* (ex), *decapentaplegic* (*dpp*) and *cyclinE* were able to dominantly enhance *Snr1* phenotypes (Annual Report Year 1). Alleles of these genes have previously been shown to interact with *merlin*, the Drosophila *NF2* ortholog (McCartney et al., 2000; Hamaratoglu et al., 2006). Since *SMARCB1* and *NF2* are both inactivated in at least some schwannomatosis tumors, reflecting a unique four-hit mechanism (Sestini et al., 2008), we analyzed genetic interactions using the hypomorphic *merlin* allele, Mer^3 (as described in detail in Annual Reports Years 1 and 2).

• ***Other Brm complex constituents also genetically interact with Merlin***

As reported previously (Annual Report Year 1) we found that other Brahma complex genes (*osa*, *mor* and *brm*) also each resulted in a strong dominant enhancement of the Mer^3 eye and wing phenotypes (Table 1 and Fig.

5). In contrast, alleles of BAP180 and BAP170 do not interact with *Mer*^{3}. Since these subunits are exclusive to the PBAP complex, it suggests that the BAP complex, rather than the PBAP, is involved in Merlin function or regulation.

A

Allele	Eye Phenotype penetrance	Eye Phenotype severity	Wing Phenotype
WT	16%		
Snr1^{01319}	71%	increased severity	MWP
Mor^{1}	100%	increased severity	MWP
Mor^{2}	89%	increased severity	MWP - incl. PCV disruption
Brm^{2}	DEAD		
Brm^{5}	45%	increased severity	MWP
Osa^{1}	DEAD		
Osa^{2}	43%		MWP
BAP180^{A36}	16%		
BAP170^{A135}	13%		
kto	21%		
kis	21%		
skd	78%	increased severity	MWP - incl. PCV disruption
Pc^{3}	31%		
Ash1^{81}	75%		

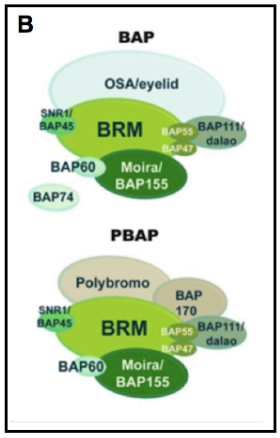

Table 1. Mutants of other Brahma complex components also dominantly modify the *Mer*^{3} phenotypes. A. Percentage values refer to the number of eye phenotype, with at least one eye showing enhancement of the ectopic vibrissae. Severity Mutations in the genes crossed to *Mer*^{3}/+ females and male progeny (*Mer*^{3}/Y) scored for. MWP (modified wing phenotype) was scored as an increase in the severity of overgrowth of wing tissue, often resulting in crinkled deformed wings. In some cases disruption of the posterior cross vein (PCV) was noted. Interactions were noted for alleles of *Snr1*, *mor* and *brm*. Alleles of *osa* (outlined in green), a component of the BAP complex also interact with *Mer*^{3}. In contrast, alleles of *BAP180* and *BAP170* (outlined in red) failed to enhance the *Mer*^{3} phenotype, indicating that the BAP, complex, rather than the PBAP complex is involved in *Mer* regulation (B).

Figure 5. Generic enhancement of *Merlin* phenotypes by Brahma complex mutants. A-D Scanning electron micrographs of respective genotypes. Note invasion of eye by ectopic vibrissae. % refers to the number of flies with at least one eye showing ectopic vibrissae.E. *Mer*^{3} wing shows overgrowth and disruption of vein structure. F. Alleles of *mor* enhances this overgrowth and causes increased interruption of the posterior cross vein.

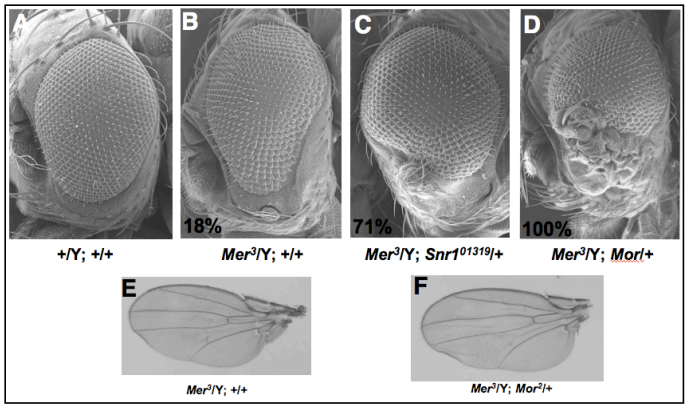

- ***The Brm Complex Interacts with NF2/Mer independently of the Hippo Pathway***

Since Merlin functions in the Salvador-Warts-Hippo (SWH) pathway (Oh and Irvine, 2010), we explored the hypothesis that Snr1, as part of the Brahma complex, may function to regulate this pathway at some level. We tested whether

loss of Brm complex genes have a transcriptional affect on *Mer* using qRT-PCR. Arguing against the former, we found no significant difference in *Mer* mRNA levels in wing discs with either *Brm* or *Snr1* RNAi driven with the *en-Gal4* driver (Figure 6A). We found no evidence that reduced levels *Snr1* affect the SWH pathway using FLP-FRT clonal experiments and transgenic reporters of the SWH pathway (described in the Year 3 Report). We therefore hypothesized that *Snr1* affects signaling downstream of *Mer,* independent of the SWH pathway. Possible mechanisms for the *Snr1-Mer* interaction include the Brm complex regulating expression of *Mer* itself, or another protein that alters Mer function/signaling. Next we employed a transgene to express a dominant negative form of Merlin ($Mer^{\Delta BB}$) under the control of the *apterous-Gal4* (kindly provided by Dr. R. Fehon) that gives ectopic veins in the wing anterior. This transgenic $Mer^{\Delta BB}$ phenotype does not rely on the endogenous *Mer* promoter. Arguing that reductions in Brm complex components affect Merlin protein activity itself, reducing Snr1 levels by RNAi modified the wing phenotype in flies (Figure 6D). Additionally, an allele of Snr1 also enhanced the defects in *Ap-Gal4> $Mer^{\Delta BB}$* wings (Figure 6E).

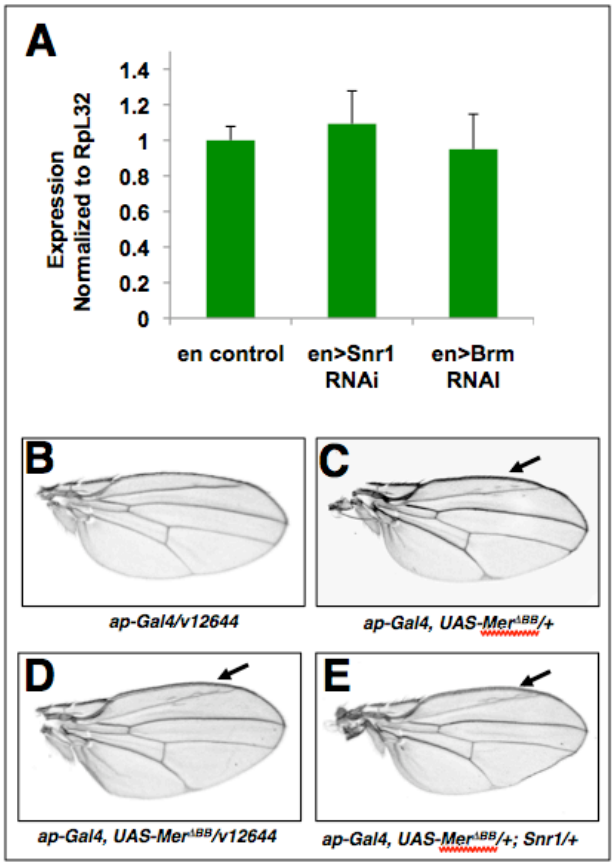

Figure 6. *Snr1* affects *Mer* protein function rather than transcription of *Mer* A. qRT-PCR of RNA from wing discs with knocked down levels of Snr1 and Brm (from *en-GAL4>Snr1 RNAi* and *en-GAL4>Brm RNAi* animals) to assess *Mer* mRNA levels. Results were normalized to *RpL32* expression. B. Snr1 RNAi using the weak *UAS-shRNAi* line v12644 and the *apterous-Gal4* driver gives no obvious defects. C-E Expressing a *UAS-$Mer^{\Delta BB}$* transgene under the control of *ap-Gal4* driver result in ectopic veins (arrows). This phenotype (C) is enhanced by addition of the *UAS-shRNAi* line v12644 targeting Snr1 (D) or dominantly using a Snr1 allele (E).

• ***Using Snr1 transgenic RNAi to screen for novel Snr1/SMARCB1 interactors***

For our initial screens we decided to use a strong *UAS-Snr1-shRNA* transgene (*v12645*) with the *ey-Gal4* driver (Figure 7A). This combination results in a highly penetrant roughened eye of reduced size. This line was used in a screen with molecularly defined deficiencies from the Bloomington Stock Collection (including Exelixis, BSC and DrosDel deficiencies). We concentrated our efforts to the 2nd chromosome for technical reasons. Table 2 describes the number of deficiencies screened and the initial hits. In many cases, not only did the deficiency reduce the severity of the eye phenotype, but also increased the viability of *ey-Gal4>UAS-Snr1-shRNA* flies, resulting in greater than usual numbers of progeny obtained (compared to the control crosses). Modifying deficiencies represent genetic interactions between genes uncovered by the deletion with *Snr1*. The two most exciting hits from the screen are discussed below and are shown in Fig. 7.

Chromosome	# deficiencies screened	Enhancers	Suppressors
2L	144	8	13
2R	103	5	7
X	26	2	1

Table 2 Results of deficiency screen using *ey-Gal4>Snr1 RNAi.* Table shows number of deficiencies screened on each chromosome arm and the number of enhancers and suppressors. These include modifiers that may be non-specific and have effects on the *UAS-Gal4* system or RNAi independently of *Snr1*.

• ***The Cyclin E agonist dacapo genetically interacts with Snr1***

As discussed in Annual Report Year 3, two overlapping deficiencies that both strongly suppress the eye phenotype of *ey-Gal4>UAS-Snr1-shRNA* (Figure 7C) and follow up experiments using alleles of *dap* were used to identify *dacapo* (*dap*), an agonist of Cyclin E, as a genetic interactor of *Snr1.* Mutations in the Brm complex genes have been isolated as dominant suppressors of S-phase defects associated with cyclin E (Brumby et al., 2002). Further, *Snr1* has

previously been shown to interact genetically with a subset of genes involved in cell cycle control, including *cyclin E* (Zraly et al., 2004).

• ***A regulator of the Hedgehog pathway, second wave mitotic (swm), genetically interacts with Snr1***

Also detailed in Annual Report Year 3, we found a second suppressing locus, represented by another two overlapping deficiencies (Fig. 7D), which uncover *second mitotic wave missing* (*swm*) as a potent genetic interactor of the *Snr1* RNAi phenotype. Subsequent testing of alleles of *swm* (swm^{F14} and $swm^{37Dh\text{-}1}$) was used to confirm the interaction. *swm* encodes a zinc finger protein that might be involved in protein- protein interactions or nucleic acid binding, an RNA-recognition motif (RRM) and nuclear localization signals. It was initially identified in a genetic screen for. *smoothened* (*smo*) interactors and has been shown to be involved in the negative regulation of the hedgehog (Hh) signaling pathway (Casso *et al*., 2008).

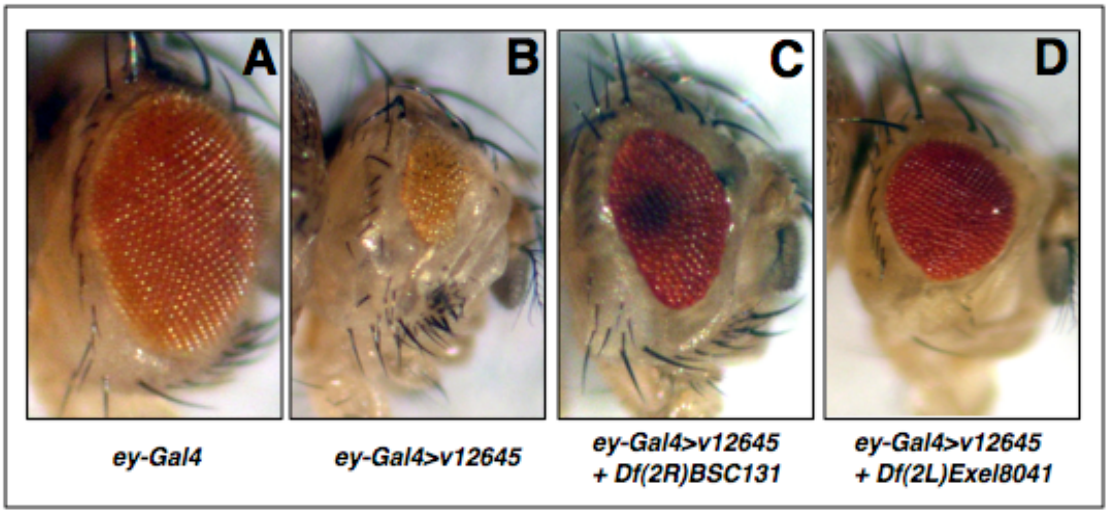

Figure 7. *Snr1* RNAi eye phenotypes. Driving the *UAS-Snr1-shRNA* transgene (v12645) with *ey-Gal4* results in a highly penetrant reduced eye phenotype (B). The control fly without the RNAi line has a wild type appearance (A). The effect of two suppressing deficiencies on the *Snr1* RNAi defect are shown (C and D) and are described in the text

Signaling by Hedgehog (Hh) proteins shapes most tissues and organs in both vertebrates and invertebrates, and its misregulation has been implicated in many human diseases, including tumorigenesis. Recently, the glioma-associated oncogene family zinc finger-1 (GLI1), a crucial effector of Hh signaling, was shown to interact physically with SMARCB1 (Jagani *et al.*, 2010). Further, SMARCB1 was shown to localize to Gli1-regulated promoters and loss of SMARCB1 was demonstrated to result in activation of the Hh-Gli pathway.

Other experiments have implicated SMARCB1 as a key mediator of Hh signaling and that aberrant activation of GLI1 is a previously undescribed targetable mechanism contributing to the growth of malignant rhabdoid tumor cells. Our finding of a genetic interaction between *Snr1* and *swm* in *Drosophila* therefore demonstrates that the link between SMARCB1 (whether it be SWI/SNF dependent or not) and the Hh pathway is conserved between humans and flies and is therefore worthy of further investigation.

Spatially and temporally choreographed cell cycles accompany the differentiation of the *Drosophila* retina. Recent studies indicate that signaling pathways with well-known roles in patterning also directly regulate cell proliferation. During the differentiation of the retina, Hh, Dpp, Notch and the EGF receptor regulate proliferation spatially through transcriptional regulation of *string*, *dacapo*, and as yet unidentified regulators of Retinoblastoma and Cyclin E/Cdk2 activities (reviewed in Baker, 2007). We hypothesize that when *Snr1* levels are reduced in the developing eye, these signaling pathways are disrupted.

• ***Functional relevance of Snr1 interactors***

There are two human homologues of swm - RBM26 (chromosome 13) and RBM27 (chromosome 5) – so unfortunately neither represent the elusive potentially other causative schwannomatosis gene on chromosome 22. However, we will continue to examine whether other Hh pathway genes could be similarly implicated. As for *dacapo*, its human homologue is cyclin-dependent kinase inhibitor 1B (p27, Kip1) and is on chromsome 12.

We crossed the deficiencies that uncover *swm* and *dacapo*, as well as *swm* and *dacapo* alleles to the *en-Gal4* and *ptc-Gal4* lines driving *UAS-Snr1-shRNA* to examine whether they can modify wing phenotypes or whether these interactions are eye-specific. We found that both the deficiencies and alleles dominantly suppress the ectopic vein phenotypes at the posterior cross vein (Figure 8). Therefore *swm* and *dacapo* interact with *Snr1* in both the eye and the wing during development.

We also used epistasis experiments to reveal that these genetic modifiers act downstream of *Snr1*. In addition, we are in the process of testing whether *dap* and/or *swm* modify *brm* and *mor* RNAi phenotypes in the eye or wing. In this way we will be able to assess whether these interactions are unique to *Snr1*. It is possible that Snr1 functions in a subset of complexes in different tissues or developmental times. By testing these modifiers with *brm* and *mor* knocked down in a variety of different tissues it is possible that we will find Snr1 functions independent from that of the Brm complex. In addition, we will investigate the possible role of the Hh pathway in the glial phenotype that we identified using *Snr1* knockdown using the *repo-Gal4* driver that we described in the second Annual Report.

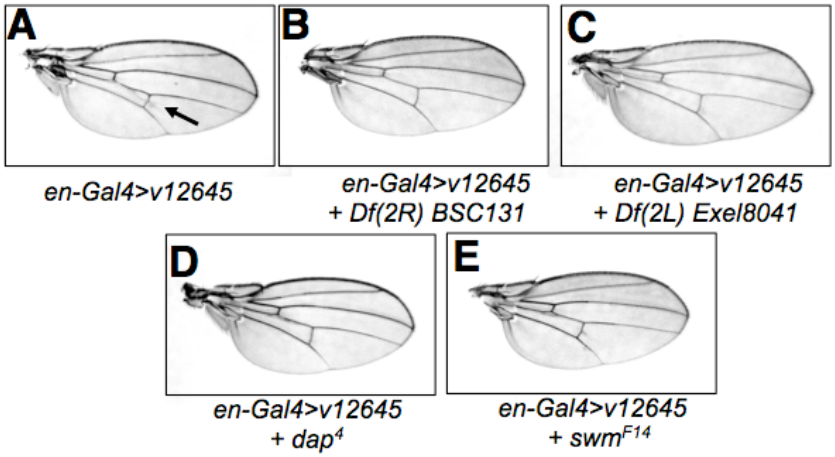

Figure 8. *swm* and *dap* interact with *Snr1* in the wing. Larvae with *Snr1* knockdown in the wing (e*n-Gal4>v12645*) were reared at room temperature to reduce the blistering phenotype (seen in Figure 1 B and C). A. At RT the wing shows an ectopic vein at the posterior cross vein (PCV) – indicated by an arrow. Introduction of the deficiencies that uncover *dap* and *swm* respectively (B and C) or alleles (D and E) suppress the appearance of the ectopic veins.

Specific Aim 3. To analyze genes which are aberrantly expressed in *Snr1* mutants.

- Used dsRNA to knockdown Snr1 expression in S2 cell lines; FACS analysis revealed G2 arrest in cell cycle
- Simultaneous Snr1 knockdown and induction of expression of wild type human SMARCB1, or SMARCB1 with missense mutations. FACS analysis to examine if G2 arrest is relieved.
- Prepared RNA from Snr1 knockdown experiments and performed microarray analysis.
- Microarray analysis of eye imaginal discs in which Snr1 knocked down using RNAi transgenes

• ***Knockdown of Snr1 in Drosophila S2 cells and test whether SMARCB1 can relieve cell cycle arrest***

As reported in the Annual Report Year 1, we knocked down *Snr1* expression in Drosophila S2 cells using dsRNA (Figure 9). The level of Snr1 protein is progressively reduced after several days of treatment, resulting in a G2/M arrest of the cell cycle (Figure 9 B and C). As a test to examine whether schwannomatosis *SMARCB1* missense mutants interfere with complex assembly, we used this system coupled with an add-back experiment. S2 cells that had been depleted of endogenous Snr1 by RNAi knockdown, resulting in a

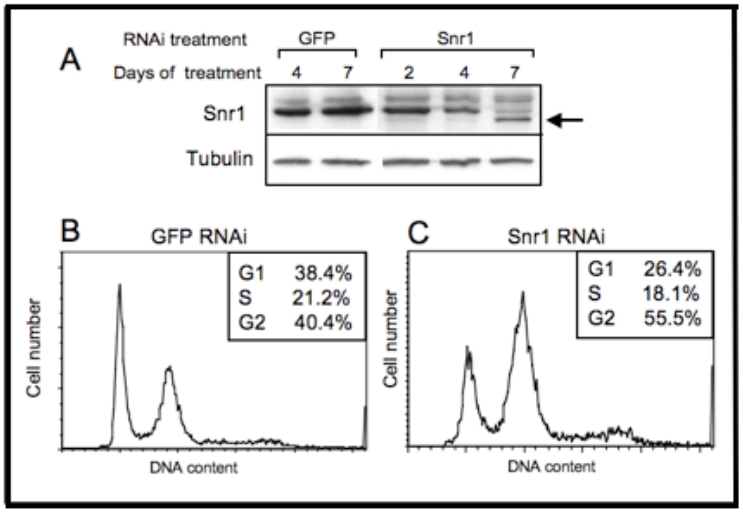

Figure 9. RNAi knock-down of Snr1 in Drosophila S2 tissue culture cells. A. Western blot of Snr1 and tubulin over a time course experiment with dsRNA knockdown of either GFP (control) or Snr1 RNAi. B and C FACS analysis of S2 cells with either GFP or Snr1 RNAi knockdown after 7 days.

G2 arrest, were subsequently transfected with constructs to express either wild type SMARCB1 or SMARCB1 with patient mutations. As shown in Table 3, FACS analysis revealed that only wild type SMARCB1 could effectively rescue the cell cycle arrest of *Snr1* depleted S2 cells, demonstrating that the disease-causing missense mutations alter the function of SMARCB1 in this assay.

Table 3. S2 cells were depleted of endogenous Snr1 by RNAi knockdown, which results in a G2 arrest of the cell cycle after 7 days. Subsequent transfection of these cells with wild type SMARCB1-A is able to rescue the cells from this arrest (+). Transfections of SMARCB1 bearing patient missense mutations are unable to rescue. The Exon4 deletion gives a partial rescue.

	Rescue of G2 Arrest
SMARCB1-A	+
SMARCB1 P14H	-
SMARCB1 R53L	-
SMARCB1 R374Q	-
SMARCB1 ΔExon4	+/-

• ***Snr1 knockdown in S2 cells: microarray analysis.***

We prepared RNA from S2 cells in which *Snr1* had been knocked down using dsRNA and performed microarray analysis. In concordance with a previous study (Zraly *et al*., 2006), we found the hormone-responsive ecdysone-induced genes (*Eig*) *Eig71Eh* and *Eig71Ei* were significantly up-regulated (~5-fold) when *Snr1* levels are reduced. We also found that *Cyclin G* (*CycG*) mRNA levels were significantly reduced (~4-fold) on *Snr1* RNAi. *Drosophila* CycG has recently been shown to negatively regulate cell growth and also has prominent effect on G1 and S phases (Faradji *et al.*, 2011). We speculate that the reduction of CycE levels upon *Snr1* RNAi could be responsible for the cell cycle arrest that we observed and/or the *Snr1* RNAi-induced cell size increase previously observed (Zraly *et al*., 2006). Follow up experiments to investigate this hypothesis are currently underway but unfortunately were not able to be concluded in time for inclusion in this report.

• ***Knock down the expression of Snr in developing fly tissues using RNAi to examine transcriptional targets***

We hypothesized that examining the transcriptional targets of *Snr1* in developing tissues would be more physiologically relevant than in S2 cells. Previous microarray studies used RNA from the pupal stage and also identified ecdysone-regulated genes as being Brm complex targets (Zraly *et al*., 2006). Given our success with *Snr1* RNAi knockdown in the developing eye and wing imaginal discs in identifying novel genetic interactions, we focused our attention of using these tissues for microarray experiments. Driving the *UAS-Snr1 RNAi* line using ey-*Gal4* has profound effects on development of the eye (Figure 7A), which undoubtedly are due to transcriptional defects. We are therefore attempting to examine changes in gene expression in the developing eye in the context of our identification of regulators of CycE and the Hedgehog pathway as novel genetic interactors of *Snr1* in this tissue.

We have spent considerable time amplifying suitable fly lines to generate sufficient material for dissection of eye imaginal discs, prepare RNA and subsequent microarray analysis. These experiments are technically difficult and required a great deal of effort including identifying animals of the correct genotype from cultures, quality control analysis of RNA and checking for sufficient knockdown. These experiments therefore took considerably longer than anticipated and we are currently in the process of submitting these samples for analysis.

Specific Aim 4. To identify and analyze the functional significance of proteins that associate with Snr1/SMARCB1.

• Subcloned cDNAs encoding SMARCB1, both wild type and with patient mutations into vectors for TAP-tag expression in tissue culture cells.

- Tandem Affinity Purification (TAP) of complexes with SMARCB1 from S2 cells. Purified complexes analyzed using mass spectroscopy.

- ***Testing whether SMARCB1 mutants have altered interactions in the Brahma Complex***

Previously we reported the generation of constructs for expression of SMARCB1 (both wild type and with patient mutations) in Drosophila S2 cells (Figure 10). Tagging of these proteins with N-terminal tandem FLAG and HA epitopes allowed us to purify them along with their associated proteins.

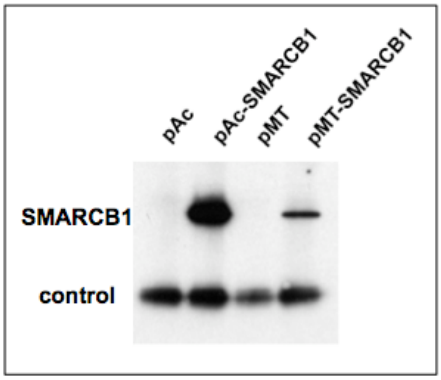

Figure 10. S2 cells were transfected with pAc or pMT(empty vectors) or these vectors containing SMARCB1 cDNA. Cells transfected with pMT and pMT-SMARCB1 were induced by addition of $CuSO_4$. After 24h whole cell lysates were made and proteins were subjected to western blotting using an anti-SMARCB1 antibody. The lower band is a non-specific protein that acts as a loading control. Based on this and similar experiments we have established the conditions to obtain optimal expression of SMARCB1 in S2 cells.

We purified wild type SMARCB1 using the FLAG epitope. Using whole cell lysates from S2 cells 48 hours post-transfection we successfully purified FLAG-SMARCB1 and associated proteins. Mass spectrometry of precipitated protein complexes showed that known components of the Brm complex were purified along with FLAG-SMARCB1, as expected. These included Brm, Mor, Osa and BAP60 (Table 4). We also found a large number of other proteins that were likely contaminants (data not shown). Purification of the disease-causing mutant SMARCB1 proteins from total S2 cell lysates showed a similar complement of interacting proteins, with no significant differences from that of wild type SMARCB1 (Table 4). However, since the purifications did not detect all the known Brm complex members, we are unable to conclude that the SMARCB1 point mutations disrupt specific protein-protein interactions that we were unable to detect, even in the wild type control.

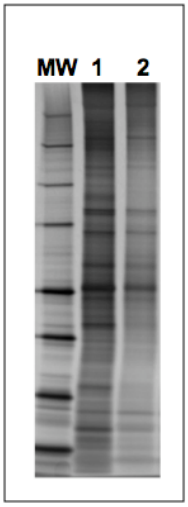

Figure 11. Purification of FLAG-tagged wild type SMARCB1 from whole cell lysates (S2 cells). Purified proteins were eluted from FLAG M2 beads using a FLAG peptide and resolved using SDS-polyacrylamide gel electrophoresis and silver stained. Lanes 1 and 2 are two independent preparations.

To circumvent this we subsequently employed a protocol to purify nuclei from S2 cells, with the idea that nuclear lysates may help us reveal other interacting proteins. Unfortunately, despite repeated attempts to purify FLAG-SMARCB1 complexes from nuclear fractions and extensive trouble-shooting, we were unsuccessful with this approach.

Protein	Mol. Mass (kDa)	SMARCB1-WT	SMARCB1-P14H	SMARCB1-R53L	SMARCB1-R374Q
Snr1	42	15	12	13	11
Brm	185	7	8	6	3
Osa	285	6	4	7	4
Mor	134	7	7	5	4
BAP60	58	2	2	1	2

Table 4 Results of protein interactors detected using FLAG-tagged SMARCB1 in S2 cells. Drosophila S2 cells were transfected with constructs expressing either wild–type or mutant SMARCB1 proteins. After purification using an anti-FLAG column, precipitated proteins were subjected to mass spectroscopy. The number of detected peptides for each protein is indicated. Only the known Brahma complex components that were detected are shown. An extensive list of other proteins was also detected, presumed to be contaminants.

• ***Tandem Affinity Purification (TAP) of complexes with Snr1 in flies***

A similar approach of examining altered protein complexes *in vivo* is underway in flies, using Snr1 fused to Streptavidin binding protein (SBP) and protein G as tags in the *pUAST-TAP-SG* vector. We have generated transgenic

lines of these flies and they are currently being crossed into the Snr1 mutant background along with the *actin5C-Gal4* driver. Initial experiments suggest that the Snr1-TAP transgene can rescue the lethality of Snr1 null mutants. We have found that the *pUAST-TAP-SG* vector drives at considerably higher levels that the *pUAST* vector used in Aim1. Consequently, we prepared for purifying Snr1 complexes from flies at different developmental stages (embryo, larva, adult) in the absence of endogenous Snr1. These samples have yet to be analyzed by mass spectroscopy and so unfortunately we are unable to report on the conclusions of these experiments here.

Key Research Accomplishments

- Generated multiple transgenic lines representing six *SMARCB1* mutations found in schwannomatosis.
- Determined that both *Snr1* and *SMARCB1* have differential ability to rescue the lethality of a *Snr1* null mutant.
- Determined that three *SMARCB1* missense mutant transgenes do not modify either the lethality of a *Snr1* null mutant; two of three missense mutations rescue an Snr1-RNAi-induced phenotype, suggesting they have residual function.
- Identified novel wing, bristles and eye phenotypes caused by RNAi knockdown of *Snr1* in the developing fly.
- Identified a potent genetic interaction between Drosophila *Snr1* (and other Brahma complex mutants) and *NF2/merlin*
- Snr1 does not appear to play a role in regulating the SWH (Hippo) pathway. Loss of *Snr1* appears to affect Merlin protein function (not *Mer* transcriptional regulation)
- Completed 2nd chromosome deficiency screen to look for modifiers of the *Snr1* RNAi-induced phenotypes in the eye (*ey-Gal4>UAS-Snr1 RNAi*). Secondary screens in wing (*en-Gal4>* and *ptc>UAS-Snr1 RNAi*)
- Identified *second wave mitotic* (*swm*) and *dacapo* (*dap*) as *Snr1* genetic suppressors
- Knockdown of *Snr1* in larval glia results in abnormal cell growth in the CNS (Annual Report Year 2)
- Disease-causing missense mutations in SMARCB1 are unable to effectively rescue the cell cycle arrest of *Snr1* depleted S2 cells
- RNAi knockdown of *Snr1* in S2 cells results in gene expression changes similar to those seen in a previous study. RNA from *Snr1* RNAi knockdown in eye imaginal discs prepared for subsequent microarray analysis.

- Purification of mutant SMARCB1 proteins (encoded by disease-causing mutations) from total S2 cell lysates showed a similar complement of interacting proteins, with no significant differences from that of wild type SMARCB1

Reportable Outcomes

- Published four papers (see Bibliography below and Appendix for copies of publications)
- Preseneted findings at The Children's Tumor Foundation NF Conference, Baltimore, MD (June 5th-8th 2010)
- The research findings were also presented at invited seminars at the following institutions:
  St. George's Medical School, University of London, UK 19th January 2012
  University of Manchester, Nowgen Centre, UK 24th January 2012
  Southampton University, Center for Biological Sciences, 26th January 2012
  University of Cambridge, Dept. of Zoology, UK 10th May 2012

Bibliography (*see Appendix for original of each publication)*

Di Stefano, L., Walker, J.A., Burgio, G., Corona, D., Mulligan, P., Näär, A. and Dyson, N.J. (2011) Functional antagonism between histone H3K4 demethylases *in vivo*. Genes & Dev. 25 (1) 17-28.

Miles, W.O., Dyson, N.J. and Walker, J.A. (2011) Modeling tumor invasion and metastasis in Drosophila. *Dis. Model Mech.* 4(6): 753-761

Longworth, M.S., Walker, J.A., Anderssen, E., Moon, N-S., Gladden, A., Heck, M.M., Ramaswamy, S. and Dyson, N.J. (2012) A shared role for RBF1 and dCAP-D3 in the regulation of transcription with consequences for innate immunity. *PLoS Genet.* 8(4):e1002618.

Smith, M.J., Walker, J.A., Shen, Y., Stemmer-Rachamimov, A., Gusella, J.F. and Plotkin, S.R. (2012) cDNA analysis of *SMARCB1 (INI1)* mutations in familial and

sporadic schwannomatosis. *Hum. Mol. Genet.* 21 (24) 5239-5245 *doi: 10.1093/hmg/dds370*

Meeting Abstracts

• Drosophila as a model to study the role of SMARCB1 in Schwannomatosis
The Children's Tumor Foundation NF Conference, Baltimore, MD (June 5th-8th 2010)

Reported in Huson et al., (2011) *Back to the future*: *proceedings from the 2010 NF Conference*. Am J Med Genet A. 2011 Feb;155A(2):307-21.

List of Personnel

• Dr. James Walker	July 2009 - January 2014
• Ms. Tram Hoang	August 2009 - May 2010
• Mr. Arjun Ray	February 2010 - May 2010
• Mr. Robert Maher	June 2010 - January 2014

Conclusions

We have examined mutations in the tumor suppressor gene SMARCB1 that are found in familial cases of schwannomatosis. *Drosophila* was used to investigate the nature of the SMARCB1 mutations and their molecular consequences, which give rise to schwannomas.

In Specific Aim 1 we examined the differential ability of transgenic expression of human SMARCB1 to rescue phenotypes caused by RNAi knockdown of Snr1, the fly ortholog of SMARCB1. These assays revealed that SMARCB1 missense mutations from patients have varying degrees of residual function suggesting that, at least some of them, are hypomorphic in nature and so differ from SMARCB1 mutations that are found in the case of early onset AT/RT.

For Specific Aim 2 we completed a deficiency screen to look for modifiers of the *Snr1* RNAi-induced phenotypes in the eye (*ey-Gal4>UAS-Snr1 RNAi*). This identified several potent *Snr1* interactors – the CycE regulator *dacapo* and *second wave mitotic* (*swm*), a negative regulator the Hedgehog pathway. These may represent important clues to the pathways that are misregulated when *Snr1* is lost in both the developing eye and wing. The recent finding by others of a physical interaction of SMARCB1 with GLI1, an effector of Hh signaling, suggests that our *Drosophila* model will be useful for gaining further insights into the interaction of the SWI/SNF complex with this important signaling pathway.

For Specific Aim 3 we developed a *Drosophila* S2 tissue culture system in which we can knockdown *Snr1* using dsRNA. We showed by add-back assays that SMARCB1 bearing disease-causing missense mutations is unable to effectively rescue the cell cycle arrest. We used this system to examine the consequences of *Snr1* knockdown on gene expression using microarrays. The changes in gene expression were similar to those reported in a previous study. However, our finding that *CycG* expression is reduced suggests further experiments to investigate whether misregulation of this cell cycle regulator on *Snr1* knockdown could account for the observed differences in cell growth.

For Specific Aim 4 we successfully developed a protocol to allow us to purify proteins complexed with FLAG-SMARCB1 transfected into S2 cells. By conducting the same procedure with SMARCB1 bearing mutations from schwannomatosis patients, we have so far been unable to identify any altered protein-protein interactions or complex formation.

We are in the process of writing up the results from Specific Aims 1 and 2 for publication and anticipate a second paper on completion of experiments that will build on the completed experiments under Specific Aims 3 and 4. Together, these approaches in *Drosophila* will address the functional consequences of the disease-causing mutations in SMARCB1 from familial cases of schwannomatosis.

References

Baker, N.E. (2007) Patterning signals and proliferation in Drosophila imaginal discs. *Curr Opin Genet Dev.* 2007 Aug;17(4):287-93.

Biegel, J. A., Zhou, J. Y., Rorke, L. B., Stenstrom, C., Wainwright, L. M., and Fogelgren, B. (1999). Germ-line and acquired mutations of INI1 in atypical teratoid and rhabdoid tumors. *Cancer Res 59*, 74-79.

Boyd, C., Smith, M.J., Kluwe, L., Balogh, A., Maccollin, M., and Plotkin, S.R. (2008). Alterations in the SMARCB1 (INI1) tumor suppressor gene in familial schwannomatosis. *Clin Genet 74*, 358-366.

Brumby, A.M, Zraly, C.B, Horsfield, J.A, Secombe, J., Saint, R., Dingwall, A.K, Richardson, H. (2002) Drosophila cyclin E interacts with components of the Brahma complex. *EMBO J.* 2002 Jul 1;21(13):3377-89.

Casso, D.J, Liu, S., Iwaki, D.D., Ogden, S.K and Kornberg, T.B. (2008) A screen for modifiers of hedgehog signaling in Drosophila melanogaster identifies swm and mts. *Genetics.* 178(3):1399-413.

Christiaans I, Kenter SB, Brink HC, van Os TA, Baas F, van den Munckhof P, Kidd AM, Hulsebos TJ. (2011) Germline SMARCB1 mutation and somatic NF2 mutations in familial multiple meningiomas. J Med Genet. 2011 Feb;48(2):93-7.

Dietzl, G., Chen, D., Schnorrer, F., Su, K. C., Barinova, Y., Fellner, M., Gasser, B., Kinsey, K., Oppel, S., Scheiblauer, S.*, et al.* (2007). A genome-wide transgenic RNAi library for conditional gene inactivation in Drosophila. Nature *448*, 151-156.

Euskirchen G, Auerbach RK, Snyder M. (2012) SWI/SNF chromatin-remodeling factors: multiscale analyses and diverse functions. *J Biol Chem.* 287(37): 30897-905. doi: 10.1074/jbc.R111.309302. Epub 2012 Sep 5.

Faradji F, Bloyer S, Dardalhon-Cuménal D, Randsholt NB, Peronnet F. (2011) Drosophila melanogaster Cyclin G coordinates cell growth and cell proliferation. *Cell Cycle.* 10(5):805-18.

Hadfield, K. D., Newman, W. G., Bowers, N. L., Wallace, A., Bolger, C. M., Colley, A., McCann, E., Trump, D., Prescott, T., and Evans, G. (2008). Molecular characterisation of SMARCB1 and NF2 in familial and sporadic schwannomatosis. *J Med Genet.* 45, 332-339.

Hamaratoglu F, Willecke M, Kango-Singh M, Nolo R, Hyun E, Tao C, Jafar-Nejad H, Halder G. (2006) The Tumor suppressor genes NF2/Merlin and Expanded act

through Hippo signaling to regulate cell proliferation and apoptosis. *Nat Cell Biol.* 8(1):27-36

Hulsebos, T.J., Plomp, A.S., Wolterman, R.A., Robanus-Maandag, E.C., Baas, F., and Wesseling, P. (2007). Germline mutation of INI1/SMARCB1 in familial schwannomatosis. *Am J Hum Genet 80*, 805-810.

Jagani Z, Mora-Blanco EL, Sansam CG, McKenna ES, Wilson B, Chen D, Klekota J, Tamayo P, Nguyen PT, Tolstorukov M, Park PJ, Cho YJ, Hsiao K, Buonamici S, Pomeroy SL, Mesirov JP, Ruffner H, Bouwmeester T, Luchansky SJ, Murtie J, Kelleher JF, Warmuth M, Sellers WR, Roberts CW, Dorsch M. (2010) Loss of the tumor suppressor Snf5 leads to aberrant activation of the Hedgehog-Gli pathway. *Nat Med.*16(12):1429-33.

MacCollin, M., Willett, C., Heinrich, B., Jacoby, L. B., Acierno, J. S., Jr., Perry, A., and Louis, D. N. (2003). Familial schwannomatosis: exclusion of the NF2 locus as the germline event. *Neurology 60*, 1968-1974.

Marenda, D. R., Zraly, C. B., and Dingwall, A. K. (2004). The Drosophila Brahma (SWI/SNF) chromatin remodeling complex exhibits cell-type specific activation and repression functions. Dev Biol *267*, 279-293.

McCartney, B.M., Kulikauskas, R.M., LaJeunesse, D.R., and Fehon, R.G. (2000). The neurofibromatosis-2 homologue, Merlin, and the tumor suppressor expanded function together in Drosophila to regulate cell proliferation and differentiation. *Development 127*, 1315-1324.

Moertel, C., Biegel, J., Dahlheimer, T. and Berry, S., (2009) Report of a Patient with Constitutional Missense Mutation of INI1/SMARCB1. Abstract from Children's Tumor Foundation Conference, Portland, Oregon 2009

Oh, H. and Irvine, K.D. (2010) Yorkie: the final destination of Hippo signaling. *Trends in Cell Biol.* 20(7), 410-417.

Rousseau G, Noguchi T, Bourdon V, Sobol H, Olschwang S. (2011) SMARCB1/INI1 germline mutations contribute to 10% of sporadic schwannomatosis. BMC Neurol. 2011 Jan 24;11:9. doi: 10.1186/1471-2377-11-9.

Sestini, R., Bacci, C., Provenzano, A., Genuardi, M., and Papi, L. (2008). Evidence of a four-hit mechanism involving SMARCB1 and NF2 in schwannomatosis-associated schwannomas. *Hum Mutat 29*, 227-231.

Smith MJ, Boyd CD, MacCollin MM, Plotkin SR. (2009) Identity analysis of schwannomatosis kindreds with recurrent constitutional SMARCB1 (INI1) alterations. Clin Genet. 75(5):501-2.

Smith, M.J., Walker, J.A., Shen, Y., Stemmer-Rachamimov, A., Gusella, J.F. and Plotkin, S.R. (2012) cDNA analysis of *SMARCB1 (INI1)* mutations in familial and sporadic schwannomatosis. *Hum. Mol. Genet.* 21 (24) 5239-5245 *doi: 10.1093/hmg/dds370*

Versteege, I., Sevenet, N., Lange, J., Rousseau-Merck, M. F., Ambros, P., Handgretinger, R., Aurias, A., and Delattre, O. (1998). Truncating mutations of hSNF5/INI1 in aggressive paediatric cancer. *Nature 394*, 203-206.

Zraly, C. B., Marenda, D. R., and Dingwall, A. K. (2004). SNR1 (INI1/SNF5) mediates important cell growth functions of the Drosophila Brahma (SWI/SNF) chromatin remodeling complex. *Genetics 168*, 199-214.

Zraly, C.B., Middleton, F.A and Dingwall, A.K. (2006) Hormone-response genes are direct in vivo regulatory targets of Brahma (SWI/SNF) complex function. *J Biol Chem.* 281(46):35305-15.

Functional antagonism between histone H3K4 demethylases in vivo

Luisa Di Stefano,[1,2] James A. Walker,[1,3] Giosalba Burgio,[4,5] Davide F.V. Corona,[4,5] Peter Mulligan,[1] Anders M. Näär,[1,6] and Nicholas J. Dyson[1,7]

[1]Massachusetts General Hospital Cancer Center, Harvard Medical School, Charlestown, Massachusetts 02129, USA; [2]Computer Science and Artificial Intelligence Laboratory, Massachusetts Institute of Technology, Cambridge, Massachusetts 02139, USA; [3]Center for Human Genetic Research, Massachusetts General Hospital, Boston, Massachusetts 02114, USA; [4]Dipartimento di Biologia Cellulare e dello Sviluppo, c/o Universitá degli Studi di Palermo, Palermo 90128, Italy; [5]Istituto Telethon Dulbecco, c/o Universitá degli Studi di Palermo, Palermo 90128, Italy; [6]Department of Cell Biology, Harvard Medical School, Boston, Massachusetts 02115, USA

Dynamic regulation of histone modifications is critical during development, and aberrant activity of chromatin-modifying enzymes has been associated with diseases such as cancer. Histone demethylases have been shown to play a key role in eukaryotic gene transcription; however, little is known about how their activities are coordinated in vivo to regulate specific biological processes. In *Drosophila*, two enzymes, dLsd1 (*Drosophila* ortholog of lysine-specific demethylase 1) and Lid (little imaginal discs), demethylate histone H3 at Lys 4 (H3K4), a residue whose methylation is associated with actively transcribed genes. Our studies show that compound mutation of *Lid* and *dLsd1* results in increased H3K4 methylation levels. However, unexpectedly, *Lid* mutations strongly suppress *dLsd1* mutant phenotypes. Investigation of the basis for this antagonism revealed that Lid opposes the functions of dLsd1 and the histone methyltransferase Su(var)3–9 in promoting heterochromatin spreading at heterochromatin–euchromatin boundaries. Moreover, our data reveal a novel role for dLsd1 in Notch signaling in *Drosophila*, and a complex network of interactions between dLsd1, Lid, and Notch signaling at euchromatic genes. These findings illustrate the complexity of functional interplay between histone demethylases in vivo, providing insights into the epigenetic regulation of heterochromatin/euchromatin boundaries by Lid and dLsd1 and showing their involvement in Notch pathway-specific control of gene expression in euchromatin.

[*Keywords*: *Drosophila*; histone demethylases; H3K4me; H3K9me; heterochromatin; Notch signaling]

Supplemental material is available for this article.

Received August 18, 2010; revised version accepted November 16, 2010.

In eukaryotic cells, genomic DNA is packaged with histone and nonhistone proteins to form chromatin. The combined action of chromatin remodeling activities and histone-modifying enzymes dynamically regulates the chromatin status and has been implicated in the control of numerous biological processes, including transcription, cell division, differentiation, and DNA repair. Furthermore, aberrant activity of chromatin-modifying enzymes has been strongly associated with diseases such as cancer (Chi et al.2010).

The methylation pattern of histones is believed to define transcriptionally active and inactive chromatin domains. For example, methylation at Lys 9 of histone H3 (H3K9) is associated with silenced chromatin (heterochromatin), while methylation of Lys 4 of histone H3 (H3K4) is an important mark of actively transcribed genes (Bannister and Kouzarides 2005; Martin and Zhang 2005; Trewick et al. 2005; Wysocka et al. 2005). H3K4 can be mono-, di-, or trimethylated, and several histone methyltransferases act at this residue, including MLL1, which is frequently translocated in leukemias (Krivtsov and Armstrong 2007). Levels of H3K4 trimethylation peak around promoters of actively transcribed genes (Bernstein et al. 2005), while H3K4me2 is highest just downstream from transcriptional start sites, and monomethylation is more dispersed throughout the body of genes (Liu et al. 2005). In addition to the promoter regions, these modifications are also detected in intergenic regions, and H3K4me1 signals have been correlated with functional enhancers (Roh et al. 2004; Heintzman et al. 2007). These observations suggest that different levels of methylation may have different functional consequences, and that the transition from mono- to di- to trimethyl moieties is likely to be a critical and highly regulated event.

Until recently, histone methylation was regarded as an irreversible modification. The discovery of the first histone lysine demethylase LSD1/KDM1 (lysine-specific demethylase 1), and subsequently of a second family of

[7]Corresponding author.
E-MAIL dyson@helix.mgh.harvard.edu; FAX (617) 726-7808.
Article is online at http://www.genesdev.org/cgi/doi/10.1101/gad.1983711.

histone demethylases, including members of the Jmj domain-containing proteins, suggested a more dynamic regulation of the methylation state of histones. These discoveries raise several fundamental questions: How are the activities of histone methyltransferases and demethylases coordinated to establish the appropriate patterns of methylation, and how are these patterns regulated to allow accurate chromatin dynamics and gene expression cascades contributing to animal development and homeostasis? Very little is known about the dynamic regulation of histone methylation by methyltransferases and demethylases in vivo, and even less is known about the signaling pathways that control their activity.

We and others generated mutants for the *Drosophila* ortholog of the histone demethylase LSD1 (dLsd1). Like its mammalian counterpart, dLsd1 specifically demethylates H3K4me2 and H3K4me1 residues, indicating functional conservation (Rudolph et al. 2007). We showed that *dLsd1* mutation affects male viability as well as specific developmental processes such as wing development and oogenesis (Di Stefano et al. 2007). Furthermore, mutant alleles of *dLsd1* strongly suppress positional effect variegation (PEV), indicating that dLsd1 contributes to maintaining the balance between euchromatin and heterochromatin (Di Stefano et al. 2007; Rudolph et al. 2007). Taken together, these studies showed that dLsd1 plays a crucial role in chromatin regulation during *Drosophila* development, and that its depletion impacts specific developmental processes.

An important question arising from these initial studies is how dLsd1 cooperates with other chromatin-associated proteins to dynamically control chromatin during animal development. We reasoned that, while many different chromatin regulators might have activities that could directly or indirectly interconnect with dLsd1, the clearest functional interactions would likely be seen with other enzymes that act on H3K4 methylation. In *Drosophila*, the ortholog of the Jarid 1 family of JmjC domain-containing proteins, *Lid* (little imaginal discs), has been shown to specifically demethylate H3K4me2 and H3K4me3 residues in vitro and H3K4me3 in vivo (Eissenberg et al. 2007; Lee et al. 2007; Secombe et al. 2007; Lloret-Llinares et al. 2008). Therefore, as a starting point, we generated flies that are mutant for both *dLsd1* and *Lid*. Consistent with their enzymatic activities, we find that *Lid; dLsd1* mutant flies display an increased level of H3K4 methylation. However, intriguingly, *Lid* mutations strongly suppress *dLsd1* mutant phenotypes. An analysis of the basis of this antagonism reveals that the interplay of Lid with dLsd1 occurs through distinct mechanisms in different contexts. For example, Lid opposes the function of dLsd1 and the H3K9 methyltransferase Su(var)3–9 at heterochromatin–euchromatin boundaries while cooperating with dLsd1 in regulating certain Notch target genes in euchromatic contexts. These findings illustrate the complexity of functional interactions between demethylases in vivo. To understand the functional interplay between these enzymes in animal development, we must therefore not only consider the biochemical properties of the enzymes, and the chromatin context of their targets, but also understand how their activities impact the status of key signaling pathways that define the cellular response, such as the Notch pathway.

Results

Lid suppresses phenotypes associated with dLsd1 mutation

To understand the function of the dLsd1 demethylase, it is essential to determine how its activities are integrated with other chromatin-associated proteins, since it is the concerted action of multiple enzymes that enables chromatin states to be controlled dynamically in vivo. One protein likely to impact dLsd1 function in *Drosophila melanogaster* is Lid. Lid and dLsd1 have both been shown to demethylate histone H3K4 methyl residues. dLsd1 acts specifically on mono- and dimethyl residues, while Lid can act on di- and trimethyl residues. To study the combinatorial contributions of H3K4 demethylases in vivo, we generated compound mutants for *Lid* and *dLsd1*. Given their enzymatic activities, we expected that *Lid*; *dLsd1* double-mutant flies would likely show a synergistic increase in the levels of H3K4 methylation. If these proteins act cooperatively, then the combined mutation of the two H3K4 demethylases would be expected to cause defects that were more severe than the single mutants.

We showed previously that inactivation of *dLsd1* in *Drosophila* results in specific developmental defects. Homozygous mutation of *dLsd1* leads to a held-out wing phenotype, male lethality, and defects in oogenesis (Di Stefano et al. 2007). Further analysis of $dLsd1^{\Delta N}$ mutant flies revealed an additional defect in the wing. Approximately 36% of $dLsd1^{\Delta N}$ mutants exhibit ectopic vein tissue emanating from the posterior cross-vein (pcv), posterior to the L5 longitudinal vein (Fig. 1A,A′). This phenotype, which has already been observed in mutants of chromatin remodeling complex components, such as Snr1 (Marenda et al. 2003), indicates that dLsd1 has a role in the repression of vein development in intervein cells.

Remarkably, combining homozygous *dLsd1* mutants with a loss-of-function mutation of *Lid* (Lid^{10424}) results in a strong dominant suppression of the $dLsd1^{\Delta N}$ wing vein phenotype (Fig. 1A,B; Table 1). The *Lid* mutant was further tested against the $dLsd1^{\Delta N}$ allele in a second independent assay using the held-out wing phenotype. When we quantified the number of flies with held-out wings, we found that heterozygous mutation in *Lid* reduces the penetrance of this phenotype from 87% of *dLsd1* homozygous mutant flies to 36% (Fig. 1C,D; Table 1).

Each of these wing phenotypes resulting from *dLsd1* mutation was markedly suppressed by mutant alleles of *Lid* (Fig. 1A–D; Table 1). To determine whether this suppression was limited to the wing, we tested the *Lid* mutant allele for its ability to modify the highly penetrant $dLsd1^{\Delta N}$ oogenesis defect (Di Stefano et al. 2007). To gain insights into the specific effects of *Lid* mutation on the $dLsd1^{\Delta N}$-dependent oogenesis defect, wild-type and mutant ovaries were stained with antibodies specific for ovarian cell markers. The *Drosophila* ovary consists

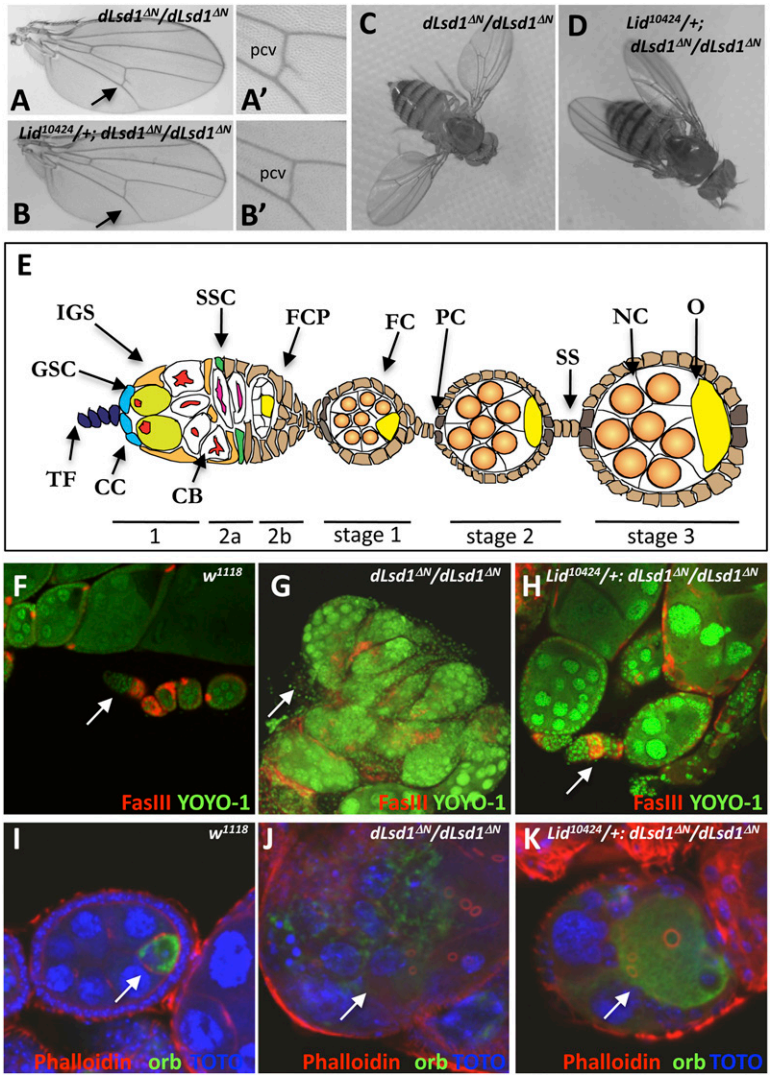

Figure 1. *Lid*^{10424} mutation suppresses phenotypes associated with *dLsd1*$^{\Delta N}$ loss-of-function mutation. (*A*) Loss of *dLsd1* results in extra wing vein tissue emanating from the pcv (indicated by arrows; closer view in *A*′). (*B*) This phenotype is rescued by heterozygous mutation of *Lid* (indicated by arrows; closer view in *B*′). (*C*,*D*) *Lid* mutation suppresses the held-out wing phenotype observed in homozygous *dLsd1* mutant flies. (*E*) Schematic representation of a wild-type ovariole, including the germarium and egg chambers (stages 1–3). Germline stem cells (GSC) reside at the tip of the germarium in a microenvironment created by the cap cells (CC) and the terminal filaments (TF). The differentiating daughter cell of a germline stem cell is the cystoblast (CB), which moves posterior and becomes encompassed by inner germarian sheath cells (IGS). Cystoblasts divide four times and generate germline cysts of 16 cells, which, after passing region 2 of the germarium, become surrounded by follicle cell precursors (FCP). Follicle cell precursors are generated by somatic stem cells (SSC) and differentiate into follicle cells (FC), polar cells (PC), and stalk cells (SC). Among the 16 germ cells, one differentiates into the oocyte (O), and the remaining 15 become nurse cells (NC). (*F*,*G*,*H*) *Lid*^{10424} mutations partially rescue *dLsd1*$^{\Delta N}$ mutant follicle cell defects. Wild-type (*w*^{1118}), *dLsd1*$^{\Delta N}$ homozygous, and *Lid*^{10424}/+; *dLsd1*$^{\Delta N}$/*dLsd1*$^{\Delta N}$ ovaries were stained with YOYO-1 (green) and anti-Fasciclin-III to outline somatic cells. (*I*,*J*,*K*) *Lid*^{10424} mutation partially rescues *dLsd1*$^{\Delta N}$ mutant defects in the germline. Wild-type (*w*^{1118}), *dLsd1*$^{\Delta N}$ homozygous, and *Lid*^{10424}/+; *dLsd1*$^{\Delta N}$/*dLsd1*$^{\Delta N}$ ovaries were stained with TOTO (blue) and anti-orb to visualize the oocyte (indicated by arrows). Cell outlines and ring canals were visualized by phalloidin staining of the actin cytoskeleton (red).

of ~14–16 ovarioles, which contain strings of developing egg chambers of progressive age with a germarium at the anterior tip (Fig. 1E; Kirilly and Xie 2007). As a consequence of *dLsd1* mutation, oogenesis arrests very early, with *dLsd1* homozygous mutant ovaries consisting of germaria that do not bud off egg chambers. Labeling the ovaries with an antibody to Fasciclin III (Fas III), a membrane-associated protein present in prefollicle and follicle cells, shows that the number of these cell types is strongly reduced in *dLsd1*$^{\Delta N}$ mutant ovaries (Fig. 1G) compared with wild-type ovaries (Fig. 1F), and that these cells fail to completely encapsulate the germline cyst. In the partially encapsulated cysts that do exist, oocyte determination/localization appears abnormal, as judged by nuclei staining and Orb accumulation (Fig. 1J). In many cases, one mutant copy of *Lid* partially rescued these defects, as shown by the presence of egg chambers at later stages of development, an increased number of cells positively staining for Fas III (Fig. 1H), and a more localized accumulation of Orb protein in the oocyte (Fig. 1K). To ensure that this suppression is due specifically to *Lid* inactivation, we tested two independently generated P-element insertions, both within the *Lid* gene, and found similar results (Supplemental Fig. S1).

To further confirm this interaction, we tested the effect of *Lid* mutation on another phenotype associated with *dLsd1* loss of function. Previously, we showed that homozygous mutation of *dLsd1* dramatically reduces male viability; in this study, we found that *Lid*^{10424} dominantly rescues *dLsd1*$^{\Delta N}$-dependent male lethality (from 1%–12% viability) (Table 2; Supplemental Table

Table 1. Lid ^{10424} *supresses* dLsd1$^{\Delta N}$ *wing phenotypes*

Genotype	Modified wing phenotype	Held-out wing phenotype
dLsd1$^{\Delta N}$/*dLsd1*$^{\Delta N}$	36% (*N* = 128)	80% (*N* = 74)
Lid^{10424}/+;*dLsd1*$^{\Delta N}$/*dLsd1*$^{\Delta N}$	7% (*N* = 179)	36% (*N* = 82)

(*N*=) The number of wings counted, in the case of the modified wing phenotype, and the number of flies counted, in the case of the held-out wing phenotype.

Table 2. *Effect of* Lid ^{10424} *and* dLsd1$^{\Delta N}$ *mutation on gender distribution*

Genotype	Females	Males
$Lid^{10424}/CyO;dLsd1^{\Delta N}/TM3$	38%	35%
Lid^{10424}/Lid^{10424}; $dLsd1^{\Delta N}/TM3$	0%	2%
Lid^{10424}/CyO; $dLsd1^{\Delta N}/dLsd1^{\Delta N}$	13%	12%
Lid^{10424}/Lid^{10424}; $dLsd1^{\Delta N}/dLsd1^{\Delta N}$	0%	0%

Percentage of males and females of the indicated genotypes obtained from Lid^{10424}/CyO; $dLsd1^{\Delta N}/TM3$ X Lid^{10424}/CyO; $dLsd1^{\Delta N}/TM3$. A total of at least 106 flies were counted for each genotype.

S1). Taken together, this set of observations shows that Lid antagonizes dLsd1 function in vivo. This antagonism is a general phenomenon that is evident in multiple tissues.

To exclude the possibility that any general manifestation of abnormal chromatin regulation could suppress *dLsd1* mutant phenotypes, we carried out a candidate genetic screen among components of chromatin remodeling complexes, Trx-G complexes, and PcG complexes for dominant modification of the homozygous $dLsd1^{\Delta N}$ wing and ovary phenotypes. The extra wing vein phenotype observed in *dLsd1* mutant flies was unaffected by mutant alleles of *ash2*, *Trl*, and *Psc*, or by mutations in *Bap180*, a specific component of the P-BAP complex (Supplemental Table S2). Hypomorphic, amorphic, null, and loss-of-function mutations in most BAP complex subunits (mor, osa, and brm) enhanced, rather than suppressed, the severity of the extra wing vein phenotype of $dLsd1^{\Delta N}$ mutants (Supplemental Fig. S2; Supplemental Table S2), suggesting that dLsd1 and the BAP complex may cooperate in the regulation of intervein-specific gene expression. In addition to *Lid* alleles, the extra vein phenotype of $dLsd1^{\Delta N}$ mutants was also strongly suppressed by *Snr1* mutations. However, unlike the *Lid* alleles, which gave a consistent pattern of interaction across all of the *dLsd1* mutant phenotypes, these other alleles that we tested had variable effects on different aspects of the *dLsd1* mutant phenotype (Supplemental Table S2). We conclude that the ability of *Lid* alleles to consistently suppress the effects of *dLsd1* mutation is an unusual property that is not seen with other general regulators of chromatin structure.

dLsd1 and Lid mutations cooperatively increase the global level of H3K4 methylation

Given that both Lid and dLsd1 have been shown to have demethylase activity toward methylated H3K4 residues, we performed an immunoblotting analysis to assess whether the combined mutation of *Lid* and *dLsd1* does indeed result in increased global levels of H3K4 methylation. As predicted from the biochemical studies, we found substantially increased levels of H3K4 monomethylation and dimethylation in $dLsd1^{\Delta N}$ homozygous mutant adult flies compared with wild type, whereas the global levels of H3K4 trimethylation were unchanged in these mutants. Mutation of *Lid*, as expected, impacted H3K4 di- and trimethylation and, most likely through an indirect mechanism, also resulted in higher H3K4 monomethylation levels. Consistent with their function as H3K4 demethylases, the combined mutation of *dLsd1* and *Lid* resulted in a significant increase in mono-, di-, and tri-H3K4 methylation in adult flies, while the global level of H3 acetylation was not affected (Fig. 2A).

To attest that methylation changes occur on H3 loaded on chromosomes, and to visualize these changes on the genome, we examined the effect of combined mutation of *Lid* and *dLsd1* on the levels of H3K4 dimethylation by immunostaining polytene chromosomes dissected from larvae. This staining showed a general increase of H3K4 dimethylation in double-mutant flies compared with the wild-type counterparts (Fig. 2B–G), while the levels of H3 are similar in all of the genotypes analyzed (Supplemental Fig. S3). Thus, the less severe phenotype of double-mutant flies is associated with a higher overall level of H3K4 methylation throughout the genome.

dLsd1 and Lid antagonistically control heterochromatin spreading in PEV

The apparent contradiction between biochemical and genetic data is very intriguing: The biochemical data,

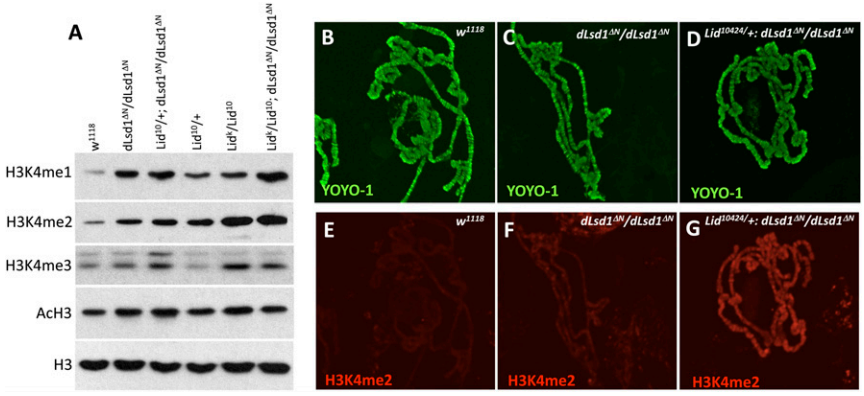

Figure 2. *dLsd1* and *Lid* mutations cooperatively increase the global level of histone H3K4 methylation. (*A*) Increase in histone H3K4 methylation level in double-mutant adult flies. Immunoblots of wild-type (wt) versus HDM mutant lysates from adult flies were probed with antibodies specific for mono-, di-, and trimethyl H3K4 and pan-acetyl H3; anti-H3 was used as a loading control. (*B–G*) H3K4 methylation levels are increased in polytene chromosomes of double mutants. Staining of polytene chromosome with an antibody specific for H3K4me2 (red) and with YOYO-1 (green). Reduced levels of Lid in combination with loss of dLsd1 results in a chromosome-wide increase in H3K4me2 levels.

showing a global increase of H3K4 methylation in the double mutants, suggest that Lid and dLsd1 cooperate, whereas the less severe phenotype of *dLsd1* mutants in a heterozygous *Lid* background indicates that the two proteins can also function antagonistically.

To understand the basis for this antagonism, we initially investigated how the combined mutation of *Lid* and *dLsd1* affects chromatin homeostasis. First, we examined the effects of these mutations on PEV. PEV is the mosaic pattern of gene silencing observed as the consequence of an abnormal juxtaposition of a gene next to a segment of heterochromatin. A prototypical example of PEV involves the *Drosophila white* gene (*w*). *white* is normally located at the distal tip of the X chromosome and is expressed in every ommatidium of the eye, resulting in a red eye phenotype. In w^{m4} mutants, a chromosomal inversion places *white* next to pericentric heterochromatin, resulting in mosaic expression of the *white* gene and patches of red and white tissue (Schotta et al. 2003).

dLsd1 has been implicated in the regulation of heterochromatin gene silencing on the basis of its function as a strong suppressor of PEV (Di Stefano et al. 2007; Rudolph et al. 2007). While *dLsd1* mutation dominantly suppresses variegation in a w^{m4h} background (Fig. 3; Di Stefano et al. 2007; Rudolph et al. 2007), *Lid* mutation, surprisingly, was shown to enhance variegation of the *white* locus (Fig. 3; Lloret-Llinares et al. 2008). This indicates opposing functions of dLsd1 and Lid in PEV regulation, and suggests a role for Lid in maintaining transcriptionally competent chromatin states at heterochromatin–euchromatin boundaries. Based on these findings, we hypothesized that reducing the level of Lid in a *dLsd1* heterozygous mutant background might restore heterochromatin formation and contribute to the suppression of *dLsd1* mutant phenotypes. To test this hypothesis, we determined the effects of *Lid; dLsd1* double mutants on w^{m4h} variegation. In accordance with our hypothesis, mutation of *Lid* suppressed the effect of *dLsd1* mutation on PEV, suggesting that Lid and dLsd1 act in an antagonistic manner in heterochromatin gene silencing. To investigate the transcriptional status of the *white* gene in these mutant flies, we measured its expression in the heads by RT-qPCR analysis. We found that *white* expression is down-regulated in w^{m4h}*; Lid* mutants and up-regulated in w^{m4h}*; dLsd1* mutants, while in double mutants its expression is more similar to wild-type levels (Fig. 3G; Supplemental Fig. S4), indicating that the positive role of dLsd1 in heterochromatin gene silencing is indeed opposed by Lid. Interestingly, the expression of the genes neighboring the *w* locus was only marginally affected by *dLsd1* and *Lid* mutations, suggesting differences in the response to expansion or contraction of heterochromatin by different genes, with *white* being the most responsive in the head tissues.

To test whether this effect on heterochromatin gene silencing is limited to the pericentric chromatin of the

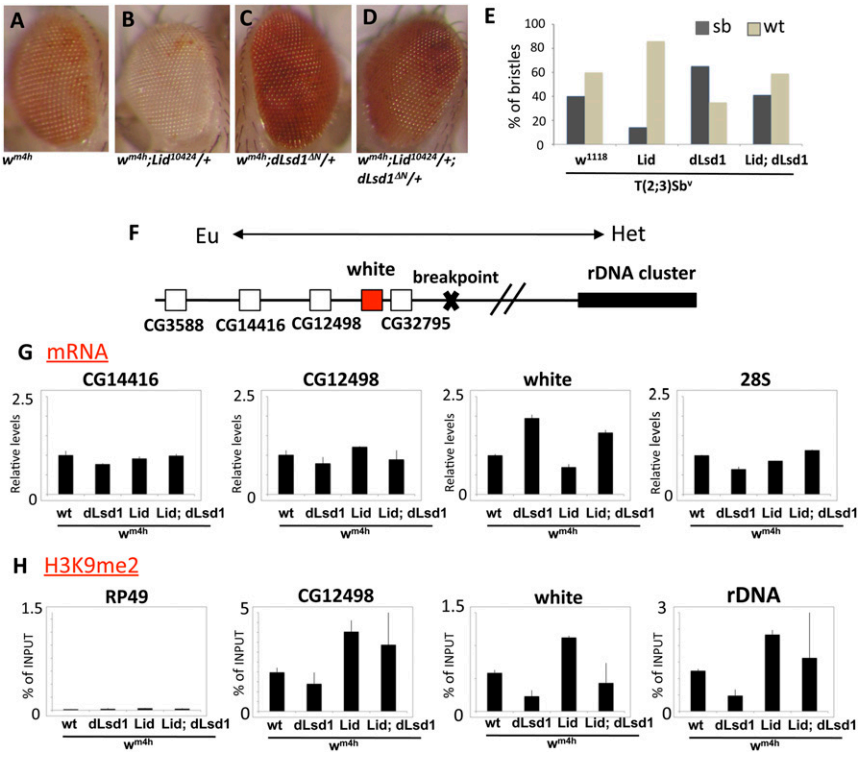

Figure 3. Lid and dLsd1 antagonistically control heterochromatin spreading in PEV. (*A–D*) The effect of a reduced dosage of Lid and dLsd1 on w^{m4h} variegation compared with control flies is shown. Reducing the dosage of dLsd1 results in suppression of variegation (*B*), while reducing the levels of Lid results in enhancement (*C*); combined reduction of Lid and dLsd1 dosage has a minimal effect on variegation (*D*). (*E*) The effect of a reduced dosage of Lid and dLsd1 on $T(2;3)Sb^{v}$ variegation compared with control flies is shown. The effect was quantified by counting the number of stubble and wild-type bristles of the thorax. A minimum of 380 bristles per genotype was counted. (*F*) A schematic representation of the white locus at the w^{m4} inversion is shown. (*G*) *dLsd1* and *Lid* mutations have opposite effects on *white* gene expression. Reducing the levels of dLsd1 results in increased expression of the *white* gene, while reducing the levels of Lid results in decreased expression as compared with wild-type flies. Combined reduction of Lid and dLsd1 dosage results in an intermediate effect compared with single mutants. (*H*) dLsd1 and Lid control H3K9 methylation levels at the *white* locus. ChIP analysis of H3K9me2 levels along the w^{m4h} inverted region. Reducing the levels of dLsd1 results in decreased levels of H3K9me2 at the *white* locus, while reducing the levels of Lid results in increased H3K9me2, and a combined reduction of Lid and dLsd1 dosage results in levels of H3K9me2 comparable with wild-type flies.

X chromosome or whether it is a more general effect, we measured the effect on PEV using the *T(2;3)Sb*^{v} translocation. In these flies, the *Stubble* (*Sb*) mutation is juxtaposed to the centric heterochromatin of the second chromosome, resulting in mosaic flies with both stubble and normal bristles (Sinclair et al. 1983; Schotta et al. 2004). When *T(2;3)Sb*^{v} was crossed to *dLsd1*$^{\Delta N}$, we observed a significant increase in the frequency of stubble bristles, indicating a suppression of variegation, while *Lid* mutation resulted in a decreased number of stubble bristles, consistent with an enhancement of PEV. We also found that combinatorial mutation of *Lid* and *dLsd1* restored the number of stubble bristles to the wild-type level (Fig. 3E). The general effect on PEV illustrates the crucial requirement of Lid and dLsd1 for heterochromatin homeostasis, and suggests that Lid and dLsd1 affect heterochromatin antagonistically, possibly by controlling the status of histone methylation at heterochromatin–euchromatin boundaries.

Heterochromatin is characterized by elevated H3K9 methylation levels, and the main histone methyltransferase responsible for H3K9 methylation at pericentric chromatin is Su(var)3–9 (Peters et al. 2003; Ebert et al. 2004). dLsd1 has been shown to physically associate with Su(var)3–9 and to control Su(var)3–9-dependent spreading of H3K9 methylation along euchromatin (Rudolph et al. 2007). To study the effects of *Lid* mutation and of the combinatorial mutation of *Lid* and *dLsd1* on H3K9 methylation at the boundary between euchromatin and heterochromatin, we performed chromatin immunoprecipitation (ChIP) for H3K9me2 across the locus of the *w*^{m4h} rearrangement. In *w*^{m4h}, the *white-rough-est* region is located next to pericentric heterochromatin, and variable spreading of H3K9 methylation results in heterochromatization and silencing of the genes located in this region. As reported previously, reducing the dosage of wild-type *dLsd1* results in a significant decrease of H3K9me2 levels across the *white-rough-est* region (Fig. 3H; Rudolph et al. 2007). Consistent with the classification of *Lid* as an enhancer of variegation (Lloret-Llinares et al. 2008), we observed that reducing the dosage of *Lid* substantially increased the levels of H3K9me2 along the *white-rough-est* locus. Interestingly, reducing the dosage of both Lid and dLsd1 had no significant effect on H3K9me2 (Fig. 3H). An opposite effect is seen on the levels of H3K4me1 along the *white-rough-est* locus; *dLsd1* mutants show high levels of H3K4me1, while *Lid* mutants exhibit a decrease in H3K4me1, and, in the double mutants, the levels are comparable with wild-type flies (Supplemental Fig. S5). The levels of H3K4me2 and H3K4me3 are negligible along this locus, and therefore do not seem to play a role in this process (Supplemental Fig. S5).

Taken together, these findings suggest that Lid is required to block dLsd1-mediated H3K4me1 demethylation and oppose Su(var)3–9-mediated spreading of H3K9me2 into euchromatin. Interestingly, at the boundaries between euchromatin and heterochromatin, the effect of Lid on the spreading of H3K9me2 is far more evident than any effect on the levels of H3K4me2 and H3K4me3.

Lid mutation results in increased levels of Su(var)3–9-dependent H3K9 methylation

To determine whether the spreading of heterochromatin observed in *Lid* mutants is dependent on Su(var)3–9, we combined *w*^{m4} with *Lid* and *Su(var)3–9* mutant alleles. Reducing the dosage of Su(var)3–9 abolished the enhancement of variegation observed in *Lid* mutants alone (Fig. 4A–H). This result suggests that Lid is required to oppose Su(var)3–9 histone methyltransferase activity and prevent Su(var)3–9-dependent spreading of heterochromatin into neighboring euchromatic regions. If this interpretation is correct, then we would expect to see an increased bulk level of H3K9 methylation in the *Lid* mutants compared with wild-type flies. Evaluation of bulk H3K9 methylation levels by immunoblot analysis in *Lid*^{10424} homozygous and heterozygous flies revealed a significant increase in H3K9me2 levels compared with wild-type flies, while intermediate levels of H3K9me2 were observed in double mutants for Lid and dLsd1 (Fig. 4I; Supplemental Fig. S6).

We then evaluated the distribution of H3K9me2 in salivary gland polytene chromosomes from third instar larvae. Immunostaining for H3K9me2 revealed that the increase in H3K9 methylation levels in *Lid* mutants is observed predominantly at the chromocenter, where pericentric heterochromatin is located. As reported previously (Rudolph et al. 2007), *dLsd1* mutation resulted in decreased levels of H3K9me2 at the chromocenter, and we found that, in double mutants for *Lid* and *dLsd1*, the levels of H3K9me2 were comparable with those of wild-type flies (Fig. 4J–Q). Taken together, these results demonstrate that Lid and dLsd1 have opposite effects on the extent of H3K9 methylation, and have a significant impact on the spreading of heterochromatin at boundaries between euchromatin and heterochromatin. While Lid opposes the spreading, dLsd1 facilitates it, and, consequently, the combined mutation of *Lid* and *dLsd1* restores the status quo by artificially resetting the balance between these two opposing activities.

Of the 450 genes predicted to be located in heterochromatic regions, ~100 have been mapped to the heterochromatin of chromosome 2 (Hoskins et al. 2002; Corradini et al. 2003; Yasuhara et al. 2003). To rule out the possibility that the effects of Lid and dLsd1 on gene expression at chromatin boundaries is limited to the artificial PEV chromosomal context, we selected several genes located in either the heterochromatic region of chromosome 2R or the proximal euchromatic region, and determined their expression levels in wild-type, *dLsd1* mutant, and *Lid; dLsd1* mutant flies. Consistent with the derepression of the *white* gene in PEV upon *dLsd1* mutation, we observed derepression of many genes located at the boundary between euchromatin and heterochromatin in *dLsd1* mutants (Fig. 5; Supplemental Table S4). Reducing the dosage of Lid abolished this effect (Fig. 5), supporting the idea that Lid and dLsd1 indeed have antagonistic roles in the control of gene expression at chromatin boundaries. Interestingly, *dLsd1* mutation also results in a reduction of expression levels of some

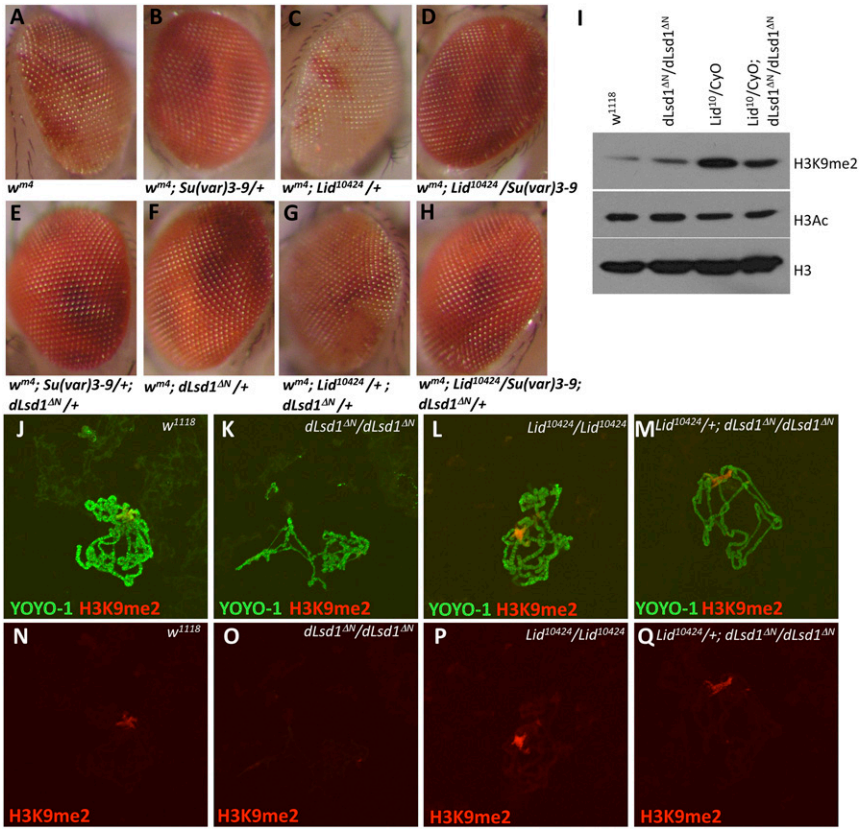

Figure 4. Enhancement of variegation due to *Lid* mutation is dependent on Su(var)3–9 dosage, and *Lid* mutation results in increased levels of H3K9 methylation. (*A–H*) The enhancer effect of *Lid* mutation on white variegation in w^{m4} is suppressed by reduction of Su(var)3–9 dosage. (*I*) H3K9 methylation levels are globally increased in *Lid* mutants. Immunoblot analysis of global levels of H3K9me2 in adult males of the indicated genotypes. Total histone H3 and acetyl-H3 levels are shown. (*J–Q*) H3K9 methylation levels are increased at the chromocenter of polytene chromosomes in mutants for the *Lid* allele. The *top* panel shows the staining of polytene chromosomes with an antibody specific for H3K9me2 (red) and with YOYO-1 (green), whereas the *bottom* panel shows anti-H3K9me2 staining alone. *dLsd1* mutation results in reduced levels of H3K9me2 at the chromocenter, while *Lid* mutation results in an increase of H3K9me2 at the chromocenter compared with w^{1118}. Reduced levels of Lid in combination with loss of dLsd1 results in H3K9me2 levels comparable with wild-type flies.

heterochromatic genes compared with wild type, a phenotype that was not rescued by *Lid* mutation. Downregulation of heterochromatic genes was observed previously in larvae carrying a mutation for an important determinant of *Drosophila* heterochromatin, HP1 (Lu et al. 2000), suggesting that HP1 might be required for proper expression of genes residing in heterochromatin. Our results suggest that dLsd1 might have a similar role. Taken together, these data show that dLsd1 is required for the silencing of some genes located at the euchromatin/heterochromatin boundaries, and that Lid opposes dLsd1 function in this context.

dLsd1 directly regulates the expression of a subset of Notch target genes

Histone H3K4 methylation is highly enriched in euchromatin and is generally associated with active transcription. Since the spreading of H3K9 methylation was the key parameter in the interaction between Lid and dLsd1 at euchromatin/heterochromatin boundaries, we reasoned that the interplay between Lid and dLsd1 in the control of gene expression might be different at euchromatic loci where H3K9 methylation is not so paramount.

Recently, the Verrijzer laboratory (Moshkin et al. 2009) reported that Lid is involved in silencing of genes regulated by the Notch signaling pathway. To determine whether dLsd1 plays a role in the control of Notch target gene expression, we used RT-qPCR to compare the expression level of *E(spl)* Notch target genes in *dLsd1* homozygous mutant flies with wild-type controls. The results showed a clear derepression of E(spl)m4, E(spl)m6, E(spl)m7, and E(spl)m8 genes in *dLsd1* mutant flies (Fig. 6A). To test whether dLsd1 directly regulates E(spl) genes, we performed ChIP analysis with an antibody specific for dLsd1 and examined binding to the E(spl)m4, E(spl)m6, E(spl)m7, and E(spl)m8 enhancers and promoters in

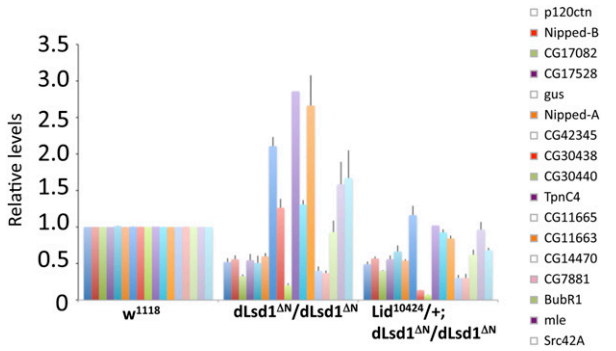

Figure 5. Increased expression of genes at the 2R euchromatin–heterochromatin boundary in *dLsd1* mutant flies. RT-qPCR analysis of the expression of the indicated genes in w^{1118} (wild-type), *dLsd1* mutant, and *Lid* and *dLsd1* double mutant ovaries is shown. The expression level is normalized against the w^{1118}, wild-type control. Experiments were performed in triplicate, and error bars indicate standard error of the mean. Supplemental Table S4 displays the sequence coordinates and the position on the cytogenetic map of each of the genes used in this expression analysis.

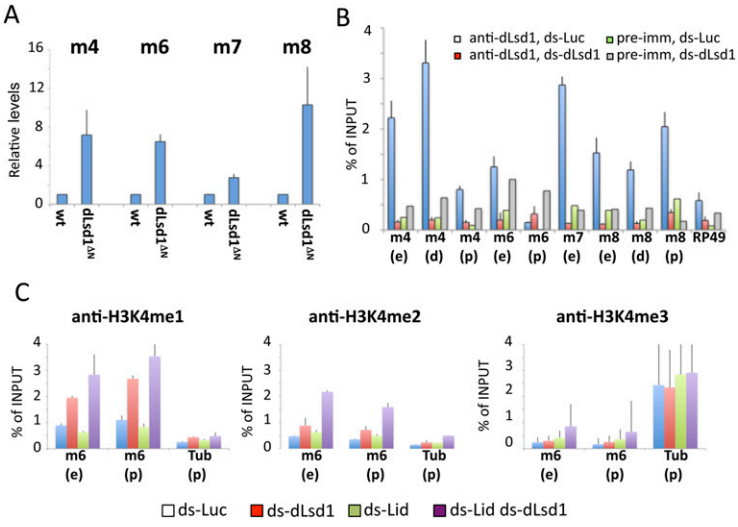

Figure 6. dLsd1 directly regulates Notch target gene expression by controlling histone methylation levels. (*A*) dLsd1 is required for repression of Notch target genes. RT-qPCR analysis of the expression of E(spl) genes in w^{1118} (wild-type, wt) and *dLsd1* mutant flies. The expression level is normalized against the w^{1118}, wild-type control. Experiments were performed in triplicate, and error bars indicate the standard error of the mean. (*B*) dLsd1 binds directly to the E(spl) locus. ChIP analysis of dLsd1 binding across the E(spl) locus using an anti-dLsd1-specific antibody in S2 cells incubated with dsRNA against Luciferase (mock) and dLsd1 to control for specificity. Preimmune serum was used as an additional control for specificity. ChIP data are the result of three independent immunoprecipitations. Error bars indicate standard deviation. Each gene is represented by two or three fragments: enhancer (e), distal (d), and proximal (p) to the transcriptional start site. (*C*) dLsd1 and Lid cooperatively control histone methylation levels at Notch target genes. Cross-linked chromatin was isolated from S2 cells incubated with dsRNA against the indicated mRNAs, and ChIP analysis was performed using antibodies specific for H3K4me1, H3K4me2, and H3K4me3. Error bars indicate standard deviation.

Drosophila S2 cells where these genes are repressed. Consistent with the in vivo gene expression data, dLsd1 binds strongly to the E(spl) locus. The dLsd1 ChIP signal was measured by comparison with preimmune serum and was absent at an unrelated control gene (RP49) (Fig. 6B). Additional confirmation of the specificity of the signal was provided by experiments showing that the ChIP signal was lost when dLsd1 was depleted using dsRNA. These data indicate that dLsd1 binds directly to the E(spl) locus and, like Lid, represses the expression of Notch target genes.

Because dLsd1 is an H3K4 demethylase, we asked whether dLsd1 might silence Notch target gene expression by directly demethylating H3K4me1 and H3K4me2. Depletion of dLsd1 in S2 cells by dsRNA resulted in increased levels of H3K4me1 and H3K4me2 at the m6 promoter and enhancer region but not at the tubulin promoter, used as a control (Fig. 6C). Consistent with our immunoblot analysis and polytene chromosome staining, upon double depletion of dLsd1 and Lid, we observed a greater increase in H3K4me1 and H3K4me2 compared with single depletions and an increase in H3K4me3 (Fig. 6C). The elevated methylation levels are accompanied by derepression of m6 expression in S2 cells upon single and double depletion of dLsd1 and Lid (Supplemental Fig. S7).

These results suggest that both dLsd1 and Lid suppress the expression of Notch target genes by removing H3K4 methyl marks associated with active transcription at E(spl) regulatory elements. In cells where Notch targets are repressed, dLsd1 and Lid seem to act synergistically, and their interaction is different from the antagonism seen at euchromatin–heterochromatin boundaries.

dLsd1 genetically interacts with the Notch signaling pathway

To determine whether the levels of Notch signaling make a functionally significant contribution to the *dLsd1* mutant phenotype, we examined the effect of introducing heterozygous mutation for $Su(H)^{05}$, the transcriptional mediator of Notch signaling, into flies that were homozygous for $dLsd1^{\Delta N}$. Remarkably, the results show that $Su(H)^{05}$ dominantly suppressed the oogenesis defects of $dLsd1^{\Delta N}/dLsd1^{\Delta N}$ mutant flies (Fig. 7A–C). We infer not only that dLsd1 is present at Notch target genes, but also that altered regulation of Notch signaling is a very important component of the *dLsd1* mutant phenotype. Indeed, we noticed the presence of other phenotypes in *dLsd1* homozygous mutants, which have been associated with mutations in the Notch pathway, such as veins broadened into deltas at the wing junction margins (Fig. 1A; Supplemental Fig. S8). As expected from the evidence that dLsd1 contributes to the repression of Notch targets, heterozygous mutations in *dLsd1* suppress the dominant wing notching associated with loss-of-function alleles of *Notch* (P Mulligan, F Yang, L Di Stefano, J Ji, J Nishikawa, Q Wang, M Kulkarni, H Najafi-Shoushtari, R Mostosvalsky, S Gygi, et al., in prep.).

More extensive genetic tests revealed that Lid and dLsd1 differ in their interaction with the Notch pathway. When we crossed *dLsd1* mutants to gain-of-function alleles of Notch (Abruptex; Ax^{E2} and Ax^{16}), we noted that *dLsd1* alleles failed to enhance the L4 and/or L5 wing defects of the *Ax* alleles, as observed with *Lid* mutant alleles (Fig. 7D–G; quantification in Supplemental Table S5–S7), and as would be expected if dLsd1 solely repressed Notch target genes. Instead, mutant alleles of *dLsd1* suppressed the Abruptex phenotype. This indicates that, in the context of a hyperactive Notch signaling pathway, dLsd1 contributes positively to the activation of Notch targets. To test this idea, we measured the expression of E(spl) genes in Ax^{E2} hemizygous mutants. Consistent with our hypothesis, we found that these targets are up-regulated in hemizygous Ax^{E2} mutants, and that the effect of heterozygous mutation of *dLsd1* is to restore wild-type levels of gene expression (Fig. 7I; Supplemental Fig. S9).

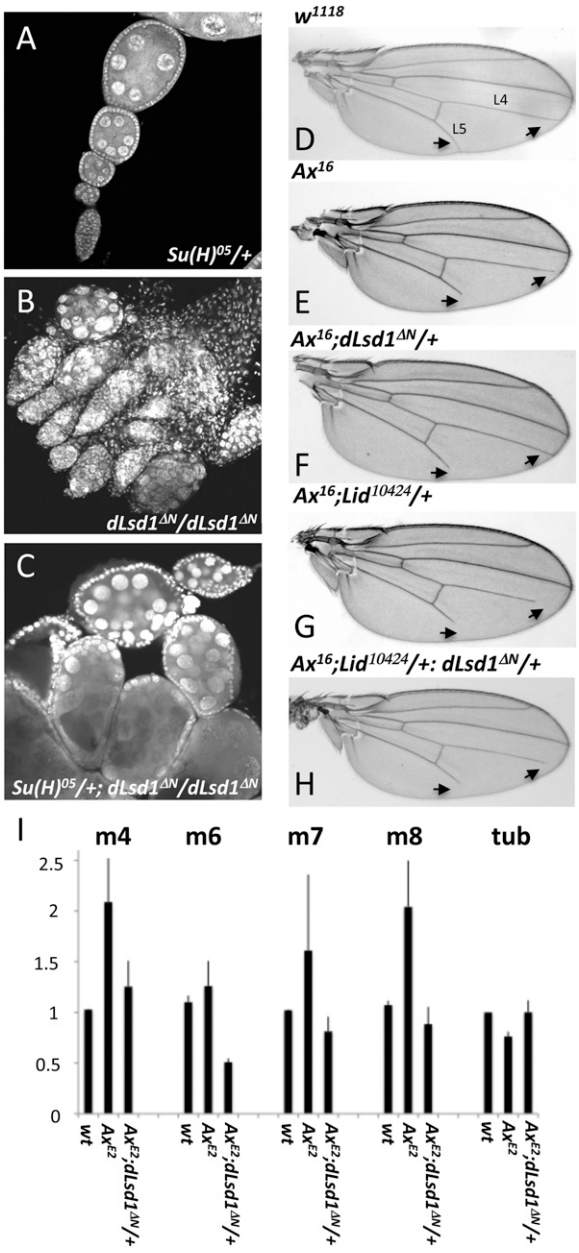

Figure 7. *dLsd1* genetically interacts with various components of the Notch signaling pathway. (*A–C*) $Su(H)^{05}$ partially suppresses the oogenesis defect in *dLsd1* homozygous mutant flies. (*D–H*) *dLsd1* mutation suppresses truncations of the L4 and L5 wing veins in flies heterozygous for the Ax^{16} gain-of-function *Notch* mutation, while *Lid* mutation enhances it. Shown are representative examples of wings of the indicated genotypes; arrows mark the distal part of L4 and L5 wing veins where the phenotype is evident. (*I*) dLsd1 is required for activation of Notch target genes. RT-qPCR analysis of the expression of E(spl) genes in w^{1118} (wild-type, wt), Ax^{E2}, and Ax^{E2}, *dLsd1* heterozygous mutant males. The expression level is normalized against the w^{1118}, wild-type control. Experiments were performed in triplicate, and error bars indicate standard error of the mean.

We infer that, in cells where Notch is inactive, such as S2 cells, Lid and dLsd1 act cooperatively to keep Notch target genes repressed. However, in the context of activated Notch signaling, such as occurs in Abruptex mutants, dLsd1 switches from being a repressor to an activator, promoting the expression of these targets. Thus, in the context of activated Notch, dLsd1 acts in opposition to Lid. In support of this hypothesis, we note that the effects of mutant *Lid* and *dLsd1* alleles on *Ax* phenotypes essentially cancel one another out, and the double mutation has, in general, an intermediate effect on phenotypes associated with gain-of-function *Ax* alleles (Fig. 7H; Supplemental Table S5–S7). Taken together, these genetic studies suggest that dLsd1 has a significant, context-dependent, role in modulating Notch signaling, and that mutant alleles that act in the Notch pathway can partly suppress *dLsd1* mutant phenotypes.

Discussion

Molecular studies have identified an increasingly large number of histone-modifying enzymes, and biochemical assays readily allow these proteins to be classified, but the more difficult and more important challenge is to understand how these various enzymatic activities are integrated, in vivo, to control biological processes. We examined the effects of combining mutations in the two H3K4 demethylases *Lid* and *dLsd1* in *Drosophila*. Our studies, performed in vivo, show that the interplay between Lid and dLsd1 is dependent on the chromatin context and active signaling pathways. Our results show a consistent pattern of genetic interactions between Lid and dLsd1 that is evident in multiple tissues and phenotypes. Unexpectedly, despite their activity as histone H3K4 demethylases, these proteins function antagonistically in a number of functional and developmental contexts. For example, dLsd1 and Lid have opposing functions in the establishment of euchromatin and heterochromatin boundaries. At these locations, the antagonism does not seem to stem from the effects of Lid on H3K4 methylation, but rather from its indirect effects on the spreading of H3K9me2. In addition, while our data show that both Lid and dLsd1 can repress Notch targets within euchromatin when Notch signaling is not active, and that Notch signaling is an important component of the *dLsd1* mutant phenotype, genetic evidence supports the hypothesis that Lid and dLsd1 have antagonistic functions in the context of activated Notch signaling. This complex pattern of interactions illustrates that the functional interplay between demethylases, and most likely between other types of chromatin-associated proteins, cannot be rationalized into a single generic model. The evidence that dLsd1 can switch from being a negative regulator of Notch target genes to a positive regulator adds an extra layer of complexity to the interplay between Lid and dLsd1, and strongly supports the concept that the activity of histone demethylases is highly regulated and context-dependent.

Antagonistic roles of Lid and dLsd1 at chromatin boundaries

Our genetic and biochemical data support a model for the creation and maintenance of heterochromatin boundaries,

proposed by Reuter and colleagues (Rudolph et al. 2007), in which dLsd1 promotes deacetylation of H3K9 by RPD3 and subsequent methylation of H3K9 by Su(var)3–9, thereby facilitating spreading of heterochromatin. In addition, we show an increase in H3K4me1 at the *white-rough-est* locus in *dLsd1* mutant flies, suggesting that active demethylation of H3K4me1 by dLsd1 is an important step in the establishment of heterochromatin. Furthermore, we find that Lid antagonizes dLsd1 function by promoting euchromatin formation, and that the spreading of heterochromatin seen in *Lid* mutants is dependent on dLsd1 and Su(var)3–9 activities. Consistent with this notion, H3K9 methylation levels are increased in *Lid* mutant flies compared with control at the *white-rough-est* locus and in pericentric heterochromatin. Interestingly, the levels of H3K4me2 and H3K4me3 at the *white-rough-est* locus are very low and increase only marginally upon *Lid* mutation, suggesting that Lid function in this context is independent of its histone H3K4 demethylase activity. Previously, Lid had been reported to facilitate activation of Myc target genes in a demethylase-independent manner (Secombe et al. 2007), and to antagonize Rpd3 histone deacetylase function (Lee et al. 2009); moreover, mutation of *Lid* has been shown to cause a decrease of H3K9 acetylation levels (Lloret-Llinares et al. 2008). It is therefore tempting to speculate that Lid opposes the spreading of heterochromatin, independent of its function as a histone H3K4 demethylase, by antagonizing the activity of the dLsd1/Su(var)3–9/Rpd3 complex. This antagonism would explain why, in double mutants for *dLsd1* and *Lid*, the balance between euchromatin and heterochromatin is artificially reset to wild-type levels. Consistently, reorganization of chromatin domains observed in *dLsd1* mutant flies affects the expression of genes located at the 2R euchromatin–heterochromatin boundary, an effect that is reversed by mutation of *Lid*.

dLsd1 is a modulator of the Notch signaling pathway

Given the predominant presence of H3K4 methylation in euchromatin and its important role in determining the transcription status of a gene, we were interested in establishing the nature of the interplay between Lid and dLsd1 in a euchromatic context. Previous studies had implicated Lid as a crucial factor in the silencing of Notch target genes (Moshkin et al. 2009). Our study shows a cooperative role for Lid and dLsd1 in repressing Notch target gene expression, and suggests that they contribute to repression by maintaining low levels of H3K4 methylation. Repression of Notch target genes is essential for the establishment of Notch-inhibited cell fates (Fiuza and Arias 2007), suggesting that Lid and dLsd1 could play a role in proper cell fate specification during *Drosophila* development. Interestingly, the role of dLsd1 does not seem to be limited to repression of Notch target genes. Indeed, our genetic analysis suggests that, in a context in which the Notch signaling pathway is active, dLsd1 switches from a repressor to an activator role. Such a dual role had already been described for Su(H), whose switch from a repressor to an activator has been suggested to be mediated through an exchange of associated proteins (Bray 2006). Similarly, in mammalian cells, studies have shown that LSD1 activity can be modulated by changes in composition of the complexes present at the Gh promoter, and, depending on the cell type (somatotroph or lactotroph), LSD1 can act as either an activator or a repressor (Wang et al. 2007). Therefore, a possible explanation for our data is that, depending on the complexes available, dLsd1 can switch from being a repressor to acting as an activator of Notch target genes. Alternatively, *dLsd1* mutation could promote derepression of negative regulators of Notch activity, or could directly modulate Notch activity by demethylating crucial components of the Notch-activating complex. Further studies are required to distinguish between these possibilities.

These results provide the basis for future studies aimed at investigating whether the dual role of dLsd1 in modulating Notch signaling is conserved in mammals. In mice, LSD1 has been shown to repress the Notch target *Hey1* in late stages of pituitary development (Wang et al. 2007), suggesting that its ability to regulate Notch target genes is conserved. This pathway-specific function of LSD1 could potentially be exploited to create novel strategies to manipulate Notch-mediated carcinogenesis.

Collectively, these results reveal an intricate interplay between the histone demethylases Lid and dLsd1 in the control of higher-order chromatin structure at euchromatin and heterochromatin boundaries affecting developmental gene silencing. They also demonstrate an involvement of dLsd1 and Lid in Notch pathway-specific control of gene expression in euchromatin, and support the idea that, depending on the context, Lid and dLsd1 can favor either transcriptional activation or transcriptional repression.

Materials and methods

Genetic analysis

The following fly stocks were obtained from the Bloomington stock collection: lid^{10424}, lid^{k06801}, $ash2^{EY03971}$, osa^{2}, brm^{2}, mor^{1}, $Snr1^{01319}$, Trl^{s2325}, esc^{1}, kis^{13416}, *Canton S*, w^{1118}, $T(2;3)Sb^{v}$, $In(1)w^{m4h}$, and $In(1)w^{m4}$; $Su(var)3–9^{1}$. brm^{1}, brm^{5}, osa^{1}, mor^{2}, and mor^{6} alleles were kindly provided by Dr. James Kennison. $Bap180^{\Delta 86}$ and $Bap170^{\Delta 65}$ alleles were kindly provided by Dr. Jessica Treisman. Psc^{h28} and $Su(z)2^{4}$ were kindly provided by Dr. Chao Ting Wu. Ax^{E2}, Ax^{16}, and $Su(H)^{05}$ were kindly provided by Dr. Spyros Artanavis-Tsakonas. Flies were grown on standard *Drosophila* medium and maintained at 25°C. Recombination of the $dLsd1^{\Delta N}$ allele with other third chromosome mutants was performed by standard means. Candidate recombinant lines were verified by testing for noncomplementation crosses with other alleles, or by using allele-specific PCR assays. The held-out wings phenotype was scored if flies had both wings extended. We categorized the rescue of the $dLsd1^{\Delta N}$-dependent oogenesis defects into moderate and weak rescues. The moderate and weak descriptors were used for those lines that showed some degree of structural organization compared with *dLsd1* mutant ovaries. For the $ISWI^{K159R}$ interaction test, *yw; eyGAL4; UAS-*$ISWI^{K159R}$*/T(2:3)* virgins were crossed with the $dLsd1^{\Delta N}$*/TM3*. The F1 progeny that did not carry any balancer were scored based on the severity of eye phenotype, as in Burgio et al. (2008). The effect

of *dLsd1* and *Lid* mutations on white variegation was studied by crossing females homozygous for the *In(1)w^{m4h}* allele with males heterozygous for *dLsd1* and *Lid* mutations. The effects on eye color variegation of the male progeny were quantified by measuring the relative expression of the *white* gene and by observing the relative red eye pigment content. The effects on stubble variegation were studied by crossing females heterozygous for the *T(2;3)Sb^{v}* allele with males heterozygous for *dLsd1* and *Lid* mutations. The effect was quantified by counting the number of stubble and wild-type bristles. The bristles examined were the dorsocentral, anterior scutellar, and posterior scutellar.

Immunostaining

Immunostaining of *Drosophila* ovaries was performed as described in Di Stefano et al. (2007). Ovaries were stained with Rhodamine-Phalloidin (Molecular Probes) and the following antibodies: anti-Fasciclin III (7G10), anti-spectrin (3A9), and anti-ORB (4H8), obtained from the Developmental Studies Hybridoma Bank. DNA was stained using YOYO-1 iodide (Molecular Probes), and ovaries were mounted for confocal microscopic imaging.

For immunostaining of polytene chromosomes, salivary glands were dissected from third instar larvae. Glands were fixed in solution 2 (3.7% formaldehyde, 1% Triton X-100/PBS at pH 7.5) and squashed in solution 3 (3.7% formaldehyde, 50% acetic acid). Chromosomes were incubated overnight at 4°C with either anti-H3K9me2 (ab1220), anti-H3 (ab1791), or anti-H3K4me2 (ab32356), followed by incubation with Cy3-conjugated secondary antibody (Molecular Probes) for 2 h at 4°C. To stain the DNA, the chromosomes were incubated with YOYO-1 iodide (Molecular Probes) for 10 min at room temperature. Preparations were examined with confocal laser-scanning microscopy. The levels of histone methylation in wild-type and mutant polytene chromosomes were compared by processing and analyzing the samples in the same experiment under identical conditions, and pictures were taken using identical exposure times (Srinivasan et al. 2005). Multiple polytene chromosomes from at least three squashes were analyzed, and representative examples are shown.

Real-time qPCR

Total RNA was prepared using Trizol (Invitrogen). RT–PCR was performed using TaqMan Reverse Transcription reagents (PE Applied Biosystems) according to the instructions provided by the manufacturer. Real-time qPCR was performed using the Roche LightCycler 480 system. Relative levels of specific mRNAs were determined using the SYBR Green I detection chemistry system (Roche). Quantification was performed using the comparative C_T method as described in the manufacturer procedures manual. RP49 was used as normalization control. Primer sequences are available on request.

ChIP

Flies were fixed in 1.8% formaldehyde for 15 min at room temperature, resuspended in lysis buffer (140 mM NaCl, 15 mM HEPES at pH 7.6, 1 mM EDTA, 0.5 mM EGTA, 1% Triton X-100, 0.5 mM DTT, 0.1% sodium deoxycholate, 0.05% SDS, 0.5% N-lauroylsarcosine, protease inhibitors), and lysed by sonication. The lysates were cleared by centrifugation, preabsorbed by incubation with protein G and A sepharose beads (GE Healthcare), and incubated overnight at 4°C with 2 μg of one of the following antibodies: anti-H3 (ab1791), anti-H3K4me1 (ab8895), anti-H3K4me2 (ab32356), anti-H3K4me3 (ab8580, ab1012), or anti-H3K9me2 (ab1220), and 8 μL of anti-dLsd1 (described in Di Stefano et al. 2007). Antibody complexes were recovered with a mixture of protein A and G sepharose. After extensive washes, immunocomplexes were eluted from the beads and cross-link-reversed, and the DNA was recovered by phenol/chloroform extraction and ethanol precipitation. DNA was resuspended in 150 μL of water, and 7.5 μL was used for real-time qPCR reactions.

S2 cells were fixed in 1.8% formaldehyde for 15 min at room temperature, resuspended in hypertonic buffer A (300 mM sucrose, 2 mM Mg acetate, 3 mM $CaCl_2$, 10 mM Tris at pH 8.0, 0.1% Triton X-100, 0.5 mM DTT), incubated for 5 min on ice, and dounced 20 times with a dounce homogenizer (tight pestle, Wheaton). Nuclei were collected by centrifuging at 720*g* for 5 min at 4°C. The pellets were washed twice in buffer A and then resuspended in buffer D (25% glycerol, 5 mM Mg acetate, 50 mM Tris at pH 8.0, 0.1 mM EDTA, 5 mM DTT). Chromatin was collected by centrifuging at 720*g* for 5 min at 4°C. The pellets were washed twice in buffer D and then resuspended in buffer MN (60 mM KCl, 15 mM NaCl, 15 mM Tris at pH 7.4, 0.5 mM DTT, 0.25 M sucrose, 1.0 mM $CaCl_2$). Nuclei were digested with 100 U of MNase (USB) and diluted in buffer MN for 30 min at room temperature. Reactions were stopped with the addition of EDTA and SDS to final concentrations of 12.5 mM and 0.5%, respectively. The samples were then processed for ChIP as described above.

Cell culture and dsRNA

S2 cells were cultured at 25°C in Schneider's insect medium (Sigma; 10% fetal bovine serum) and treated with dsRNA as described (Stevaux et al. 2002).

Immunoblot analysis and antibodies

Protein extracts were obtained by acid extraction. Briefly, flies were resuspended in lysis buffer (50 mM Tris at pH 8.0, 0.4% NP40, 300 mM NaCl, 10 mM $MgCl_2$, 0.5 mM DTT, 1.5 mM PMSF) and homogenized using a douncer with type A pestle. Lysates were incubated with 0.2 M HCl for 2 h on ice. Lysates were then centrifuged and the supernatant was dialyzed overnight using Slide-a-Lyser cassettes (Pierce) according to the manufacturer's procedure. Immunoblots were performed using standard procedures. The blots were probed using antibodies specific for anti-H3 (ab1791), anti-H3K4me1 (ab8895), anti-H3K4me2 (ab32356), anti-H3K4me3 (ab8580), anti-H3K9me2 (ab1220), and anti-acetyl-H3 (Millipore, #06-599).

Acknowledgments

We thank Dr. Spyros Artanavis-Tsakonas, Dr. James Kennison, Dr. Jessica Treisman, and Dr. Chao Ting Wu for providing fly stocks, and members of the Dyson laboratory for technical assistance and helpful discussion. We thank Dr. Kristian Helin for critical reading of the manuscript. This study was supported by NIH grants GM81607, GM53203, and CA64402 to N.J.D., and GM071449 to A.M.N. L.D.S. was supported by a fellowship from the Leukemia and Lymphoma Society. J.A.W. was supported by a grant from the DoD (W81XWH-09-1-0487). G.B. was supported by a FIRC Fellowship, and D.C. was supported by Fondazione Telethon, Giovanni Armenise Harvard Foundation, MIUR-PRIN, HFSP, AIRC, and EMBO-YIP. N.J.D. is the Saltonstall Scholar of the Massachusetts General Hospital Cancer Center.

References

Bannister AJ, Kouzarides T. 2005. Reversing histone methylation. *Nature* **436:** 1103–1106.

Bernstein BE, Kamal M, Lindblad-Toh K, Bekiranov S, Bailey DK, Huebert DJ, McMahon S, Karlsson EK, Kulbokas EJ 3rd, Gingeras TR, et al. 2005. Genomic maps and comparative analysis of histone modifications in human and mouse. *Cell* **120:** 169–181.

Bray SJ. 2006. Notch signalling: A simple pathway becomes complex. *Nat Rev Mol Cell Biol* **7:** 678–689.

Burgio G, La Rocca G, Sala A, Arancio W, Di Gesù D, Collesano M, Sperling AS, Armstrong JA, van Heeringen SJ, Logie C, et al. 2008. Genetic identification of a network of factors that functionally interact with the nucleosome remodeling ATPase ISWI. *PLoS Genet* **4:** e1000089. doi: 10.1371/journal.pgen.1000089.

Chi P, Allis CD, Wang GG. 2010. Covalent histone modifications—Miswritten, misinterpreted and mis-erased in human cancers. *Nat Rev Cancer* **10:** 457–469.

Corradini N, Rossi F, Verni F, Dimitri P. 2003. FISH analysis of *Drosophila melanogaster* heterochromatin using BACs and P elements. *Chromosoma* **112:** 26–37.

Di Stefano L, Ji JY, Moon NS, Herr A, Dyson N. 2007. Mutation of *Drosophila* Lsd1 disrupts H3-K4 methylation, resulting in tissue-specific defects during development. *Curr Biol* **17:** 808–812.

Ebert A, Schotta G, Lein S, Kubicek S, Krauss V, Jenuwein T, Reuter G. 2004. Su(var) genes regulate the balance between euchromatin and heterochromatin in *Drosophila*. *Genes Dev* **18:** 2973–2983.

Eissenberg JC, Lee MG, Schneider J, Ilvarsonn A, Shiekhattar R, Shilatifard A. 2007. The trithorax-group gene in *Drosophila* little imaginal discs encodes a trimethylated histone H3 Lys4 demethylase. *Nat Struct Mol Biol* **14:** 344–346.

Fiuza UM, Arias AM. 2007. Cell and molecular biology of Notch. *J Endocrinol* **194:** 459–474.

Heintzman ND, Stuart RK, Hon G, Fu Y, Ching CW, Hawkins RD, Barrera LO, Van Calcar S, Qu C, Ching KA, et al. 2007. Distinct and predictive chromatin signatures of transcriptional promoters and enhancers in the human genome. *Nat Genet* **39:** 311–318.

Hoskins RA, Smith CD, Carlson JW, Carvalho AB, Halpern A, Kaminker JS, Kennedy C, Mungall CJ, Sullivan BA, Sutton GG, et al. 2002. Heterochromatic sequences in a *Drosophila* whole-genome shotgun assembly. *Genome Biol* **3:** RESEARCH0085. doi: 10.1186/gb-2002-3-12-research0085.

Kirilly D, Xie T. 2007. The *Drosophila* ovary: An active stem cell community. *Cell Res* **17:** 15–25.

Krivtsov AV, Armstrong SA. 2007. MLL translocations, histone modifications and leukaemia stem-cell development. *Nat Rev Cancer* **7:** 823–833.

Lee N, Zhang J, Klose RJ, Erdjument-Bromage H, Tempst P, Jones RS, Zhang Y. 2007. The trithorax-group protein Lid is a histone H3 trimethyl-Lys4 demethylase. *Nat Struct Mol Biol* **14:** 341–343.

Lee N, Erdjument-Bromage H, Tempst P, Jones RS, Zhang Y. 2009. The H3K4 demethylase lid associates with and inhibits histone deacetylase Rpd3. *Mol Cell Biol* **29:** 1401–1410.

Liu CL, Kaplan T, Kim M, Buratowski S, Schreiber SL, Friedman N, Rando OJ. 2005. Single-nucleosome mapping of histone modifications in *S. cerevisiae*. *PLoS Biol* **3:** e328. doi: 10.1371/journal.pbio.0030328.

Lloret-Llinares M, Carre C, Vaquero A, de Olano N, Azorin F. 2008. Characterization of *Drosophila melanogaster* JmjC+N histone demethylases. *Nucleic Acids Res* **36:** 2852–2863.

Lu BY, Emtage PC, Duyf BJ, Hilliker AJ, Eissenberg JC. 2000. Heterochromatin protein 1 is required for the normal expression of two heterochromatin genes in *Drosophila*. *Genetics* **155:** 699–708.

Marenda DR, Zraly CB, Feng Y, Egan S, Dingwall AK. 2003. The *Drosophila* SNR1 (SNF5/INI1) subunit directs essential developmental functions of the Brahma chromatin remodeling complex. *Mol Cell Biol* **23:** 289–305.

Martin C, Zhang Y. 2005. The diverse functions of histone lysine methylation. *Nat Rev Mol Cell Biol* **6:** 838–849.

Moshkin YM, Kan TW, Goodfellow H, Bezstarosti K, Maeda RK, Pilyugin M, Karch F, Bray SJ, Demmers JA, Verrijzer CP. 2009. Histone chaperones ASF1 and NAP1 differentially modulate removal of active histone marks by LID–RPD3 complexes during NOTCH silencing. *Mol Cell* **35:** 782–793.

Peters AH, Kubicek S, Mechtler K, O'Sullivan RJ, Derijck AA, Perez-Burgos L, Kohlmaier A, Opravil S, Tachibana M, Shinkai Y, et al. 2003. Partitioning and plasticity of repressive histone methylation states in mammalian chromatin. *Mol Cell* **12:** 1577–1589.

Roh TY, Ngau WC, Cui K, Landsman D, Zhao K. 2004. High-resolution genome-wide mapping of histone modifications. *Nat Biotechnol* **22:** 1013–1016.

Rudolph T, Yonezawa M, Lein S, Heidrich K, Kubicek S, Schafer C, Phalke S, Walther M, Schmidt A, Jenuwein T, et al. 2007. Heterochromatin formation in *Drosophila* is initiated through active removal of H3K4 methylation by the LSD1 homolog SU(VAR)3–3. *Mol Cell* **26:** 103–115.

Schotta G, Ebert A, Dorn R, Reuter G. 2003. Position-effect variegation and the genetic dissection of chromatin regulation in *Drosophila*. *Semin Cell Dev Biol* **14:** 67–75.

Schotta G, Lachner M, Sarma K, Ebert A, Sengupta R, Reuter G, Reinberg D, Jenuwein T. 2004. A silencing pathway to induce H3-K9 and H4-K20 trimethylation at constitutive heterochromatin. *Genes Dev* **18:** 1251–1262.

Secombe J, Li L, Carlos L, Eisenman RN. 2007. The Trithorax group protein Lid is a trimethyl histone H3K4 demethylase required for dMyc-induced cell growth. *Genes Dev* **21:** 537–551.

Sinclair DAR, Mottus RC, Grigliatti TA. 1983. Genes which suppress position-effect variegation in *Drosophila melanogaster* are clustered. *Mol Gen Genet* **191:** 326–333.

Srinivasan S, Armstrong JA, Deuring R, Dahlsveen IK, McNeill H, Tamkun JW. 2005. The *Drosophila* trithorax group protein Kismet facilitates an early step in transcriptional elongation by RNA Polymerase II. *Development* **132:** 1623–1635.

Stevaux O, Dimova D, Frolov MV, Taylor-Harding B, Morris E, Dyson N. 2002. Distinct mechanisms of E2F regulation by *Drosophila* RBF1 and RBF2. *EMBO J* **21:** 4927–4937.

Trewick SC, McLaughlin PJ, Allshire RC. 2005. Methylation: Lost in hydroxylation? *EMBO Rep* **6:** 315–320.

Wang J, Scully K, Zhu X, Cai L, Zhang J, Prefontaine GG, Krones A, Ohgi KA, Zhu P, Garcia-Bassets I, et al. 2007. Opposing LSD1 complexes function in developmental gene activation and repression programmes. *Nature* **446:** 882–887.

Wysocka J, Milne TA, Allis CD. 2005. Taking LSD 1 to a new high. *Cell* **122:** 654–658.

Yasuhara JC, Marchetti M, Fanti L, Pimpinelli S, Wakimoto BT. 2003. A strategy for mapping the heterochromatin of chromosome 2 of *Drosophila melanogaster*. *Genetica* **117:** 217–226.

Disease Models & Mechanisms 4, 753-761 (2011) doi:10.1242/dmm.006908

Modeling tumor invasion and metastasis in *Drosophila*

Wayne O. Miles[1], Nicholas J. Dyson[1] and James A. Walker[1,2,*]

Conservation of major signaling pathways between humans and flies has made *Drosophila* a useful model organism for cancer research. Our understanding of the mechanisms regulating cell growth, differentiation and development has been considerably advanced by studies in *Drosophila*. Several recent high profile studies have examined the processes constraining the metastatic growth of tumor cells in fruit fly models. Cell invasion can be studied in the context of an in vivo setting in flies, enabling the genetic requirements of the microenvironment of tumor cells undergoing metastasis to be analyzed. This Perspective discusses the strengths and limitations of *Drosophila* models of cancer invasion and the unique tools that have enabled these studies. It also highlights several recent reports that together make a strong case for *Drosophila* as a system with the potential for both testing novel concepts in tumor progression and cell invasion, and for uncovering players in metastasis.

Introduction

Cancer is a leading cause of death worldwide and, according to the World Health Organization, was responsible for the death of 7.9 million people in 2007 (www.who.int). This disease is characterized by the uncontrolled malignant growth of cells; however, the vast majority of human fatalities arise from secondary metastatic tumors. These secondary tumors generally spread from the original site via the blood or lymphatic system and are highly invasive and aggressive. The metastatic process involves several discrete biological steps: loss of cellular adhesion, increased motility and invasiveness, entry and survival of tumor cells in the circulation, their exit into new tissue, and their eventual colonization of a distant site (Chambers et al., 2002; Gupta and Massague, 2006). Understanding the mechanisms that promote tumor invasion and the role of the microenvironment is important for developing therapeutic strategies to treat metastatic cancers (Yang and Weinberg, 2008; Nguyen et al., 2009; Hanahan and Weinberg, 2011).

Over the last decade, the fruit fly *Drosophila melanogaster* has become an important model system for cancer studies. Reduced redundancy in the *Drosophila* genome compared with that of humans, coupled with the ability to conduct large-scale genetic screens in this organism, has enabled its use to determine the molecular characterization of important signaling cascades, developmental processes and growth control. For example, our understanding of the Hippo, Notch, Dpp and JAK-STAT signaling pathways, all of which are involved in tumor formation, has been enhanced by research in *Drosophila* (for reviews, see Brumby and Richardson, 2005; Vidal and Cagan, 2006; Januschke and Gonzalez, 2008). *Drosophila* genetics has revealed many genes that, when mutated or dysregulated, result in or contribute to tumorigenesis. Hyperplastic tumor suppressors, including components of the Hippo pathway, promote increased proliferation or survival, but do not disrupt tissue structure or differentiation. By contrast, *Drosophila* neoplastic tumor suppressors, such as the apical-basal cell polarity regulators (e.g. Lgl), lead to loss of tissue architecture, defects in differentiation and failure to exit the cell cycle. Elegant genetic and cell biology techniques have enabled the effects of tumor suppressors and oncogenes to be examined in the context of the whole animal. The capacity to generate patches (clones) of mutant tissue for specified genes during fly development has facilitated investigations into the role of the microenvironment in tumor development. Similarly, studies using clonal analysis in *Drosophila* have begun to elucidate cell competition mechanisms, which could potentially confer malignant cells with a growth advantage over their neighbors.

In conjunction with studies using other model organisms, flies have contributed greatly to our understanding of the mechanisms involved in cancer initiation and progression, revealing previously unknown molecular components and concepts. In turn, these have served to guide researchers who use mammalian systems to study cancer. This Perspective focuses on recent developments using fly tumor models that have been generated by tumor suppressor mutations or oncogene overexpression to induce neoplastic tumors of neuronal and epithelial origin as a means to probe the mechanisms involved in cellular invasion and metastasis.

Insights from metastatic neuronal tumors in the developing larval brain

Single gene mutations in a unique subset of genes {*lethal (3) malignant brain tumor* [*l(3)mbt*], *brain tumor* (*brat*), *discs large*

[1]Massachusetts General Hospital Center for Cancer Research and Harvard Medical School, 149, 13th Street, Charlestown, MA 02129, USA
[2]Center for Human Genetic Research, Massachusetts General Hospital, Boston, MA 02114, USA
*Author for correspondence (jwalker@helix.mgh.harvard.edu)

(*dlg*), *scribble* (*scrib*), *lethal giant larvae* (*lgl*), *miranda* (*mira*), *prospero* (*pros*), *partner of inscuteable* (*pins*) (for reviews see Januschke and Gonzalez, 2008; Froldi et al., 2008)} cause malignant neoplastic tumors in the *Drosophila* larval brain. These genes have crucial roles in regulating proliferation and development [*l(3)mbt*] (Gateff et al., 1993) and apical-basal cell polarity (*dlg* and *scrib*) (Woods et al., 1989; Bilder et al., 2000).

The human homologs of Dlg, Scrib and Lgl are important regulators of cell polarity, and mutations or splice variants have been linked to poor prognosis for colorectal (Schimanski et al., 2005) and hepatocarcinoma (Lu et al., 2009) patients. Importantly, all three complex components are targets for E6 papillomavirus-mediated degradation (Nakagawa and Huibregtse, 2000; Humbert et al., 2003; Handa et al., 2007). L(3)mbt has also been linked to various myeloid haemopoietic disorders (Boccuni et al., 2003) and is important for DNA replication and genomic stability (Gurvich et al., 2010).

Of these fly neoplastic tumor suppressors, *lgl* and *brat* are the best characterized. Lgl is localized to the cellular cortex, and functions in the same genetic pathway as *dlg* and *scrib* to maintain cellular polarity. Neuroblasts from *lgl* mutant larvae undergo aberrant symmetrical cell divisions, rather than the normal asymmetric divisions that are required for neuroblast and ganglion mother cell production (Mechler et al., 1985). Brat regulates ribosomal RNA (rRNA) synthesis and is a translational repressor. Brat is also asymmetrically localized to the ganglion mother cell after neuroblast division and is necessary for neuronal differentiation and proliferation control (Arama et al., 2000). Malignant tumors resulting from mutations in these fly neoplastic tumor suppressors cause late larval lethality but can be propagated and will metastasize when allografted into a recipient adult host (Gateff, 1978; Januschke and Gonzalez, 2008).

Metastasis of *lgl* and *brat* tumors

The Shearn group has utilized allograft experiments to investigate the metastatic behavior of *lgl* and *brat* mutant cells (Fig. 1A). Neoplastic brain tumors labeled with β-galactosidase (encoded by *lacZ*) from mutant larvae were dissected and allografted into the abdomens of wild-type adult flies. These tumors grew rapidly and resulted in host lethality within 12 days. Ovaries from allograft recipients were dissected and assayed for cells expressing *lacZ*. Because the ovary is contained in a non-porous epithelial sheet and muscle layers surround the ovarioles, only cells that are capable of metastasizing can invade into this organ (Fig. 1A). *lacZ*-positive cells were detected in recipient ovarioles from *lgl* and *brat* mutant tumors but not from control brains. These *lacZ*-positive cells in the ovary were shown to retain their neuronal and glial cell markers. This work provided the first evidence that *Drosophila* cells can metastasize through epithelial tissue and colonize new sites distant from the initial tumor (Beaucher et al., 2007a).

To understand the processes regulating this metastasis, a candidate approach was used to identify genes that are required for invasion by *lgl* and *brat* cells. Matrix metalloproteases (MMPs) have long been linked to metastasis in human cancer and were therefore excellent candidates. The *Drosophila* genome encodes two MMPs (MMP1 and MMP2). MMP1 expression is strongly upregulated in *lgl* mutant cells and is necessary for their metastatic behavior (Beaucher et al., 2007b). By contrast, MMP1 expression is not required in *brat* mutant cells but is required in the host tissue, suggesting that MMP1 co-operates non-cell-autonomously with *brat* mutant cells to enable their metastasis.

Molecular profiling of *l(3)mbt* neuronal tumors

Recent studies from the Gonzalez group have taken a fresh approach to identifying genes required for *l(3)mbt* tumor growth (Janic et al., 2010). *l(3)mbt* is a substoichiometric member of the *Drosophila* dREAM-Myb complex, which is required for gene silencing, and functions in establishing and maintaining differentiation states (Lewis et al., 2004). Similar to *lgl* and *brat* tumors, those arising from *l(3)mbt* mutations result in larval lethality and can be allografted (Fig. 1B).

By conducting extensive expression arrays on larval neuronal and allograft cultured tumors, gene expression profiles were identified for tumors that result from single gene mutations [in *l(3)mbt*, *brat*, *lgl*, *mira*, *pros* and *pins*] (Janic et al., 2010). By comparing profiles, Janic and colleagues characterized an *l(3)mbt*-specific tumor signature. The concatenate sequencing of Piwi-interacting RNAs (piRNAs) and microRNAs from these tumors identified small RNA changes that are characteristic of the *l(3)mbt* tumors. Together with immunohistochemical analyses, these approaches provide a basis for understanding the gene expression changes that are specific to *l(3)mbt* tumors. The *l(3)mbt* tumor signature surprisingly contains a disproportionately high number of germline-specific genes and microRNAs. This result suggests that a germline fate is associated with *l(3)mbt* tumor growth, and is in agreement with studies from *Caenorhabditis elegans* that linked soma-to-germline transition with increased fitness and longevity (Curran et al., 2009; Wang et al., 2005).

Genetic studies then tested the capacity of mutations in upregulated germline-specific genes to modify *l(3)mbt* tumor formation and allograft metastasis (Janic et al., 2010). Interestingly, only mutations in a subset of germline-specific genes (*piwi*, *vasa*, *aub* and *nos*) could suppress *l(3)mbt* tumor formation. By contrast, other upregulated germline-specific transcripts (*zpg*, *Pxt* and *AGO*) were unable to prevent tumor formation or metastatic growth. This result suggests that only a limited number of germline-specific genes are capable of restricting tumor growth. These findings provide a detailed understanding of the gene expression and small RNA changes in *l(3)mbt* neoplastic tumors, and highlight the possibility that a soma-to-germline transition accompanies metastasis. However, this approach has not yet identified genes that are specifically required for invasion, because all metastatic suppressors also prevented *l(3)mbt* tumor growth. Further analysis of the *l(3)mbt* tumor signature will hopefully identify other metastasis-promoting factors.

Using mutations to generate neoplastic tumors has significant advantages. First, only a single mutational event is required to initiate tumor growth in an isogenic background. Second, the *l(3)mbt* alleles are particularly advantageous because they are temperature sensitive, permitting gene expression arrays to be conducted from a single stock at both permissive and restrictive temperatures. Finally, these tumors develop rapidly and metastasize when allografted. These experiments permit expansion of the tumor mass for biochemical analysis and metastasis modeling.

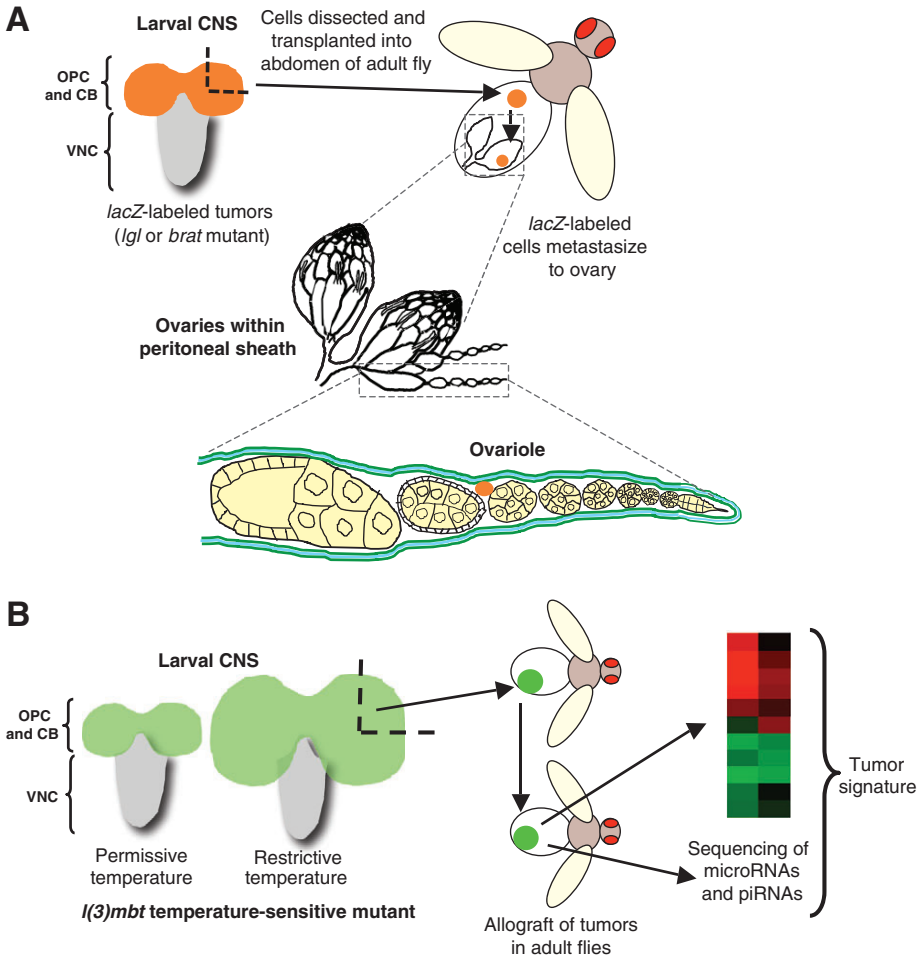

Fig. 1. *Drosophila* models of tumor metastasis caused by loss-of-function mutations in *lgl or brat* and *l(3)mbt*. The *Drosophila* larval brain is composed of two hemispheres and the ventral nerve cord (VNC). Mutant tumorous tissue in these models is restricted to the outer proliferative center (OPC) and central brain (CB) regions. (A) Neoplastic brain tumors caused by mutations in either *lgl* or *brat* can be engineered to express a reporter gene (*lacZ*; orange). Larval brains from these *lgl* or *brat* mutant animals are quartered and transplanted into the abdomens of adult female flies. The transplanted tissue continues to proliferate in the abdomen and, after several days, the ovaries of the host can be dissected and examined by immunofluorescence to detect labeled tumor cells that have metastasized. *Drosophila* ovaries are encased within a peritoneal sheath. Each ovary consists of 15-20 ovarioles, which are surrounded by an epithelial sheath of cells in addition to a muscle layer (blue) between two layers of extracellular matrix (green). Any *lacZ*-expressing cells found within the ovarioles must have traversed these layers and are therefore considered to have undergone metastasis. (B) Modeling metastasis using tumors caused by loss-of-function mutations in *l(3)mbt*. Temperature-sensitive mutations in *l(3)mbt* result in tissue overgrowth in the developing larval CNS when grown at restrictive temperatures (29°C). Tumor tissue (engineered to express GFP) can be dissected and transplanted into the abdomens of wild-type adult flies (allografts). These can be maintained and multiple rounds of allografts can be performed by transplantation into other flies, thereby generating sufficient material for biochemical analysis (e.g. microarray analysis, sequencing and western blotting). Comparison of the expression profiles of *l(3)mbt* and *brat* mutant tumors enabled an *l(3)mbt*-specific tumor expression signature to be obtained (Janic et al., 2010).

Insights from neuronal metastatic tumors induced by oncogene overexpression

Modeling *Ras*^{V12} tumors in the larval eye neural epithelium

Overexpression of oncogenic Ras protein (Ras^{V12}) causes benign tumor growth in *Drosophila*. This model has been used to identify pathways that are required for tumor development and metastasis. The mosaic analysis with a repressible cell marker (MARCM) technique can be used to generate clones expressing activated Ras^{V12} by FLP-FRT-mediated mitotic recombination; clones are concomitantly labeled with a visible marker (*UAS-GFP*) (Theodosiou and Xu, 1998; Lee and Luo, 2001; Elliott and Brand, 2008). Using an eye-specific flippase (*ey-FLP*) to convert an inactive *GAL4* driver (*Act>y+>GAL4*) to an active conformation (*Act>GAL4*) enables the ectopic expression of *UAS* transgenes to be stimulated in the larval neural tissue, in an otherwise wild-type animal (Pagliarini and Xu, 2003). Expression of activated Ras (*UAS-Ras*^{V12}) causes benign tumor growth in the larval midbrain, which can be visualized through imaging living larvae or pupae directly. These benign tumors can then be used to identify genetic modifiers that are required for either initial tumor development and/or metastasis (Fig. 2A).

This system identified the cell polarity genes *scrib*, *lgl* and *dlg* as being crucial for constraining metastatic growth (Pagliarini and Xu,

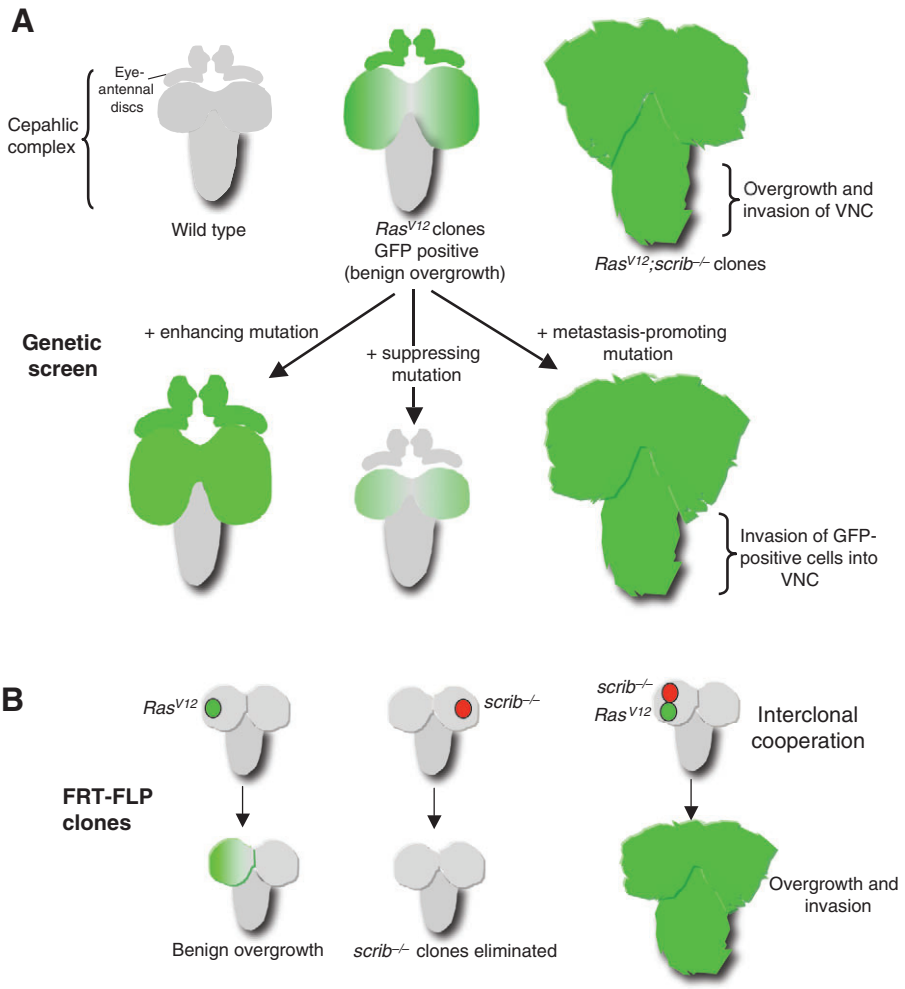

Fig. 2. Modeling tumor invasion and metastasis in the *Drosophila* larval brain. (A) Ras^{V12} overexpression clones generated by the MARCM system in eye-antennal discs. These clones (marked with GFP, and shown in green) produce a benign overgrowth throughout the cephalic complex. When *Ras^{V12}* clones are also mutant for *scrib*, they become tumorigenic and metastasize, as shown by invasion of GFP-labeled cells into the ventral nerve cord (VNC). Genetic screens have identified modifiers of the *Ras^{V12}* phenotype [suppressor, JNK; enhancer, *large giant lethal* (*lgl*); metastatic enhancer, *deep orange* (*dor*)] (Chi et al., 2010; Wu et al., 2010). (B) Interclonal cooperation of *Ras^{V12}* and *scrib$^{-/-}$* clones. As described in A, Ras^{V12} overexpression produces benign overgrowth. *scrib$^{-/-}$* clones grow at a reduced rate and are excluded via cell competition. Adjacent *Ras^{V12}* and *scrib$^{-/-}$* clones cooperate to overproliferate and undergo metastasis. The large tumor and metastatic growth consists almost exclusively of *Ras^{V12}* cells, suggesting that *scrib$^{-/-}$* cells actively cooperate with *Ras^{V12}* cells during the early stages of tumor growth and metastasis (Wu et al., 2010).

2003). All three of them genetically interact and cause overgrowth of *Ras^{V12}* tissue when mutated. These studies also identified *bazooka*, *stardust* and *cdc42* as factors that do not induce overgrowth when mutated singly but can strongly stimulate oncogenic Ras-mediated tumor growth and metastasis (Pagliarini and Xu, 2003). Each of these genes can also regulate cell polarity and E-cadherin expression. Crucially, although downregulation of E-cadherin is necessary for *Ras^{V12};scrib$^{-/-}$*-induced metastasis, it is not sufficient, implicating other contributing factors in metastatic growth.

The relationship between oncogenic Ras and JNK signaling

Several *Drosophila* laboratories have highlighted the importance of the oncogenic cooperation between Ras and JNK signaling. Constitutive activation of the Ras signaling pathway prevents fly cells from undergoing JNK-mediated apoptosis in response to cellular stresses (Brumby and Richardson, 2003; Brumby and Richardson, 2005). The Xu group has linked JNK upregulation to cell polarity and changes in E-cadherin expression in *Ras^{V12};scrib$^{-/-}$* clones (Igaki et al., 2006). They also demonstrated that overexpression of negative regulators of the JNK pathway [using a transgene to express a dominant-negative form of *Drosophila* JNK (encoded by the *bsk* gene)] prevents tumor formation and metastasis (Igaki et al., 2006). The Bohmann laboratory has shown that the invasion potential of *Ras^{V12};scrib$^{-/-}$* clones is dependent on the Fos-mediated transcriptional activation of *mmp1* downstream of JNK (Uhlirova and Bohmann, 2006). Expression of the MMP inhibitor, TIMP, or *mmp1* RNA interference (RNAi) knockdown, was able to suppress cell invasiveness (Uhlirova and Bohmann, 2006).

Recent studies of the *sds22* gene in *Drosophila* have strengthened the idea that epithelial integrity and JNK signaling cooperate to drive the metastatic growth of *Ras^{V12};scrib$^{-/-}$* clones (Jiang et al., 2011). Sds22 is a conserved regulatory subunit of protein phosphatase 1 (PP1), and acts as a regulator of epithelial polarity and as a neoplastic tumor suppressor in *Drosophila* (Grusche et al., 2009). Loss of *sds22* in *Ras^{V12}* clones results in reduced epithelial integrity, and the clones become invasive. Overexpression of Sds22 in *Ras^{V12};scrib$^{-/-}$* cells largely suppresses their tumorigenic growth, and mechanistic studies suggest that Sds22-PP1 inhibits non-muscle myosin II and JNK activity (Jiang et al., 2011). The authors of this study also showed that human *SDS22* is deleted or downregulated in multiple types of carcinoma.

A recent study by the Richardson group identified key regulators of the actin cytoskeleton and cell morphology, including Rho1-

family GTPases and RhoGEFs, as Ras-cooperating proteins (Brumby et al., 2011). The hyperplastic eye phenotype produced by driving *UAS-Ras^{V12}* with *ey-GAL4* was screened for modifiers using a collection of P-element enhancer insertion lines bearing *UAS* promoter sequences. These lines result in overexpression of the gene adjacent to the insertion element in *Ras^{V12}* cells. JNK pathway activation is crucial for the cooperation of these actin cytoskeletal regulators with Ras^{V12}. The relevance to human cancer of the collaboration between oncogenic Ras and JNK was demonstrated in this study by correlating JNK signaling with the upregulation of Ras in breast cancers (Brumby et al., 2011).

The role of JNK signaling in promoting metastatic behavior seems to be context specific. In contrast to the promotion of Ras-induced metastasis by JNK, analysis of *lgl$^{-/-}$* clones suggests that the activity of Diap1 (a caspase inhibitor) and JNK loss are essential for invasion of mutant cells out of the clone (Grzeschik et al., 2010a; Grzeschik et al., 2010b). Although Diap1 expression is sufficient to inhibit widespread apoptosis, cells at the boundary of *lgl$^{-/-}$* clones undergo cell death in a JNK-dependent manner. By blocking the JNK signaling cascade, apoptosis of these cells is specifically inhibited, stimulating de-differentiation and cellular invasion.

Lysosome dysfunction in *Ras^{V12}* tumor growth and invasion

Recent studies from the Xu laboratory have used genetic screens to identify mutations that promote *Ras^{V12}* cell metastasis (Fig. 2A). The authors tested 3119 ethyl-methanesulfonate-mutagenized lines (on the X chromosome) for their capacity to modify *Ras^{V12}* larval tumors. This screen identified 516 suppressors and 351 enhancers of tumor growth, of which 23 enhanced tumor growth as well as metastasis (Chi et al., 2010). Two of these metastasis-promoting mutations occurred within the class C vacuolar protein sorting (VPS) complex member *deep orange* (*dor*). By testing mutations in genes encoding other components of this lysosome complex, namely *carnation* and *vps16A*, they confirmed that loss of lysosome activity stimulates metastatic growth of the *Ras^{V12}* tissue (Chi et al., 2010). Characterization of other modifiers from this screen might provide a clearer understanding of the mechanisms underlying Ras-mediated tumor growth in *Drosophila*. This study also confirmed their genetic findings: feeding chemical inhibitors of lysosomal function to larvae with *Ras^{V12}* overgrowths promoted tumor development and metastasis. This work illustrates the potential of *Drosophila* to screen for therapeutic cancer drugs in vivo, a system that might one day provide a cheap and rapid means for drug discovery.

Interclonal cooperation between *Ras^{V12}* and *scrib* mutant cells

Exciting recent work using the *Ras^{V12}-scrib$^{-/-}$* system has demonstrated a non-cell-autonomous effect between neighboring clones (called interclonal cooperation; Fig. 2B). Adjacent *Ras^{V12}* clones and *scrib$^{-/-}$* clones actively cooperate to form tumors and can metastasize (Wu et al., 2010). Interclonal tumors and metastatic growths are smaller than those produced from a single *Ras^{V12};scrib$^{-/-}$* clone but still represent a significant tumor burden to the hosts (Fig. 2B). During later stages of tumor development, these interclonal tumors are made up almost exclusively of Ras^{V12}-expressing cells, suggesting that the *scrib$^{-/-}$* mutant cells are only required for the initial stages of tumor formation and metastasis (Wu et al., 2010). These studies also identified the JAK-STAT signaling pathway as being a crucial downstream target of JNK activity, implicating JNK and JAK-STAT as important oncogenic drivers for *Ras*-mediated tumor growth (Wu et al., 2010). In agreement with these findings, the authors went on to demonstrate that JNK activation after wounding is also able to promote the overgrowth of *Ras^{V12}* cells. This study potentially forges a link between tissue damage and Ras-stimulated JNK activity – a situation resembling the chronic inflammation that has been reported to contribute to tumorigenesis in humans (Mantovani, 2010). Other recent *Drosophila* studies have also highlighted the role of the immune response in tumor growth (Box 1).

Screening for regulators of invasive growth caused by activation of the Notch pathway

The Notch signaling cascade was originally identified as an important regulator of proliferation and differentiation in flies. Extensive genetic and biochemical studies have identified and characterized the components and regulators of this pathway (Artavanis-Tsakonas and Muskavitch, 2010). *Drosophila* studies have revealed that, similar to oncogenic Ras, Notch signaling cooperates with JNK to promote dysregulation of epithelial integrity (Brumby and Richardson, 2003; Leong et al., 2009). Aberrant Notch signaling is associated with several human cancers, including skin, breast, lung and ovarian cancer (for a review, see Allenspach et al., 2002). Tumors containing amplifications of genes encoding Notch signaling components (e.g. Notch and Jagged) tend to be highly aggressive and metastatic.

Overexpression of the Notch activator Delta (Dl) using the *eyeless-GAL4* driver (*ey-GAL4>UAS-Dl*) stimulates a non-metastatic overproliferation of eye tissue. Flies treated with a γ-secretase inhibitor to prevent Notch receptor proteolysis showed complete rescue of the *ey-GAL4>UAS-Dl* phenotype (Palomero et al., 2007). This model has been employed by the Dominguez group to screen for modifiers of this phenotype using a library of P-element UAS insertion lines that result in gene overexpression

Box 1. The role of the immune system in tumor growth in *Drosophila*

Several recent reports suggest that the immune system plays a crucial role in *Drosophila* tumor models, as is the case in mammalian tumors. Circulating blood cells, known in *Drosophila* as hemocytes, are part of the fly immune system and have been found to associate with *Ras^{V12};scrib$^{-/-}$* tumors and to reduce tumor growth in *scrib$^{-/-}$* animals (Pastor-Pareja et al., 2008). The *Drosophila* genome encodes a single member of the tumor necrosis factor (TNF) family, named Eiger (Egr). Egr has been shown to be required for the JNK-dependent cell death of *scrib* or *dlg* clonal tissue (Igaki et al., 2009). In the absence of *egr*, these mutant clones grow aggressively and develop into tumors (Igaki et al., 2009). By contrast, another study showed that loss of *egr* in *Ras^{V12};scrib$^{-/-}$* tumors prevented invasive overgrowth, which was correlated with reduced JNK activation and a failure to express MMP1 (Cordero et al., 2010). Therefore, in the presence of oncogenic Ras, Egr seems to play a role as a tumor promoter. This study also revealed that Egr is produced in the hemocytes associated with *Ras^{V12};scrib$^{-/-}$* tumors (Cordero et al., 2010). Together, these *Drosophila* models might provide an excellent parallel to mammalian tumors, in which TNF is produced in both tumor cells and associated immune cells, where it has been shown to have both oncogenic and tumor-suppressive roles (Balkwill, 2009).

(Ferres-Marco et al., 2006). One of these lines, *eyeful*, strongly promoted the metastatic growth of *ey-GAL4>UAS-Dl* eye tissue, resulting in secondary eye growths throughout the body. Using various tissue-specific *GAL4* drivers, the authors demonstrated that co-expression of *Dl* and *eyeful* could stimulate massive overgrowth and metastatic invasion in multiple tissue settings. The *eyeful* construct was mapped within the divergently transcribed genes of *longitudinals lacking* (*lola*) and *pipsqueak* (*psq*), which produce a myriad of alternatively spliced BTB (BR-C, ttk and bab) proteins, which are required for the recruitment of histone deacetylases and Polycomb complexes to promoter regions. Further biochemical studies demonstrated that silencing of Retinoblastoma (Rbf) expression via promoter hypermethylation strongly contributed to the metastatic phenotype (Ferres-Marco et al., 2006).

This screen also identified the P-element insertion GS1D233C as an enhancer of the *ey-GAL4>UAS-Dl* phenotype. This insertion was mapped to the *Akt1* locus, which encodes an important serine/tyrosine kinase linked to phosphatase and tensin homolog (PTEN) and Notch signaling (Palomero et al., 2007). These results suggest that flies will provide a useful system to test new pharmacological reagents targeted against the Notch pathway.

The Hassan group used the *ey-GAL4>UAS-Dl/eyeful* phenotype to screen for mutations that could further enhance metastatic growth (Bossuyt et al., 2009). This screen identified *atonal* (*ato*), a transcription factor required for retinal terminal differentiation, as a crucial tumor suppressor. Mutations affecting *ato* dramatically enhanced tumor burden and metastasis rates, and tumors displayed elevated levels of proliferation markers (such as phosphorylated histone H3). Conversely, overexpression of *atonal* upregulated both Decapo (also known as p21 cell-cycle inhibitor) and phosphorylated-JNK levels, inhibiting proliferation and inducing apoptosis. Furthermore, overexpressing dominant-negative JNK (*bsk*) partially mimics *ato* downregulation in the *eyeful* (*ey-GAL4>UAS-Dl/eyeful*) model, indicating that JNK signaling is downstream of *atonal* and that *atonal* requires active JNK signaling to inhibit overgrowth (Bossuyt et al., 2009).

Modeling glioma in *Drosophila*

Developing *Drosophila* models of specific human tumor types is limited in many cases owing to the lack of directly homologous organs (e.g. pancreas, liver and lung). However, recent studies have capitalized on the similarity of mammalian and *Drosophila* glial cells to model glioblastoma in flies (Read et al., 2009; Witte et al., 2009). Glioblastomas are the most common tumors of the central nervous system (CNS), and their rapid proliferation and malignancy result in poor patient prognosis.

Mutation or amplification of the gene encoding epidermal growth factor receptor (EGFR) tyrosine kinase, loss of PTEN [which antagonizes the growth promoting effects of phosphoinositide 3-kinase (PI3K) signaling] or activating mutations in PI3K (Furnari et al., 2007) are genetic lesions that are commonly associated with gliomas. Consequently, the glial-specific *Repo-GAL4* driver (incorporating the promoter *reversed polarity*) was used to simultaneously express transgenes encoding constitutively active EGFR and PI3K in larval glia. Co-activation of EGFR (or Ras) and PI3K in larval glia results in neoplasia, neurological defects and lethality (Read et al., 2009; Witte et al., 2009). The overproliferation and neoplastic transformation seems to be specific for glia, because overexpression of EGFR and PI3K in neurons, neuroblasts or other glial cells (such as oligodendrocyte-like neuropil glia and astrocyte-like cortex glia) failed to transform them.

The neoplastic glia induced in this *Drosophila* model mimic the highly proliferative anaplastic glia from high-grade human gliomas. They ectopically express Cyclin-B (CycB), Cyclin-E (CycE) and MMP1, promoting cell cycle entry and invasive growth. These studies demonstrated that glia expressing activated EGFR or Ras and PI3K invade into inappropriate areas of the brain, such as along Bolwig nerves, which are not normally accompanied by glial cells (Read et al., 2009; Witte et al., 2009).

Genetic experiments have revealed that the malignant neoplastic transformation of larval glia induced by EGFR and PI3K occurs via a complex network of genetic factors that are commonly mutated or activated in human gliomas. These downstream effectors include Tor, Myc, G1 cyclin-Cdk complexes (such as those including Cyclin B or E) and the Rb-E2F pathway. Interestingly, pharmacological inhibitors, including compounds that are used to treat patients, rescued these phenotypes in larvae. An EGFR inhibitor (gefitinib) partially reduced the migration of EGFR- and PI3K-transformed glia, whereas a PI3K inhibitor (wortmannin) and an Akt inhibitor (triciribine) completely prevented invasion (Witte et al., 2009). Together, these studies suggest that this *Drosophila* model is useful for deciphering the signaling cascades underlying the abnormal behavior of glioma cells, including their metastatic potential.

Modeling tumor invasion in the epithelia of the *Drosophila* wing disc

Roles for both receptor and non-receptor tyrosine kinases in cell transformation and progression towards malignant phenotypes are well established (Blume-Jensen and Hunter, 2001). The SRC family kinases (SFKs) are membrane-linked non-receptor tyrosine kinases that are required for regulating adhesion and cytoskeleton reorganization, cell cycle progression, and migration (Guarino, 2010; Thomas and Brugge, 1997). Elevated SRC levels have been reported in a wide variety of human cancers, including those of the colon, liver, lung, breast and pancreas (Ishizawar and Parsons, 2004; Summy and Gallick, 2003). SFK activity is inhibited by the C-terminal SRC kinase (CSK) family of tyrosine kinases [CSK and CSK homologous kinase (CHK)] (Chong et al., 2005); both CSK and CHK phosphorylate and inactivate SFKs, and mutations disrupting this activity have been implicated in a plethora of cancers. Elevated SRC levels (either by amplification of SRC or loss of CSK function) promote anchorage-independent cell growth, tumor cell invasion and metastasis (Guarino, 2010). Although SRC is a crucial regulator of epithelial-mesenchymal transition (EMT), the exact mechanism of how SRC promotes metastatic growth remains elusive.

Recent studies from the Cagan group have utilized the pseudostratified epithelia of the *Drosophila* larval wing imaginal disc to model invasive cell growth (Vidal et al., 2006). Global depletion of the sole *Drosophila* CSK/CHK ortholog, Csk, using either RNAi or *Csk* mutations, elevates active levels of Src, leading to significant overgrowth in developing larvae. By contrast, targeting *Csk* depletion to a discrete stripe along the anterior-posterior (A-P) boundary of the larval wing disc using a *patched-GAL4* driver (*ptc-GAL4*) to express a *Csk* RNAi transgene (*UAS-Csk-RNAi*) produces a metastatic phenotype (Vidal et al., 2006).

Src-transformed cells lose their apical profile and are excluded from the epithelium. These cells invasively migrate through the basal extracellular matrix, and eventually apoptose (Fig. 3). This invasive migration has been used to model tumor metastasis. Invasion occurs only at the boundaries between *Csk* mutant cells and the adjacent wild-type cells, suggesting that the microenvironment is crucial in determining the outcome of the Src-activated cells (Vidal et al., 2006).

By utilizing this model of metastasis, Vidal and co-authors examined the capacity of GFP-labeled *Csk-RNAi* cells to invasively migrate in different mutant backgrounds. These studies implicate JNK signaling in the apoptotic response of *Csk-RNAi* cells. Mutations in *puckered* (*puc*), a *Drosophila* JNK-specific phosphatase, cause an upregulation in JNK signaling and enhance both the apoptotic and the invasion phenotype of *ptc>Csk-RNAi* cells. Conversely, *puc* overexpression (*UAS-puc*) using *ptc-GAL4* prevents apoptosis within the stripe. Similar experiments revealed that the small GTPase Rho1 is a positive mediator of the JNK signal in *Csk-RNAi* boundary cells, similar to that seen in activated Ras^{V12} tumors in the eye epithelia (discussed above) (Brumby et al., 2011).

Cadherin-containing complexes are required for maintaining adherens junctions, which are important for cell adhesion and tissue structure. Src modulates the integrity of these adhesion sites: E-cadherin-dependent adhesion is reduced in *ptc>Csk-RNAi* tissue. These results implicated E-cadherin in the recognition and elimination of *Csk-RNAi* cells. Depletion of E-cadherin suppresses both the migratory and apoptotic phenotypes of *ptc>Csk-RNAi* boundary cells. Using candidate approaches, p120-catenin and both MMPs (MMP1 and MMP2) were found to be important for the *Csk-RNAi* invasive phenotype (Vidal et al., 2006; Vidal et al., 2010).

mmp1 transcript levels were specifically upregulated at the leading edge of *Csk-RNAi* migrating cells (Singh et al., 2010; Vidal et al., 2010), suggesting that rearrangement of the extracellular matrix is crucial for this invasive growth.

In a separate study, the capacity of Src to contribute to Ras^{V12}-induced tumor growth was tested (Vidal et al., 2007), and malignant overgrowth of Ras^{V12} tumors was found to correlate with elevated Src levels. These studies suggest a progressive role for Src, whereby low levels promote proliferation during early tumorigenesis and high levels are required for the later stages of invasive migration and metastasis (Vidal et al., 2007).

Invasive migration phenotypes similar to those of *ptc>Csk-RNAi* cells are produced by the overexpression of the oncogene *Abl* in the A-P boundary of the wing disc (Singh et al., 2010). Co-expression of *ptc>Csk-RNAi* and *UAS-Abl* results in synergistic enhancement of the invasive phenotype. Conversely, the migration phenotype induced by *UAS-Csk-RNAi* is suppressed by reducing Abl function using RNAi. Together, these findings suggest that Abl functions downstream of Csk and Src to mediate cell invasion. In addition to activating JNK (required for cell invasion and apoptosis), Abl overexpression also stimulates ERK signaling, further promoting cellular proliferation. Interestingly, the authors of this study defined a positive feedback loop whereby Abl increases the activity of Src, resulting in signal amplification (Singh et al., 2010).

This system provides an excellent model in which to study the function of genes in cell proliferation, survival and invasive behavior in the context of cell polarity. Although these reports only tested candidate genes for their ability to modify the invasion phenotype induced by *Csk* RNAi, the system should prove amenable to genetic screening using *UAS-RNAi* fly lines to identify genes involved in

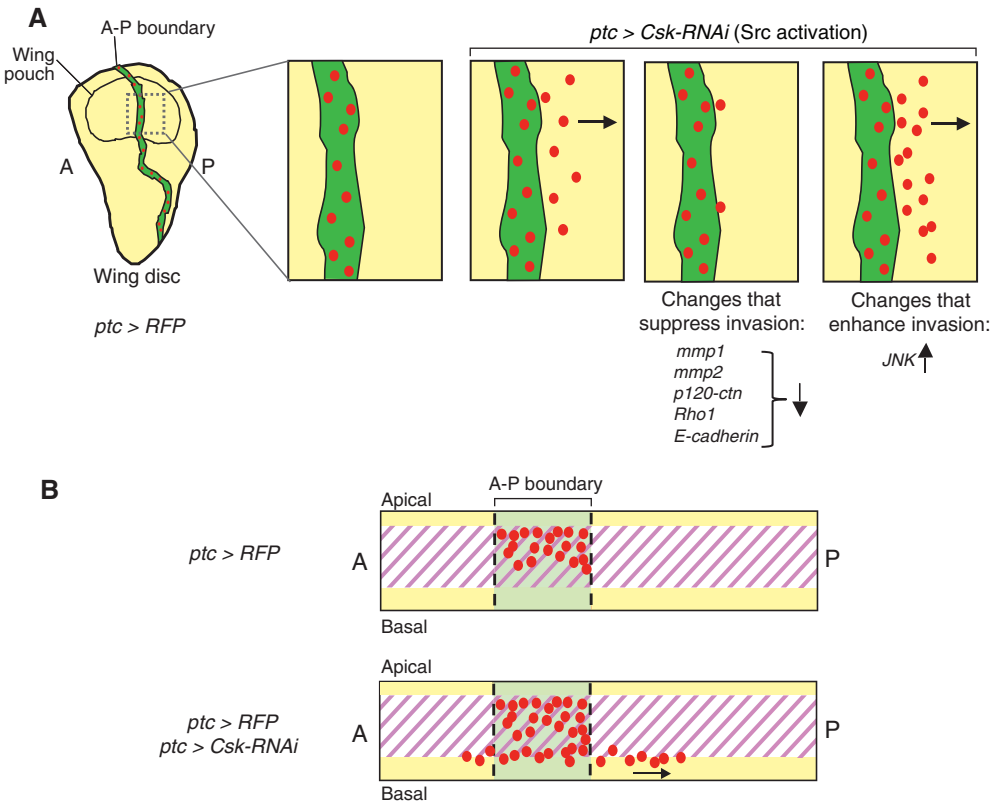

Fig. 3. Modeling tumor invasion in the *Drosophila* larval wing disc. (A) The larval wing disc consists of a sheet of epithelial cells (yellow). A *ptc-GAL4* driver is used to knock down Csk, a negative regulator of Src, specifically in a stripe along the A-P boundary, using an RNAi transgene (*UAS-Csk-RNAi*). The Src-transformed cells are labeled with red fluorescent protein (RFP). The *ptc* domain is shown in green. The *Csk-RNAi* cells at the boundary of the *ptc* domain have the potential to invade into the surrounding tissue. Activation of the JNK pathway or knockdown of regulators of the cytoskeleton (*mmp1*, *mmp2*, *p120-ctn*, *Rho1* and *E-cadherin*) using transgenic overexpression, different genetic backgrounds or RNAi, can either enhance or suppress the invasion of the *Csk-RNAi* cells, highlighting the importance of the tumor microenvironment (Vidal et al., 2006). (B) Horizontal cross-section of the boxed area of the wing disc shown in A. On silencing of Csk, labeled cells (red) are basally excluded and migrate from the boundary through the extracellular matrix (purple hatch).

metastasis. In addition, the identification of the factors that collaborate to control cell migration suggests possible approaches for dual therapeutic targeting in combating metastasis in various cancers.

Conclusions, limitations and perspectives

This review has highlighted the many advantages of *Drosophila* as a model for studying tumor progression. A streamlined genome, coupled with powerful genetic tools, provides a unique system in which to explore the mechanisms regulating the metastatic growth of tumor cells. However, as with any model organism, it has several limitations that should be considered. In mammals, malignant cells undergoing metastasis enter a local blood or lymph vessel before colonizing a distant tissue and forming secondary tumors. This is difficult to model in *Drosophila* because flies have rudimentary hematopoietic systems and a dramatically different lymphatic system compared with mammals. In addition, the metastatic potential of tumors induced in *Drosophila* is greatly reduced compared with their mammalian counterparts; tumor cells tend to invade the local surrounding tissue distally (e.g. in the cephalic complex in the case of Ras^{V12} overexpression).

Tumor formation is generally stimulated by a single mutation or activated oncogene expression in *Drosophila*. However, as the examples outlined here demonstrate, *Drosophila* has also proved to be a powerful experimental system for examining 'two-hit' models of tumor overgrowth and invasion. Although the *Drosophila* models discussed here are largely limited to tumors that develop in the larval stage, adult flies can be employed to examine the metastatic potential of these tumors using allografts, providing an ideal way to propagate tumors for extended studies.

The systems of modeling tumor development in *Drosophila* capitalize on the unique advantages of this model organism coupled with recent innovative technologies (see Box 2). Undoubtedly, the major strength of *Drosophila* is the ease of conducting large-scale genetic screens, which can now make use of the large publicly available collections of isogenic deficiencies and RNAi lines that cover the entire genome (Dietzl et al., 2007; Parks et al., 2004). Elegant targeting techniques – including the UAS/GAL4 system, FLP-FRT-mediated recombination and MARCM clonal analysis – enable gene knockdown in specific tissues or patches of cells, bypassing issues of organism lethality. Because these cancer models involve an in vivo setting, they are also ideally suited for studies that examine the role of the microenvironment. In addition, *Drosophila* offers the potential for drug screening. Together, these approaches make *Drosophila* an excellent model organism to elucidate the basic mechanisms governing tumorigenesis and tumor progression. Validation of this research in mammalian cancer models and human cancer cell lines could lead to new insights into tumor invasion. Metastasis modeling in *Drosophila* is in its infancy but, as better tools and models of specific tumor types are developed, it offers the potential to probe the basic mechanisms regulating cancer cell invasion.

Box 2. Advantages of *Drosophila* for modeling tumor invasion and metastasis

- The signaling pathways controlling growth, differentiation and development that are involved in tumorigenesis and tumor progression are largely conserved between *Drosophila* and humans.
- Models of tumor formation and cell invasion have been created in *Drosophila* using a wide variety of gene targeting strategies, such as loss-of-function mutations and tissue-specific RNAi knockdown, as well as transgenic overexpression of activated oncogenes found in human cancers.
- The ability to generate clones that are mutant for specific genes juxtaposed with wild-type cells using the FLP-FRT and MARCM systems allows the genetics of the tumor microenvironment required for invasion and metastasis to be examined.
- Genome-wide screens using either de novo mutagenesis or tissue-specific knockdown by RNAi in *Drosophila* can identify genes with previously unidentified roles in cancer progression.
- *Drosophila* tumor models can be used for pharmacological screening.

FUNDING

Work in the authors' laboratories is supported by the National Institutes of Health (NIH) [R01GM53202] to N.J.D.; and the Department of Defense (DOD) [W81XWH-09-1-0487] to J.A.W.

COMPETING INTERESTS

The authors declare that they do not have any competing or financial interests.

REFERENCES

Allenspach, E. J., Maillard, I., Aster, J. C. and Pear, W. S. (2002). Notch signaling in cancer. *Cancer Biol. Ther.* **1**, 466-476.

Arama, E., Dickman, D., Kimchie, Z., Shearn, A. and Lev, Z. (2000). Mutations in the beta-propeller domain of the *Drosophila* brain tumor (brat) protein induce neoplasm in the larval brain. *Oncogene* **19**, 3706-3716.

Artavanis-Tsakonas, S. and Muskavitch, M. A. (2010). Notch: the past, the present, and the future. *Curr. Top. Dev. Biol.* **92**, 1-29.

Balkwill, F. (2009). Tumour necrosis factor and cancer. *Nat. Rev. Cancer* **9**, 361-371.

Beaucher, M., Goodliffe, J., Hersperger, E., Trunova, S., Frydman, H. and Shearn, A. (2007a). *Drosophila* brain tumor metastases express both neuronal and glial cell type markers. *Dev. Biol.* **301**, 287-297.

Beaucher, M., Hersperger, E., Page-McCaw, A. and Shearn, A. (2007b). Metastatic ability of *Drosophila* tumors depends on MMP activity. *Dev. Biol.* **303**, 625-634.

Bilder, D., Li, M. and Perrimon, N. (2000). Cooperative regulation of cell polarity and growth by *Drosophila* tumor suppressors. *Science* **289**, 113-116.

Blume-Jensen, P. and Hunter, T. (2001). Oncogenic kinase signalling. *Nature* **411**, 355-365.

Boccuni, P., MacGrogan, D., Scandura, J. M. and Nimer, S. D. (2003). The human L(3)MBT polycomb group protein is a transcriptional repressor and interacts physically and functionally with TEL (ETV6). *J. Biol. Chem.* **278**, 5412-5420.

Bossuyt, W., De Geest, N., Aerts, S., Leenaerts, I., Marynen, P. and Hassan, B. A. (2009). The atonal proneural transcription factor links differentiation and tumor formation in *Drosophila*. *PLoS Biol.* **7**, e40.

Brumby, A. M. and Richardson, H. E. (2003). scribble mutants cooperate with oncogenic Ras or Notch to cause neoplastic overgrowth in *Drosophila*. *EMBO J.* **22**, 5769-5779.

Brumby, A. M. and Richardson, H. E. (2005). Using *Drosophila melanogaster* to map human cancer pathways. *Nat. Rev. Cancer* **5**, 626-639.

Brumby, A. M., Goulding, K. R., Schlosser, T., Loi, S., Galea, R., Khoo, P., Bolden, J. E., Aigaki, T., Humbert, P. O. and Richardson, H. E. (2011). Identification of novel ras-cooperating oncogenes in *Drosophila melanogaster*: a RhoGEF/Rho-family/JNK pathway is a central driver of tumorigenesis. *Genetics* **188**, 105-125.

Chambers, A. F., Groom, A. C. and MacDonald, I. C. (2002). Dissemination and growth of cancer cells in metastatic sites. *Nat. Rev. Cancer* **2**, 563-572.

Chi, C., Zhu, H., Han, M., Zhuang, Y., Wu, X. and Xu, T. (2010). Disruption of lysosome function promotes tumor growth and metastasis in *Drosophila*. *J. Biol. Chem.* **285**, 21817-21823.

Chong, Y. P., Mulhern, T. D. and Cheng, H. C. (2005). C-terminal Src kinase (CSK) and CSK-homologous kinase (CHK)-endogenous negative regulators of Src-family protein kinases. *Growth Factors* **23**, 233-244.

Cordero, J. B., Macagno, J. P., Stefanatos, R. K., Strathdee, K. E., Cagan, R. L. and Vidal, M. (2010). Oncogenic Ras diverts a host TNF tumor suppressor activity into tumor promoter. *Dev. Cell* **18**, 999-1011.

Curran, S. P., Wu, X., Riedel, C. G. and Ruvkun, G. (2009). A soma-to-germline transformation in long-lived *Caenorhabditis elegans* mutants. *Nature* **459**, 1079-1084.

Dietzl, G., Chen, D., Schnorrer, F., Su, K. C., Barinova, Y., Fellner, M., Gasser, B., Kinsey, K., Oppel, S., Scheiblauer, S. et al. (2007). A genome-wide transgenic RNAi library for conditional gene inactivation in *Drosophila*. *Nature* **448**, 151-156.

Elliott, D. A. and Brand, A. H. (2008). The GAL4 system: a versatile system for the expression of genes. *Methods Mol. Biol.* **420**, 79-95.

Ferres-Marco, D., Gutierrez-Garcia, I., Vallejo, D. M., Bolivar, J., Gutierrez-Avino, F. J. and Dominguez, M. (2006). Epigenetic silencers and Notch collaborate to promote malignant tumours by Rb silencing. *Nature* **439**, 430-436.

Froldi, F., Ziosi, M., Tomba, G., Parisi, F., Garoia, F., Pession, A. and Grifoni, D. (2008). *Drosophila* lethal giant larvae neoplastic mutant as a genetic tool for cancer modeling. *Curr. Genomics* **9**, 147-154.

Furnari, F. B., Fenton, T., Bachoo, R. M., Mukasa, A., Stommel, J. M., Stegh, A., Hahn, W. C., Ligon, K. L., Louis, D. N., Brennan, C. et al. (2007). Malignant astrocytic glioma: genetics, biology, and paths to treatment. *Genes Dev.* **21**, 2683-2710.

Gateff, E. (1978). Malignant neoplasms of genetic origin in *Drosophila melanogaster*. *Science* **200**, 1448-1459.

Gateff, E., Loffler, T. and Wismar, J. (1993). A temperature-sensitive brain tumor suppressor mutation of *Drosophila melanogaster*: developmental studies and molecular localization of the gene. *Mech. Dev.* **41**, 15-31.

Grusche, F. A., Hidalgo, C., Fletcher, G., Sung, H. H., Sahai, E. and Thompson, B. J. (2009). Sds22, a PP1 phosphatase regulatory subunit, regulates epithelial cell polarity and shape [Sds22 in epithelial morphology]. *BMC Dev. Biol.* **9**, 14.

Grzeschik, N. A., Parsons, L. M., Allott, M. L., Harvey, K. F. and Richardson, H. E. (2010a). Lgl, aPKC, and Crumbs regulate the Salvador/Warts/Hippo pathway through two distinct mechanisms. *Curr. Biol.* **20**, 573-581.

Grzeschik, N. A., Parsons, L. M. and Richardson, H. E. (2010b). Lgl, the SWH pathway and tumorigenesis: it's a matter of context & competition! *Cell Cycle* **9**, 3202-3212.

Guarino, M. (2010). Src signaling in cancer invasion. *J. Cell. Physiol.* **223**, 14-26.

Gupta, G. P. and Massague, J. (2006). Cancer metastasis: building a framework. *Cell* **127**, 679-695.

Gurvich, N., Perna, F., Farina, A., Voza, F., Menendez, S., Hurwitz, J. and Nimer, S. D. (2010). L3MBTL1 polycomb protein, a candidate tumor suppressor in del(20q12) myeloid disorders, is essential for genome stability. *Proc. Natl. Acad. Sci. USA* **107**, 22552-22557.

Hanahan, D. and Weinberg, R. A. (2011). Hallmarks of cancer: the next generation. *Cell* **144**, 646-674.

Handa, K., Yugawa, T., Narisawa-Saito, M., Ohno, S., Fujita, M. and Kiyono, T. (2007). E6AP-dependent degradation of DLG4/PSD95 by high-risk human papillomavirus type 18 E6 protein. *J. Virol.* **81**, 1379-1389.

Humbert, P., Russell, S. and Richardson, H. (2003). Dlg, Scribble and Lgl in cell polarity, cell proliferation and cancer. *BioEssays* **25**, 542-553.

Igaki, T., Pagliarini, R. A. and Xu, T. (2006). Loss of cell polarity drives tumor growth and invasion through JNK activation in *Drosophila*. *Curr. Biol.* **16**, 1139-1146.

Igaki, T., Pastor-Pareja, J. C., Aonuma, H., Miura, M. and Xu, T. (2009). Intrinsic tumor suppression and epithelial maintenance by endocytic activation of Eiger/TNF signaling in *Drosophila*. *Dev. Cell* **16**, 458-465.

Ishizawar, R. and Parsons, S. J. (2004). c-Src and cooperating partners in human cancer. *Cancer Cell* **6**, 209-214.

Janic, A., Mendizabal, L., Llamazares, S., Rossell, D. and Gonzalez, C. (2010). Ectopic expression of germline genes drives malignant brain tumor growth in *Drosophila*. *Science* **330**, 1824-1827.

Januschke, J. and Gonzalez, C. (2008). *Drosophila* asymmetric division, polarity and cancer. *Oncogene* **27**, 6994-7002.

Jiang, Y., Scott, K. L., Kwak, S. J., Chen, R. and Mardon, G. (2011). Sds22/PP1 links epithelial integrity and tumor suppression via regulation of myosin II and JNK signaling. *Oncogene* **30**, 3248-3260.

Lee, T. and Luo, L. (2001). Mosaic analysis with a repressible cell marker (MARCM) for *Drosophila* neural development. *Trends Neurosci.* **24**, 251-254.

Leong, G. R., Goulding, K. R., Amin, N., Richardson, H. E. and Brumby, A. M. (2009). Scribble mutants promote aPKC and JNK-dependent epithelial neoplasia independently of Crumbs. *BMC Biol.* **7**, 62.

Lewis, P. W., Beall, E. L., Fleischer, T. C., Georlette, D., Link, A. J. and Botchan, M. R. (2004). Identification of a *Drosophila* Myb-E2F2/RBF transcriptional repressor complex. *Genes Dev.* **18**, 2929-2940.

Lu, X., Feng, X., Man, X., Yang, G., Tang, L., Du, D., Zhang, F., Yuan, H., Huang, Q., Zhang, Z. et al. (2009). Aberrant splicing of Hugl-1 is associated with hepatocellular carcinoma progression. *Clin. Cancer Res.* **15**, 3287-3296.

Mantovani, A. (2010). Molecular pathways linking inflammation and cancer. *Curr. Mol. Med.* **10**, 369-373.

Mechler, B. M., McGinnis, W. and Gehring, W. J. (1985). Molecular cloning of lethal(2)giant larvae, a recessive oncogene of *Drosophila melanogaster*. *EMBO J.* **4**, 1551-1557.

Nakagawa, S. and Huibregtse, J. M. (2000). Human scribble (Vartul) is targeted for ubiquitin-mediated degradation by the high-risk papillomavirus E6 proteins and the E6AP ubiquitin-protein ligase. *Mol. Cell. Biol.* **20**, 8244-8253.

Nguyen, D. X., Bos, P. D. and Massague, J. (2009). Metastasis: from dissemination to organ-specific colonization. *Nat. Rev. Cancer* **9**, 274-284.

Pagliarini, R. A. and Xu, T. (2003). A genetic screen in *Drosophila* for metastatic behavior. *Science* **302**, 1227-1231.

Palomero, T., Sulis, M. L., Cortina, M., Real, P. J., Barnes, K., Ciofani, M., Caparros, E., Buteau, J., Brown, K., Perkins, S. L. et al. (2007). Mutational loss of PTEN induces resistance to NOTCH1 inhibition in T-cell leukemia. *Nat. Med.* **13**, 1203-1210.

Parks, A. L., Cook, K. R., Belvin, M., Dompe, N. A., Fawcett, R., Huppert, K., Tan, L. R., Winter, C. G., Bogart, K. P., Deal, J. E. et al. (2004). Systematic generation of high-resolution deletion coverage of the *Drosophila melanogaster* genome. *Nat. Genet.* **36**, 288-292.

Pastor-Pareja, J. C., Wu, M. and Xu. T. (2008). An innate immune response of blood cells to tumors and tissue damage in Drosophila. *Dis. Model Mech.* **1**, 144-154.

Read, R. D., Cavenee, W. K., Furnari, F. B. and Thomas, J. B. (2009). A *Drosophila* model for EGFR-Ras and PI3K-dependent human glioma. *PLoS Genet.* **5**, e1000374.

Schimanski, C. C., Schmitz, G., Kashyap, A., Bosserhoff, A. K., Bataille, F., Schafer, S. C., Lehr, H. A., Berger, M. R., Galle, P. R., Strand, S. et al. (2005). Reduced expression of Hugl-1, the human homologue of *Drosophila* tumour suppressor gene lgl, contributes to progression of colorectal cancer. *Oncogene* **24**, 3100-3109.

Singh, J., Aaronson, S. A. and Mlodzik, M. (2010). *Drosophila* Abelson kinase mediates cell invasion and proliferation through two distinct MAPK pathways. *Oncogene* **29**, 4033-4045.

Summy, J. M. and Gallick, G. E. (2003). Src family kinases in tumor progression and metastasis. *Cancer Metastasis Rev.* **22**, 337-358.

Theodosiou, N. A. and Xu, T. (1998). Use of FLP/FRT system to study *Drosophila* development. *Methods* **14**, 355-365.

Thomas, S. M. and Brugge, J. S. (1997). Cellular functions regulated by Src family kinases. *Annu. Rev. Cell Dev. Biol.* **13**, 513-609.

Uhlirova, M. and Bohmann, D. (2006). JNK- and Fos-regulated Mmp1 expression cooperates with Ras to induce invasive tumors in *Drosophila*. *EMBO J.* **25**, 5294-5304.

Vidal, M. and Cagan, R. L. (2006). *Drosophila* models for cancer research. *Curr. Opin. Genet. Dev.* **16**, 10-16.

Vidal, M., Larson, D. E. and Cagan, R. L. (2006). Csk-deficient boundary cells are eliminated from normal *Drosophila* epithelia by exclusion, migration, and apoptosis. *Dev. Cell* **10**, 33-44.

Vidal, M., Warner, S., Read, R. and Cagan, R. L. (2007). Differing Src signaling levels have distinct outcomes in *Drosophila*. *Cancer Res.* **67**, 10278-10285.

Vidal, M., Salavaggione, L., Ylagan, L., Wilkins, M., Watson, M., Weilbaecher, K. and Cagan, R. (2010). A role for the epithelial microenvironment at tumor boundaries: evidence from *Drosophila* and human squamous cell carcinomas. *Am. J. Pathol.* **176**, 3007-3014.

Wang, D., Kennedy, S., Conte, D., Jr, Kim, J. K., Gabel, H. W., Kamath, R. S., Mello, C. C. and Ruvkun, G. (2005). Somatic misexpression of germline P granules and enhanced RNA interference in retinoblastoma pathway mutants. *Nature* **436**, 593-597.

Witte, H. T., Jeibmann, A., Klambt, C. and Paulus, W. (2009). Modeling glioma growth and invasion in *Drosophila melanogaster*. *Neoplasia* **11**, 882-888.

Woods, D. F. and Bryant, P. J. (1989). Molecular cloning of the lethal(1)discs large-1 oncogene of *Drosophila*. *Dev. Biol.* **134**, 222-235.

Wu, M., Pastor-Pareja, J. C. and Xu, T. (2010). Interaction between Ras(V12) and scribbled clones induces tumour growth and invasion. *Nature* **463**, 545-548.

Yang, J. and Weinberg, R. A. (2008). Epithelial-mesenchymal transition: at the crossroads of development and tumor metastasis. *Dev. Cell* **14**, 818-829.

OPEN ACCESS Freely available online

PLoS GENETICS

A Shared Role for RBF1 and dCAP-D3 in the Regulation of Transcription with Consequences for Innate Immunity

Michelle S. Longworth[1]*, James A. Walker[2,3], Endre Anderssen[2], Nam-Sung Moon[4], Andrew Gladden[5], Margarete M. S. Heck[6], Sridhar Ramaswamy[2], Nicholas J. Dyson[2]

1 Department of Molecular Genetics, The Lerner Research Institute, Cleveland Clinic, Cleveland, Ohio, United States of America, **2** Massachusetts General Hospital Cancer Center and Harvard Medical School, Charlestown, Massachusetts, United States of America, **3** Center for Human Genetic Research, Massachusetts General Hospital, Boston, Massachusetts, United States of America, **4** Department of Biology, Developmental Biology Research Initiative, McGill University, Montreal, Canada, **5** Department of Genetics, The University of Texas MD Anderson Cancer Center, Houston, Texas, United States of America, **6** Centre for Cardiovascular Science, Queen's Medical Research Institute, University of Edinburgh, Edinburgh, United Kingdom

Abstract

Previously, we discovered a conserved interaction between RB proteins and the Condensin II protein CAP-D3 that is important for ensuring uniform chromatin condensation during mitotic prophase. The *Drosophila melanogaster* homologs RBF1 and dCAP-D3 co-localize on non-dividing polytene chromatin, suggesting the existence of a shared, non-mitotic role for these two proteins. Here, we show that the absence of RBF1 and dCAP-D3 alters the expression of many of the same genes in larvae and adult flies. Strikingly, most of the genes affected by the loss of RBF1 and dCAP-D3 are not classic cell cycle genes but are developmentally regulated genes with tissue-specific functions and these genes tend to be located in gene clusters. Our data reveal that RBF1 and dCAP-D3 are needed in fat body cells to activate transcription of clusters of antimicrobial peptide (AMP) genes. AMPs are important for innate immunity, and loss of either dCAP-D3 or RBF1 regulation results in a decrease in the ability to clear bacteria. Interestingly, in the adult fat body, RBF1 and dCAP-D3 bind to regions flanking an AMP gene cluster both prior to and following bacterial infection. These results describe a novel, non-mitotic role for the RBF1 and dCAP-D3 proteins in activation of the *Drosophila* immune system and suggest dCAP-D3 has an important role at specific subsets of RBF1-dependent genes.

Citation: Longworth MS, Walker JA, Anderssen E, Moon N-S, Gladden A, et al. (2012) A Shared Role for RBF1 and dCAP-D3 in the Regulation of Transcription with Consequences for Innate Immunity. PLoS Genet 8(4): e1002618. doi:10.1371/journal.pgen.1002618

Editor: Giovanni Bosco, Univeristy of Arizona, United States of America

Received May 10, 2011; **Accepted** February 8, 2012; **Published** April 5, 2012

Funding: MSL was supported by a Leukemia and Lymphoma Society Career Development Fellowship Award, by a Charles King Trust Fellowship Award, and by Cleveland Clinic Foundation Seed funds. JAW was supported by a grant from the DOD (W81XWH-09-1-04871). NJD is the Saltonstall Scholar of the Massachusetts General Hospital Cancer Center. This study was supported by NIH grants GM53203 and CA64402 (to NJD) and CIHR grant MOP-93666 (to N-SM). The funders had no role in study design, data collection and analysis, decision to publish, or preparation of the manuscript.

Competing Interests: The authors have declared that no competing interests exist.

* E-mail: longwom@ccf.org

Introduction

The RB family proteins (pRB, p130 and p107 in humans; RBF1 and RBF2 in *Drosophila*) co-ordinate changes in gene expression. Understanding the types of programs that these proteins regulate is important because of the unequivocal link between the inactivation of RB proteins and human cancer. Mutation of the retinoblastoma tumor susceptibility gene (*RB1*) is the rate-limiting step in the genesis of retinoblastoma and over 90% of human tumors exhibit reduced pRB function [1,2].

RB family members are best-known for their roles in the regulation of E2F-dependent transcription. E2F-controlled genes are needed for cell proliferation and RB proteins suppress the expression of these targets during G0 and G1 of the cell cycle [3]. In addition, RB proteins are also important for the regulation of genes that are not involved in cell cycle progression. For example, osteoblast differentiation is modulated by pRB through its interaction with Runx2 [4]; in muscle cells, pRB promotes the expression of muscle-specific differentiation markers, enabling these cells to irreversibly exit the cell cycle [5–7]; in *Drosophila*, RBF1 cooperates with the Hippo pathway to maintain photoreceptor differentiation, independent of dE2F1 activity [8]. Such E2F-independent functions may help to explain why the inactivation of RB proteins can have very different consequences in different cellular contexts. However, many of the E2F-independent activities of RB proteins are not well-understood. At present, it is unclear if pRB has different activities in different cell types, or whether there is a yet-to-be discovered, general process that allows RB proteins to activate or repress the expression of variable sets of genes in different cell types.

Recent studies have suggested that pRB family members may impact the organization of higher-order chromatin structures, in addition to their local effects on the promoters of individual genes [9]. Mutation of pRB causes defects in pericentric heterochromatin [10] and RBF1 is necessary for uniform chromatin condensation in proliferating tissues of *Drosophila* larvae [11]. Part of the explanation for these defects is that RBF1 and pRB promote the localization of the Condensin II complex protein, CAP-D3 to DNA both in *Drosophila* and human cells [11]. Depletion of pRB from human cells strongly reduces the level of CAP-D3 associated with centromeres during mitosis and causes centromere dysfunction [12].

Condensin complexes are necessary for the stable and uniform condensation of chromatin in early mitosis [13–16]. They are

Author Summary

The retinoblastoma protein (pRB) is a tumor suppressor protein known for its ability to repress transcription of E2F-dependent genes and induce cell cycle arrest. We have previously shown that RB proteins in *Drosophila* and human cells interact with the Condensin II subunit, CAP-D3, in an E2F-independent manner. Condensins promote condensation of chomosomes in mitosis. Our previous studies suggested that the *Drosophila* pRB and CAP-D3 homologs, RBF1 and dCAP-D3, co-localize on DNA and may share a function in cells that never undergo mitosis. In this study, we show that one non-mitotic function shared between RBF1 and dCAP-D3 is the regulation of many non-cell-cycle-related, clustered, and cell-type-specific transcripts including a conserved family of genes that are important for the immune response in the fly. In fact, results show that normal levels of dCAP-D3 and RBF1 expression are necessary for the ability of the fly to clear infection with human bacterial pathogens. This work demonstrates that dCAP-D3 proteins can regulate a unique subset of RBF1-dependent transcripts *in vivo* and identifies a novel role for both RBF1 and dCAP-D3 protein in activation of innate immune genes, which may be conserved in human cells.

conserved from bacteria to humans with at least two types of Condensin complexes (Condensin I and II) present in higher eukaryotes. Both Condensin I and II complexes contain heterodimers of SMC4 and SMC2 proteins that form an ATPase which acts to constrain positive supercoils [17,18]. Each type of Condensin also contains three specific non-SMC proteins that, upon phosphorylation, stabilize the complex and promote ATPase activity [14,19,20]. The kleisin CAPH and two HEAT repeat containing subunits, CAP-G and CAP-D2 are components of Condensin I, while the kleisin CAP-H2 and two HEAT repeat containing subunits, CAP-G2 and CAP-D3, are constituents of Condensin II.

Given the well-established functions of Condensins during mitosis, and of RBF1 in G1 regulation, the convergence of these two proteins was unexpected. Nevertheless, mutant alleles in the non-SMC components of Condensin II suppress RBF1-induced phenotypes, and immunostaining experiments revealed that RBF1 displays an extensive co-localization with dCAP-D3 (but not with dCAP-D2) on the polytene chromatin of *Drosophila* salivary glands [11]. This co-localization occurs in cells that will never divide, suggesting that Condensin II subunits and RBF1 co-operate in an unidentified process in non-mitotic cells. In various model organisms, the mutation of non-SMC Condensin subunits has been associated with changes in gene expression [21–24] raising the possibility that dCAP-D3 may affect some aspect of transcriptional regulation by RBF1. However, the types of RBF1-regulated genes that might be affected by dCAP-D3, the contexts in which this regulation becomes important, and the consequences of losing this regulation are all unknown.

Here we identify sets of genes that are dependent on both *rbf1* and *dCap-D3*. The majority of genes that show altered expression in both *rbf1* and *dCap-D3* mutants (larvae or adults) are not genes involved in the cell cycle, DNA repair, proliferation, but are genes with cell type-specific functions and many are spaced within 10 kb of one another in "gene clusters". To better understand this mode of regulation we have investigated the effects of RBF1 and dCAP-D3 on one of the most highly misregulated clusters which includes genes coding for antimicrobial peptides (AMPs). AMPs are produced in many organs, and one of the major sites of production is in the fat body. Following production in the fat body, AMPs are subsequently dumped into the hemolymph where they act to destroy pathogens [25]. RBF1 and dCAP-D3 are required for the transcriptional activation of many AMPs in the adult fly. Analysis of one such gene cluster shows that RBF1 and dCAP-D3 bind directly to this region and that they bind, in the fat body, to sites flanking the locus. RBF1 and dCAP-D3 are both necessary in the fat body for maximal and sustained induction of AMPs following bacterial infection, and RBF1 and dCAP-D3 deficient flies have an impaired ability to respond efficiently to bacterial infection. These results identify dCAP-D3 as an important transcriptional regulator in the fly. Together, the findings suggest that RBF1 and dCAP-D3 regulate the expression of clusters of genes in post-mitotic cells, and this regulation has important consequences for the health of the organism.

Results

RBF1 and dCAP-D3 regulate many of the same genes during the later stages of the *D. melanogaster* life cycle

Our previous data demonstrated that RBF1 co-localizes extensively with dCAP-D3 on polytene chromatin of non-dividing cells, leading us to hypothesize that the two proteins may co-operate to regulate transcription. To begin to test this idea, we first identified the stages of fly development where RBF1 and dCAP-D3 were most highly expressed. qRT-PCR using primers for *dCap-D3* and *rbf1* was performed on cDNA generated from various stages of the *Drosophila* life cycle (Figure 1A). The results demonstrate that both genes are transcribed at the highest levels in late third instar larval and adult stages. Concordantly, immunostaining for dCAP-D3 and RBF1 in cryosections of the abdomens of wild type flies confirmed that both proteins are highly expressed in the adult and that they are both present in the nuclei of many cells in normal adult tissues (Figure 1B).

Preliminary experiments showed that dCAP-D3 levels could influence the expression of very few of the previously identified RBF1-dependent transcripts. To gain a more complete understanding of the abundance and characteristics of RBF1/dCAP-D3 shared transcriptional targets, we carried out a microarray analysis of the entire *Drosophila melanogaster* genome and compared gene expression profiles of wild type, *dCap-D3* and *rbf1* mutant flies, at both the third instar larval and adult stages (Table S1). Since the null mutants are lethal, females expressing a transheterozygous combination of null and hypomorphic alleles were used for these experiments. The mutant flies used for microarray analysis expressed about 15% of wild type levels of each gene as judged by qRT-PCR and western blot (Figure S1). The microarray results revealed an extensive and highly significant overlap between RBF1 and dCAP-D3 regulated gene sets in both adults and larvae (Figure 2A and 2B). Shared target genes were evident in both upregulated and downregulated gene sets. Although some genes were mis-expressed in both larvae and adults, the majority of transcriptional changes were stage specific. The most highly significant p values for shared target gene sets were seen in upregulated larval genes (genes repressed by RBF1 and dCAP-D3 in the larvae, $p \leq 6.34E\text{-}130$) and downregulated adult genes (genes activated by RBF1 and dCAP-D3 in the adult, $p \leq 9.88E\text{-}95$) (Figure 2B). This suggests that RBF1 and dCAP-D3 may cooperate to repress specific programs during one stage of development and activate other programs in a later, more differentiated stage. Interestingly, at both stages, the genes dependent on both RBF1 and dCAP-D3 represented 15–17% of the total number of genes dependent on RBF1 in a given

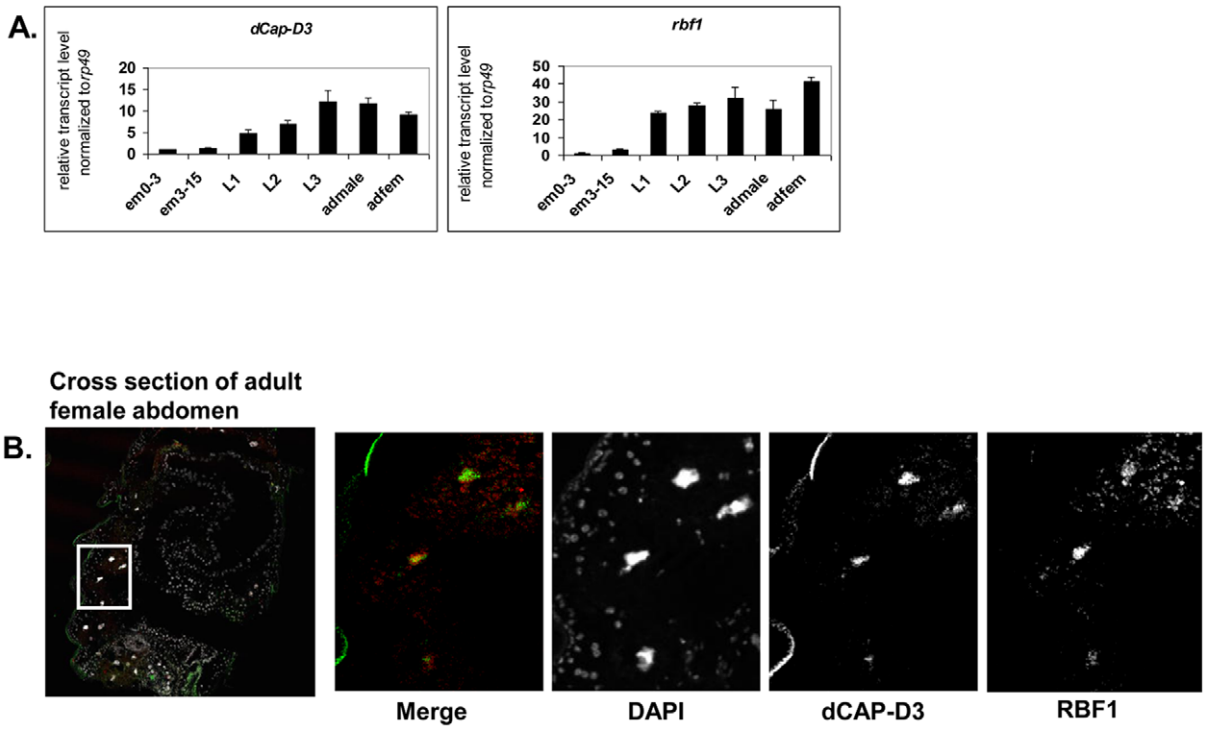

Figure 1. RBF1 and dCAP-D3 are highly expressed at later stages of development and co-localize in adult tissues. A) qRT-PCR for *rbf1* transcript levels and *dCap-D3* transcript levels in wild type *Drosophila* embryos aged for 0–3 hours (em0–3), embryos aged for 3–15 hours (em3–15), first instar larvae (L1), second instar larvae (L2), third instar larvae (L3), adult males (admale) or adult females (adfem) demonstrate high expression levels in the later life cycle stages. B) Immunostaining for RBF1 and dCAP-D3 in cryosections of adult female flies indicates co-localization in large nuclei of cells present underneath the cuticle. Images presented are a magnification of the area highlighted by the white box in the first image.
doi:10.1371/journal.pgen.1002618.g001

developmental stage and 47–55% of the total number of genes dependent on dCAP-D3 in a given developmental stage. Thus RBF1 appears to be important at close to half of the transcriptional targets of dCAP-D3.

Characteristics of RBF1/dCAP-D3 shared target genes

We noticed that the lists of RBF1/dCAP-D3 shared target genes had two general properties. First, these genes are almost completely different from the lists of E2F-regulated genes that have been reported previously [26]. As expected, many of the targets that were upregulated in *rbf1* mutant larvae could be categorized as E2F target genes involved in DNA repair, DNA replication and continuation of the cell cycle (comparison to microarray data from [26] and GO analyses of rbf1 mutant larvae-data not shown). However, few if any, of these cell cycle/proliferation related genes were altered in the *dCap-D3* mutant flies (Figure 2C) suggesting that *dCap-D3* regulates a different subset of RBF1 dependent targets. In fact, less than 6% of dCAP-D3/RBF1 shared target genes in larvae were found to be bound by dE2F1 in dE2F1 ChIP-chip experiments (Korenjak et. al., unpublished data). Unexpectedly, many of the known E2F target genes did not show a significant increase in expression in *rbf1* mutant adults (Figure 2C). This may reflect cell-type specific differences in the requirement for RBF1. In support of this idea, qRT-PCR analysis of dissected tissues showed that few E2F-regulated genes were upregulated in ovaries of *rbf1* mutants, but many did show a significant increase in the rest of the carcass (Figure S2). However, even in the tissues where these E2F-regulated proliferation genes did increase in expression levels in *rbf1* mutant adults, these transcripts were not upregulated in tissues from *dCap-D3* mutant flies (Figure S2). We infer that dCAP-D3 is not a key factor at most of the well-characterized E2F regulated genes in either larvae or adults. While unlikely, it is a formal possibility that the remaining amounts of dCAP-D3 protein present in the hypomorphic mutant flies might be sufficient for the regulation of E2F targets, but not for other target genes.

Second, we noted that genes that are similarly dependent on RBF1 and dCAP-D3 tend to be clustered on the genome and are often positioned within 10 kb of one another (Table 1). To determine whether this was an unusual feature, we compared the frequency of RBF1/dCAP-D3shared target genes positioned within 10 kb of one another to hundreds of simulations of randomly chosen *Drosophila* genes (Table 1). The results showed that genes exhibiting increased expression in *rbf1* and *dCap-D3* mutant adults (ie. genes that are apparently repressed both by RBF1 and dCAP-D3 are 25 times more likely to be clustered. Genes that were downregulated in *rbf1* and *dCap-D3* mutant adults (i.e. genes apparently activated by both RBF1 and dCAP-D3) are 15 times more likely to be clustered. Clustering of shared target genes was also seen in the larvae, although the fold difference was greatly diminished (5 fold) for the activated genes. Overall, the clustering effect was 3–7 fold more prevalent in dCAP-D3 regulated genes than in RBF-regulated genes. By way of comparison, RBF1/dCAP-D3 shared target genes in the larvae exhibited a much greater degree of clustering than the larval genes regulated by Hop or Nurf301, two other well-known chromatin remodeling proteins shown to regulate clusters of genes [27]. A list of the actual groupings of clustered genes is presented in Table S2.

Although proliferation-related genes were missing, gene ontology (GO) classification of the RBF1/dCAP-D3 shared target genes

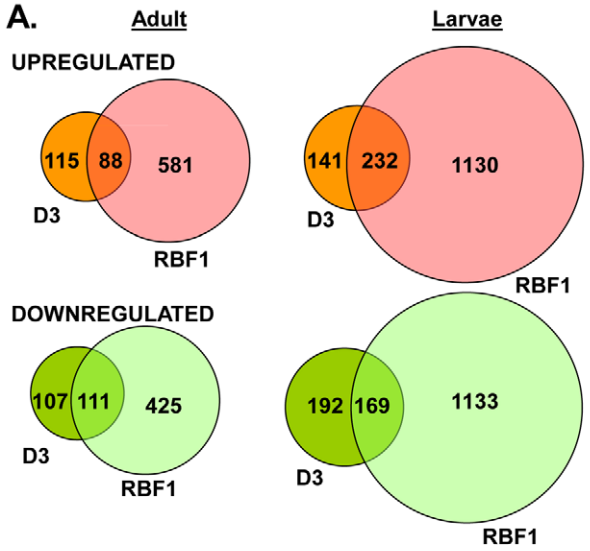

C.

	Wild Type	St Dev	dCAP-D3 mutant	St Dev	RBF1 mutant	St Dev
dnk	1.01	0.16	1.04	0.25	1.29	0.40
mus209	1.01	0.17	1.27	0.30	0.80	0.44
dup	1.01	0.22	1.12	0.24	1.22	0.04
dnapol alpha 50	1.01	0.13	1.10	0.22	1.58	0.42
dnapol delta	1.01	0.20	1.12	0.23	1.49	0.68
orc1	1.01	0.15	1.14	0.26	1.36	0.23
RnrS	1.00	0.07	1.45	0.25	1.65	0.47
Mcm7	1.00	0.04	1.38	0.16	1.59	0.75
Mcm3	1.01	0.14	1.06	0.16	1.25	0.16
Mcm2	1.01	0.15	1.33	0.19	1.07	0.40
Mcm5	1.00	0.05	1.43	0.22	1.55	0.54
CG5250	1.10	0.52	199.66	111.00	88.40	36.79

D.

UPREGULATED- larvae only	
GO:0003824	catalytic activity
GO:0008527	taste receptor activity

DOWNREGULATED-adults only	
GO:0050830	defense response to Gram-positive bacterium
GO:0001708	cell fate specification
GO:0007219	Notch signaling pathway
GO:0004252	serine-type endopeptidase activity
GO:0048513	organ development
GO:0000902	cell morphogenesis
GO:0035264	multicellular organism growth
GO:0051252	regulation of RNA metabolic process
GO:0007365	periodic partitioning
GO:0017171	serine hydrolase activity

B.

Upregulated shared target genes

	D3adult-WTadult	RBF1adult-WTadult	D3larvae-WTlarvae	RBF1larvae-WTlarvae
D3adult-WTadult		2.71E-58	7.25E-58	2.18E-23
RBF1adult-WTadult	9.88E-95		9.84E-27	5.58E-27
D3larvae-WTlarvae	1.58E-30	2.17E-15		6.34E-130
RBF1larvae-WTlarvae	4.27E-19	2.47E-37	6.98E-71	

Downregulated shared target genes

Figure 2. RBF1 and dCAP-D3 regulate many of the same transcripts in the fly. RNA was isolated from *rbf1* mutant and *dCap-D3* mutant female third instar larvae and adult flies. cDNA was hybridized to Nimblegen 385 k whole genome arrays. A) Venn diagrams show the numbers of RBF1, dCAP-D3 or RBF1/dCAP-D3 shared target genes which exhibited at least a 2 fold log change in expression with a p value of ≤0.15. Genes significantly upregulated in the mutant flies are shown in red while genes significantly downregulated are shown in green. B) P values for shared RBF1 and dCAP-D3 target genes indicate that RBF1 and dCAP-D3 regulate a significant number of the same genes in both adults and larvae. The numbers above the diagonal represent p-values for upregulated shared subsets and are colored red while the numbers below the diagonal represent p-values for downregulated shared genes and are colored green. C) qRT-PCR analyses of 12 E2F targets shows that the majority of RBF1/dCAP-D3 shared targets are not E2F targets. The one target that was significantly upregulated in dCAP-D3 and RBF1 mutant flies, *CG5250*, is highlighted in red. Results are the average of three independent experiments involving 10 female flies per genotype. D) Significant (p≤0.05) Gene Ontology (GO) groupings for shared target genes include defense response genes in the adult fly. The top box lists GO categories for upregulated shared genes in mutant larvae only, and the bottom box lists selected GO categories for downregulated shared genes in adults only. There were no significant GO groupings for upregulated shared target genes in adults or for downregulated shared target genes in the larvae.
doi:10.1371/journal.pgen.1002618.g002

revealed many significant categories in the lists of up- and downregulated genes in the adult, and for shared, repressed target genes in the larvae (Figure 2D, complete list for downregulated adult genes in Table S3). One of the most interesting GO categories represented in the adults were the defense response genes (GO:0050830). The fly relies on an innate immune system to defend against invading pathogens. This immune system is comprised of three major mechanisms: 1) phagocytosis, 2) induction of coagulation and melanization, and 3) production of Antimicrobial Peptides or AMPs.

Phagocytosis is a conserved mechanism that is often the primary cellular defense used by many organisms to engulf and destroy pathogens. In *Drosophila*, circulating blood cells called hemocytes phagocytose bacteria, fungi, and parasitic wasp eggs [28]. RBF1 and dCAP-D3 mutant adult microarray data was analyzed for changes in levels of 19 different genes reported to be involved in phagocytosis in *Drosophila* (Table S4). Of these 19 genes, 2 genes demonstrated significant changes in transcript levels in adults. *NimC1*, a gene expressed in plasmatocytes which make up 95% of *Drosophila* hemocytes, has been shown to be necessary for phagocytosis of bacteria [29], and was significantly upregulated in RBF1 and dCAP-D3 mutant adults. Embryonic and larval hematopoiesis depends on a number of transcription factors including Gcm [30,31]. *Gcm* transcripts were demonstrated to be downregulated in both RBF1 and dCAP-D3 adults (Table S4). While adult hemocytes do display phagocytic properties, they do not differentiate into specialized cells upon immune challenge [32,33], and it is therefore unlikely that misregulation of *gcm* in adults would affect phagocyte numbers.

In response to septic injury, proteolytic cascades are triggered which lead to coagulation and melanization. Reactive oxygen species formed during these processes, as well as the actual deposition of melanin, are thought to be toxic to microorganisms [34]. After scanning the literature for genes involved in coagulation and melanization, and then analyzing RBF1 and

Table 1. RBF1 and dCAP-D3 tend to regulate clusters of genes.

Gene Set	*Ratio for upregulated*^*	*Ratio for downregulated*^*
Whole adult dCAP-D3 mut	12.42	11.68
Whole adult RBF1 mut	3.93	4.41
Whole adult shared targets	25.00	15.87
Whole larvae dCAP-D3 mut	14.2	11.59
Whole larvae RBF1 mut	2.60	2.03
Whole larvae shared targets	22.58	3.68
Whole larvae Hop mut**	1.91	1.30
Whole larvae Nurf301 mut**	1.55	1.30

*The ratio of observed clustering to expected clustering for the lists of differentially expressed genes between mutant and wild -type organisms (fdr<0.15, log2 fc>0.1) shows that RBF1 and dCAP-D3 shared target genes are 6–10 fold more likely to be present in clusters. Chromosomal clustering is calculated as the number of pairs of genes within 10,000 bp among the differentially expressed genes. The expected number is the average clustering of 500 random gene lists of the same length as the corresponding list of differentially expressed genes.

**Raw data for Hop and Nurf301 mutant larvae was obtained from supplemental data files found in [27].

^False Discovery Rates for all ratios presented were <0.05.

doi:10.1371/journal.pgen.1002618.t001

dCAP-D3 mutant adult microarray data for changes in transcript levels of these genes, it was determined that only one of the reported genes, *CG8193* was significantly increased in both RBF1 and dCAP-D3 mutant adults (Table S5). CG8193/PPO2 is thought to encode a phenol-oxidase constitutively expressed in crystal cells, a type of hemocyte cell involved in melanization [35].

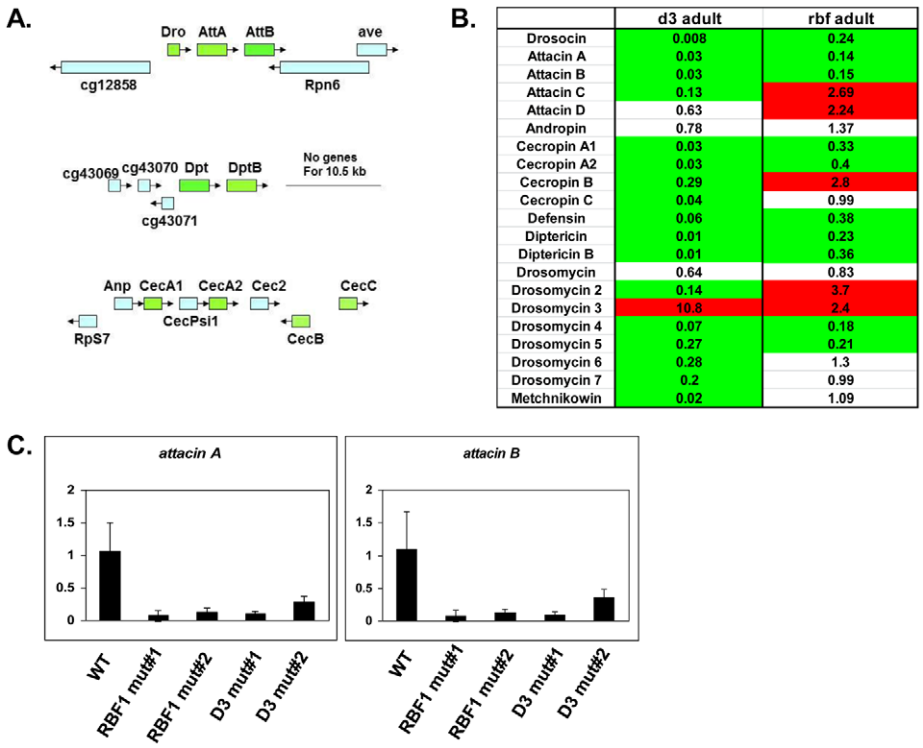

	d3 adult	rbf adult
Drosocin	0.008	0.24
Attacin A	0.03	0.14
Attacin B	0.03	0.15
Attacin C	0.13	2.69
Attacin D	0.63	2.24
Andropin	0.78	1.37
Cecropin A1	0.03	0.33
Cecropin A2	0.03	0.4
Cecropin B	0.29	2.8
Cecropin C	0.04	0.99
Defensin	0.06	0.38
Diptericin	0.01	0.23
Diptericin B	0.01	0.36
Drosomycin	0.64	0.83
Drosomycin 2	0.14	3.7
Drosomycin 3	10.8	2.4
Drosomycin 4	0.07	0.18
Drosomycin 5	0.27	0.21
Drosomycin 6	0.28	1.3
Drosomycin 7	0.2	0.99
Metchnikowin	0.02	1.09

Figure 3. RBF1 and dCAP-D3 activate basal transcript levels of genes coding for Antimicrobial Peptides (AMPs). A) Graphic depictions of three separate AMP loci. The *Attacin* and *Diptericin* loci are located on Chromosome 2R at 51C1 and 55F8, respectively. The *Cecropin* locus is located on Chromosome 3R at 99E2. Genes within each locus are drawn in correct orientation to one another but are not drawn to scale. Genes colored in green are downregulated in dCAP-D3 mutant adult carcasses dissected of ovaries and most are also downregulated RBF1 mutants. Genes colored in blue remain unchanged in dCAP-D3 and RBF1 mutants. B) qRT-PCR analyses of transcript levels for 21 AMPs in female adult bodies (N = 10) with ovaries dissected shows that dCAP-D3 and RBF1 each regulate a much larger number of AMPs than originally indicated by the microarray results. Genes significantly upregulated in the mutants are highlighted in red and genes significantly downregulated in the mutants are highlighted in green. Transcript levels were normalized to tubulin 84B. All results had false discovery rates ≤0.05. C) qRT-PCR analysis of cDNA from wild type (WT/w^{1118}), *rbf1* mutant #1 ($rbf1^{120a}/rbf1^{\Delta 14}$), *rbf1* mutant #2 ($rbf1^{120a}/rbf1^{120a}$), *dCap-D3* mutant #1 ($dCap\text{-}D3^{c07081}/dCap\text{-}D3^{\Delta 25}$) and *dCap-D3* mutant #2 ($dCap\text{-}D3^{c07081}/dCap\text{-}D3^{c07081}$) female adult whole flies confirms that two AMP target genes are regulated by both RBF1 and dCAP-D3, regardless of mutant genotype. Transcript levels were normalized to *tubulin 84B* mRNA levels.

doi:10.1371/journal.pgen.1002618.g003

However, overexpression of CG8193/PPO2 in cell lines or in flies does not induce constituitive melanization [36], nor did we see any evidence of melanotic lesions in RBF1 or dCAP-D3 mutant adults.

Several of the genes in the adult, downregulated GO category of "defense response to Gram positive bacteria" (Figure 2D and Table S3) fall into a family of proteins known as Antimicrobial Peptides or AMPs. In fact, two of these genes, *AttA* and *AttB*, represented some of the most highly deregulated targets in the mutant adults. Upon closer inspection of the microarray data, it was revealed that many other AMP genes were also deregulated in dCAP-D3 and/or RBF1 mutant adults, however their p-values were just below the confidence level. In addition, many of the AMP genes are present in clusters and located immediately next to one another in the genome (Figure 3A), making them an enticing group of genes for further study.

AMPs are shared targets of RBF1 and dCAP-D3 in the adult fat body

To confirm that the transcription of AMPs was indeed dependent on both RBF1 and dCAP-D3, qRT-PCR analysis was performed using cDNA generated from *dCap-D3* or *rbf1* transheterozygotes (using whole female mutant flies whose ovaries had been dissected) (Figure 3B). Results showed that 17 of the 21 AMPs tested were downregulated in the *Cap-D3* mutants and 10 of those genes were similarly dependent on RBF1. qRT-PCR for AMPs performed on different allelic combinations of *rbf1* and *Cap-D3* mutants gave similar results (Figure 3C).

AMPs constitute one of the major defense mechanisms against bacterial and/or fungal infection in the fly [25,37,38]. They are produced in various adult tissues but one of the main organs responsible for their production is the fat body. Once produced in the fat body, AMPs are secreted into the hemolymph where they destroy or inhibit growth of pathogens [39].

We set out to test the hypothesis that RBF1 and dCAP-D3 regulate AMP genes in the adult fat body. First, we examined whether RBF1 and dCAP-D3 are expressed in this cell type. The *yolk-GAL4* driver was used to express GFP in adult fat body cells, effectively marking this cell type in green. Combined immunostaining for RBF1 and dCAP-D3 localization in cryosections of adult wild type abdomens revealed a strong staining for both RBF1 and dCAP-D3 in the nuclei of adult fat body cells (Figure 4A, yellow arrows). *yolk-GAL4* has been characterized to drive expression in *Drosophila* at approximately 2–5 days post eclosure [40], making it possible to drive expression of transgenes after the majority of fly development has occurred. The staining for RBF1 and dCAP-D3 in the adult abdomens was specific, as *yolk-GAL4* driven expression of dsRNAs directed against RBF1 and dCAP-D3 specifically abrogated staining of their respective targets in fat body cells, without dramatically altering gross tissue morphology (Figure S3).

Next, we measured the changes in expression of AMPs in animals where *yolk-GAL4* driven expression of dsRNAs had reduced the expression of either RBF1 or dCAP-D3 in the fat body. qRT-PCR of cDNA from whole adult females showed a significant decrease in the expression of multiple AMP genes including *diptericin*, *diptericin B* and *Cecropin A2* (Figure 4B) in the knockdown flies. Interestingly, the fold change in transcript levels for *diptericin* was comparable to the changes seen in *dCap-D3* and *rbf1* mutant animals. These results suggest that the yolk-GAL4-expressing cells are a primary site of constitutive *diptericin* expression in adult flies and that in these cells, RBF1 and dCAP-D3 are both needed to drive the basal expression levels of specific AMPs.

Regulation of an AMP cluster by RBF1 and dCAP-D3 is direct and dynamically changes over the course of bacterial infection

AMP genes can be regulated by multiple transcription factors [41–44]. We sought to determine, therefore, whether transcriptional regulation of these genes by RBF1 and dCAP-D3 was direct. For our ChIP analysis we focused on *diptericin* and *diptericin B*; two AMP genes that are situated within 1200 bp of one another (Figure 5B), that have well characterized promoters [45–47], and whose basal expression was dependent on both RBF1 and dCAP-D3 in the fat body (Figure 3B and Figure 4B). In addition, the basal transcript levels of at least one other gene in the region, *CG43070*, was found to be significantly activated by both RBF1 and dCAP-D3 (Figure S4).

To study the binding of RBF1 and dCAP-D3 at the *diptericin* locus *in vivo*, transgenic fly lines were created which expressed N-terminally FLAG-HA tagged dCAP-D3 or N-terminally FLAG-HA tagged RBF1 under the control of the UAS promoter. These lines were then crossed to *yolk-GAL4/FM7* lines to create progeny in which the tagged protein was specifically expressed in the adult fat body. ChIP using FLAG antibody in FLAG-HA-dCAP-D3 expressing flies demonstrated that dCAP-D3 binds to two separate regions located approximately 3 kb upstream and 900 bp downstream of the *diptericin* locus (Figure 5A and red bars in Figure 5B). Since *diptericin* is strongly induced in response to bacterial infection, we examined the effect of infection with *S. aureus* on the binding of dCAP-D3 to the *diptericin* locus. Strikingly, dCAP-D3 binding to the upstream site significantly increased after *S. aureus* infection (compare red bars to yellow bars, Figure 5B).

ChIP for FLAG in FLAG-HA-RBF1 expressing flies indicated that RBF1 binds to the identical upstream and downstream regions of the *diptericin* locus as dCAP-D3 (red bars in Figure 5C). This binding was detected both before and after infection with *S. aureus* (blue and yellow bars in Figure 5C), but unlike the results for dCAP-D3 binding, RBF1 binding was most significant prior to infection. ChIP for FLAG protein in flies expressing the FLAG-HA construct alone showed almost no signal at any of the primer sets used in these experiments (Figure 5D). Taken together, ChIP results show that 1) RBF1 and dCAP-D3 can bind directly to an AMP gene cluster at identical binding sites, 2) that the binding sites flank the *diptericin* and *diptericin B* genes, and 3) dCAP-D3 binding increases when gene expression is induced in response to bacterial infection.

For comparison, we also performed ChIP for dCAP-D3 on the *CG5250* locus. *CG5250* was the one previously identified direct target of RBF1 [26] that we found to be repressed by RBF1 and dCAP-D3 and to be consistently upregulated in all tissues of *rbf1* and *dCap-D3* mutant animals (Figures S2 and S5A). ChIP using FLAG antibody in FLAG-HA-dCAP-D3 expressing flies demonstrated a small amount of binding in the open reading frame of *CG5250* (Figure S5B and S5C). This binding pattern obtained with the FLAG antibody closely resembled the ChIP signal found when a dCAP-D3 antibody was used to immunoprecipiate the endogenous dCAP-D3 protein expressed everywhere in the adult fly (Figure S5D).

The ability of RBF1 and dCAP-D3 to regulate basal levels of AMP transcription prompted the question of whether these proteins were also necessary for the regulation of AMP transcription in response to bacterial infection. cDNA was generated from female adult flies expressing dCAP-D3 or RBF1 dsRNAs specifically in the fat body, at various time-points post-infection with *Staphylococcus aureus* (Figure 6). dsRNAs have been used successfully in the past to decrease *in vivo* expression levels of

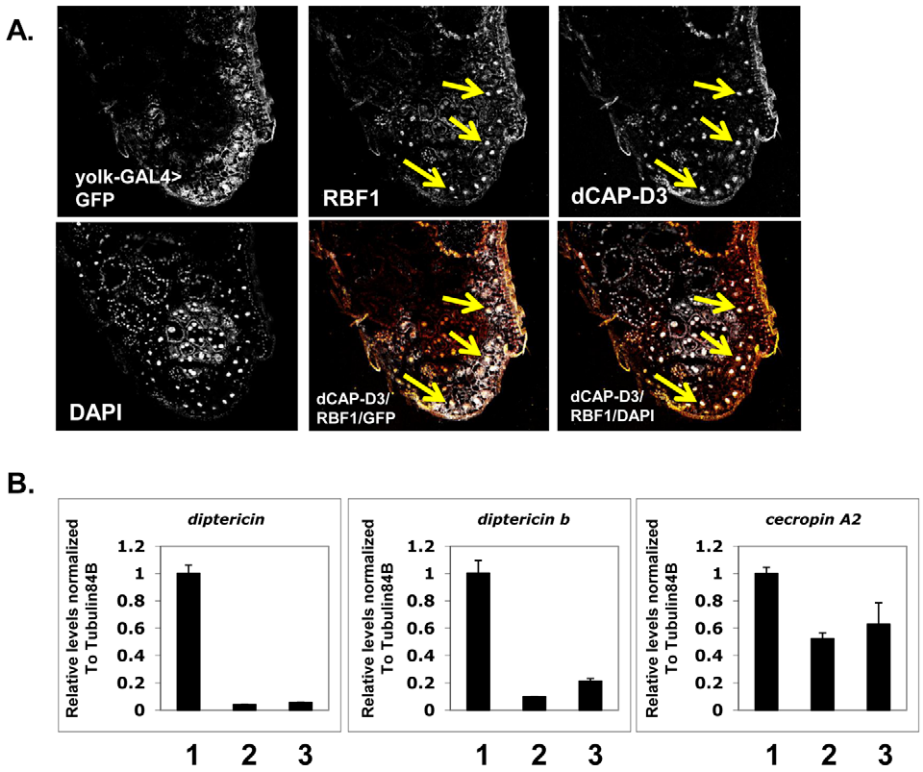

Figure 4. Basal AMP transcript levels are activated by RBF1 and dCAP-D3 specifically in the fat body. A) Immunofluorescence analysis of RBF1 and dCAP-D3 performed on cryosections of adult female flies expressing GFP under the control of the fat body specific *yolk-GAL4* driver indicates that RBF1 and dCAP-D3 co-localize in the nuclei of fat body cells. Yellow arrows highlight fat body cells. B) qRT-PCR analysis of cDNA from 1) flies expressing driver alone (*yolk-GAL4/+;+;+*), 2) flies expressing *rbf1 dsRNA (yolk-GAL4;+;UAS-rbf1 dsRNA)* in the fat body cells and 3) flies expressing *dCAP-D3 dsRNA (yolk-GAL4;+;UAS-dCAP-D3 dsRNA)* in the fat body cells shows significant decreases in AMP levels. For each genotype, N = 10.
doi:10.1371/journal.pgen.1002618.g004

proteins involved in innate immunity and to study their effects on responses to bacterial infection [48].

qRT-PCR for AMPs indicated two types of transcriptional defects in the RBF1 and dCAP-D3 deficient flies. In agreement with our earlier results, basal transcript levels of *diptericin* were reduced as a result of deficiency for either protein (Figure 6B, inset boxes). Following infection, *diptericin* transcripts remained very low in the dCAP-D3 deficient tissue and induction was minimal and severely delayed in comparison to GFP dsRNA expressing "wild type" control flies. RBF1 deficiency, however, allowed normal induction of *diptericin* transcripts. *Drosomycin* is an AMP gene downstream of the Toll pathway, and it is strongly induced following infection with Gram positive bacteria or fungi [49]. qRT-PCR for levels of *Drosomycin* revealed a much different defect in expression. Neither dCAP-D3 nor RBF1 deficiency in the fat body had any effect on basal levels of *Drosomycin*, a result consistent with our microarray data from whole flies. However, both dCAP-D3 and RBF1 deficiency caused significant decreases in the maximal expression levels of *drosomycin* at 24 hours post-infection (Figure 6A).

The biological response to bacterial infection in the fly requires dCAP-D3 and RBF1

Next, we tested whether the inefficient transcription of AMPs that results from decreased expression of RBF1 or dCAP-D3 has a significant effect on the ability of the fly to recover from exposure to pathogenic bacteria. Survival rates after infection with the Gram positive bacterium, *Staphylococcus aureus* (Figure 7A, Figure 8A) or with the Gram negative bacterium, *Pseudomonas aeruginosa* (Figure 7B, Figure 8B) were measured in five different genotypes: females expressing GFP dsRNAs under the control of the yolk-GAL4 driver ("wild-type controls", *yolk-GAL4* driving expression of dCAP-D3 dsRNA in the fat body, *yolk-GAL4* driving expression of RBF1 dsRNA in the fat body, and positive control females which were either mutant for the Eater protein or expressing dsRNAs against the IMD protein. IMD is a major mediator of innate immune signaling in *Drosophila* [50]. Eater is a known phagocytic receptor necessary for the response to infection with Gram positive bacteria [51]. We did not include data on flies expressing Eater dsRNAs under the control of yolk-GAL4, since Kocks et al [51] reported that Eater is not expressed in the fat body. In agreement with this, expression of Eater dsRNA in the fat body exhibited no changes in the ability of the fly to clear bacteria, while the Eater mutants described above showed a striking inability to phagocytize bacteria 5 hours following infection (data not shown and Figure 7). Following infection with *S. aureus*, both dCAP-D3 and RBF1 deficient flies were more susceptible to infection in comparison to flies expressing GFP dsRNAs (Figure 7A and Figure 8A). dCAP-D3 deficient flies were also more susceptible to infection with Gram negative bacteria, but this was not the case for RBF1 deficient flies, as their survival rates were not significantly decreased (Figure 7B and Figure 8B). These data demonstrate that acute knockdown of dCAP-D3 or RBF1 in the fat body of adult flies renders them more susceptible to bacterial infection, most likely due to inefficient transcription of AMP genes.

Recently, a number of reports have identified genes whose mutation can reduce the ability of the fly to survive bacterial

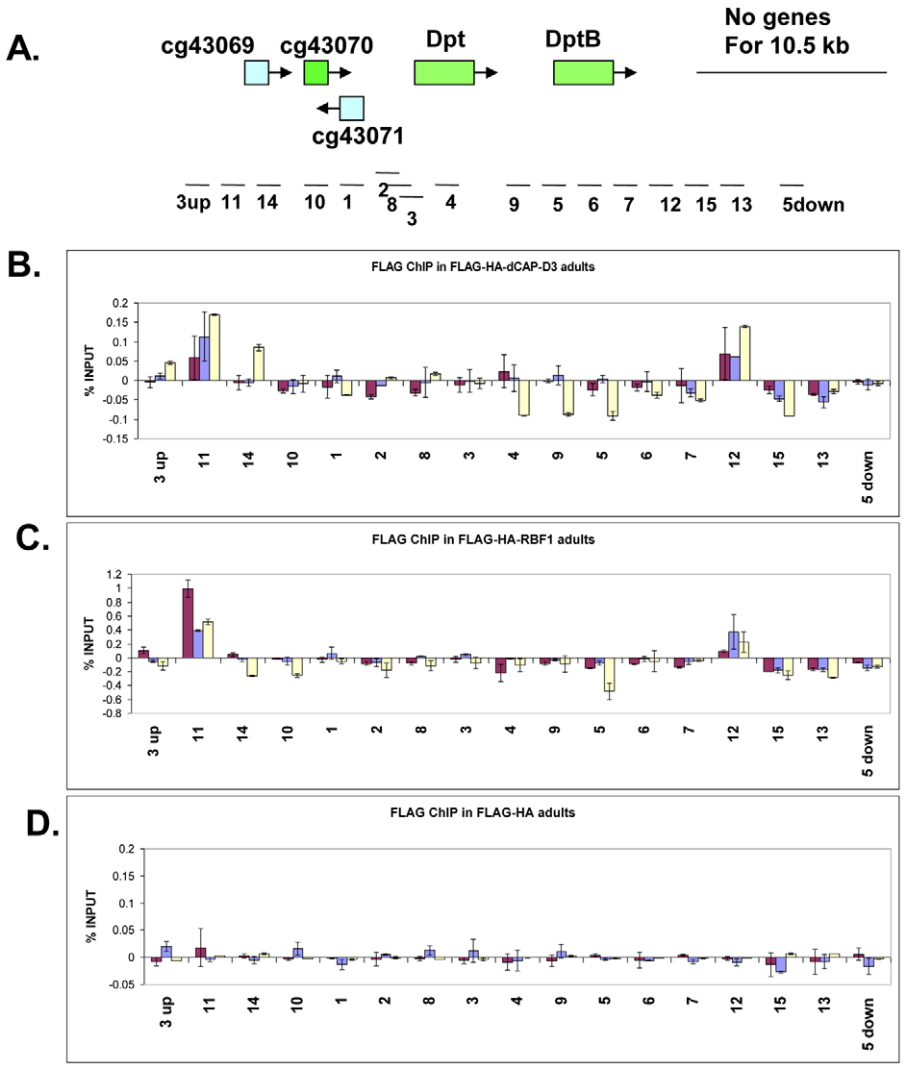

Figure 5. RBF1 and dCAP-D3 bind to an AMP locus *in vivo*. A) Graphic representation of the locus on which Chromatin Immunoprecipitation (ChIP) for RBF1 and dCAP-D3 in the adult fat body was performed. Genes highlighted in green are activated by both RBF1 and dCAP-D3 in the fat body. Positions of primer sets used are listed under the diagram of the locus. B) Chromatin immunoprecipitation for FLAG protein in female adult flies expressing FLAG-HA-dCAP-D3 in the fat body (*yolk-GAL4/+; +; UAS-FLAG-HA-dCap-D3/+*) demonstrates that the *diptericin* locus is a direct target of dCAP-D3. ChIP signal corresponding to FLAG-HA-dCAP-D3 binding in the absence of *Staphylococcus aureus* infection is colored in burgundy. ChIP signal corresponding to FLAG-HA-dCAP-D3 binding two and four hours after *S. aureus* infection is colored in blue and yellow, respectively. C) Chromatin immunoprecipitation for FLAG protein in female adult flies expressing FLAG-HA-RBF1 in the fat body (*yolk-GAL4/+; +; UAS-FLAG-HA-rbf1/+*) demonstrates that the locus is also a direct target of RBF1. Depiction of signal is as described in B. D) Chromatin immunoprecipitation for FLAG protein in female adult flies expressing FLAG-HA in the fat body (*yolk-GAL4/+; +; UAS-FLAG-HA/+*) demonstrates minimal non-specific binding of tag alone at the locus. Depiction of signal is as described in B.
doi:10.1371/journal.pgen.1002618.g005

infection, without influencing the ability of the fly to clear bacteria [52–54]. These genes have been described as having affects not on the resistance mechanisms which exist in the fly, but on the tolerance mechanisms of the fly. Tolerance mechanisms limit the damage caused to the host by the infection, but do not actually limit the pathogen burden [55]. To determine whether loss of dCAP-D3 and/or RBF1 expression in the fat body did indeed result in diminished capacity of the fly to clear bacteria, we performed bacterial clearance assays and measured the number of bacteria present in the fly from 0–20 hours post-infection (Figure 9). Results showed that flies deficient for RBF1 or dCAP-D3 behave more like positive control flies deficient for IMD or Eater proteins, and exhibit significant increases in bacterial numbers at 15 hours post-infection with *S. aureus*. This suggests that RBF1 and dCAP-D3 most likely affect the resistance mechanisms (i.e. AMP transcription), and not the tolerance mechanisms of the fly.

A second RBF family member, RBF2, regulates basal AMP transcription levels, but not induced levels, following infection

Since the observed defects in survival rates and AMP induction were not as severe for RBF1 deficient flies in comparison to dCAP-D3 deficient flies, we wondered whether the other *Drosophila* RBF member, RBF2, might compensate for loss of RBF1 activity. RBF2 has been shown to be upregulated upon depletion of RBF1, and co-regulates many genes with RBF1 as a part of the dREAM complex [26,56,57]. To address this question, we tested survival

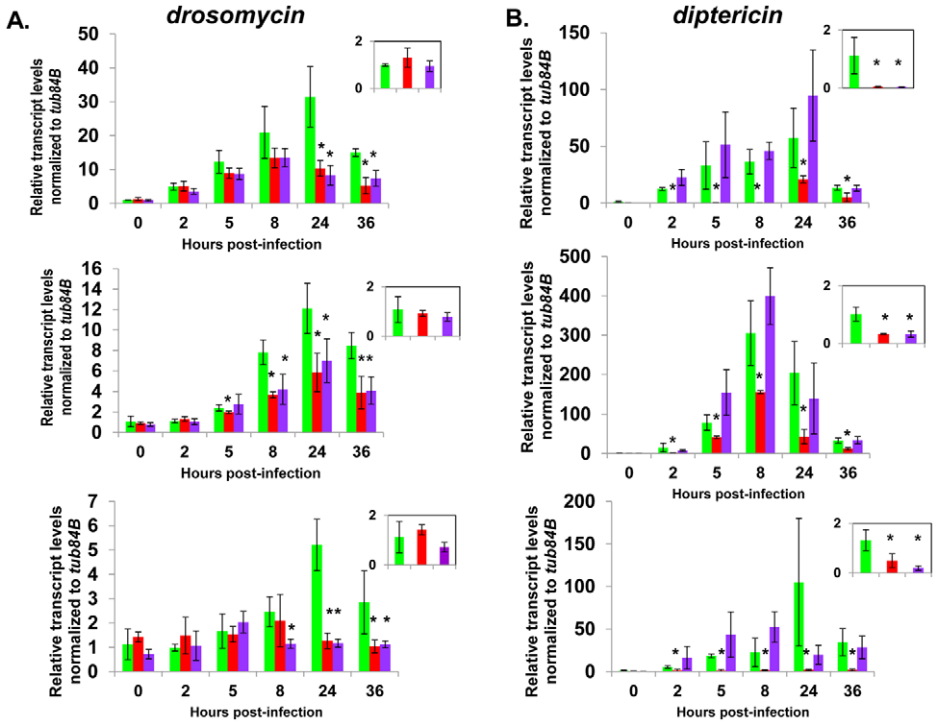

Figure 6. Complete AMP induction following bacterial infection depends on dCAP-D3 and RBF1. Adult female flies expressing RBF1 (purple) or dCAP-D3 (red) dsRNAs under the control of *yolk-GAL4* were infected with the Gram positive bacteria, *Staphylococcus aureus*. A) qRT-PCR analyses for transcript levels of the *Drosomycin* AMP gene in these flies show that while flies expressing GFP dsRNAs under the control of *yolk-GAL4* (green) undergo a large induction of AMPs at 8–24 hours post-infection, flies expressing dCAP-D3 or RBF1 dsRNA in the fat body fail to exhibit maximal, sustained induction. B) qRT-PCR analyses for transcript levels of the *Diptericin* AMP gene in these flies show that while flies expressing GFP or RBF1 dsRNAs under the control of *yolk-GAL4* (green) undergo a large induction of AMPs at 8–24 hours post-infection, flies expressing dCAP-D3 dsRNA in the fat body fail to exhibit maximal, sustained induction. The inset boxes in the upper right corner of each graph are a larger representation of the 0 hour timepoint and depict basal transcription levels. Asterisks emphasize statistical significance ($p \leq 0.05$) as determined by a students paired t-test. Three independent experiments are shown and results for each experiment are the average of three sets of five infected adults per genotype, per timepoint.
doi:10.1371/journal.pgen.1002618.g006

times and AMP induction in flies deficient for RBF2 in the fat body (yolk-GAL4<UAS-RBF2-dsRNA) or a combination of both RBF1 and RBF2 in the fat body (yolk-GAL4<UAS-RBF1 dsRNA, UAS-RBF2 dsRNA). The specific deficiencies in these flies were confirmed by qRT-PCR (Figure S6). qRT-PCR revealed that similar to the loss of RBF1 or dCAP-D3, loss of RBF2 or RBF1/RBF2 resulted in decreased basal transcript levels of *diptericin* but not *drosomycin* (Figure S7A and S7B, inset boxes). However, following infection with *S. aureus*, loss of RBF2 or RBF1/RBF2 did not cause decreased induction of either AMP transcript. In some cases, loss of both RBF1 and RBF2 actually resulted in an increase in *diptericin* transcription levels at 8 hours post infection. In response to infection with Gram positive bacteria (Figure S8A) or Gram negative bacteria (Figure S8B), RBF2 deficient or RBF1/RBF2 deficient flies did not exhibit any changes in survival rates that were significantly different from wild type control flies. These results demonstrate that RBF2 does regulate basal AMP transcript levels, but does not compensate for RBF1 in induction of AMP transcription in *Drosophila* following infection.

The shared regulation of innate immune gene clusters by RBF1 and dCAP-D3 may be conserved in human cells

AMPs are conserved in many metazoans and play a very important role in fighting pathogens in barrier epithelial cells at mucosal surfaces [58]. pRB and CAP-D3 have been previously shown to interact physically and functionally in human cells [11]. Remarkably, and perhaps unexpectedly, the regulation of AMP genes by RB and CAP-D3 proteins may also be conserved in human cells. To determine whether pRB and CAP-D3 could regulate genes in human cells and, more specifically, whether the co-regulation of AMPs was conserved, siRNAs were used to decrease pRB and CAP-D3 expression in human Retinal Pigment Epithelial (RPE-1) cells and in premonocytic U937 cells. (Figure S9A and data not shown). qRT-PCR analyses of the levels of five different AMPs revealed that two AMPs (DEFB-3 and DEFA-1) were expressed in RPE-1 cells and both genes were significantly downregulated following the depletion of either pRB or CAP-D3 (Figure S9B). Interestingly, these genes are also located in a very large gene cluster, the *Defensin* locus, encompassing over 20 different AMPs. These data raise the possibility that the regulation of AMPs by CAP-D3 and pRB, and the ability of these proteins to regulate gene clusters, are properties that may be conserved in human cells.

Discussion

In *Drosophila*, RB-family proteins are best known as transcriptional repressors of cell cycle and proliferation genes. Here we describe a different aspect of RB function and show that, together with the Condensin II protein dCAP-D3, RBF1 functions to regulate the expression of a large number of genes during *Drosophila* development. A surprising characteristic of RBF1/

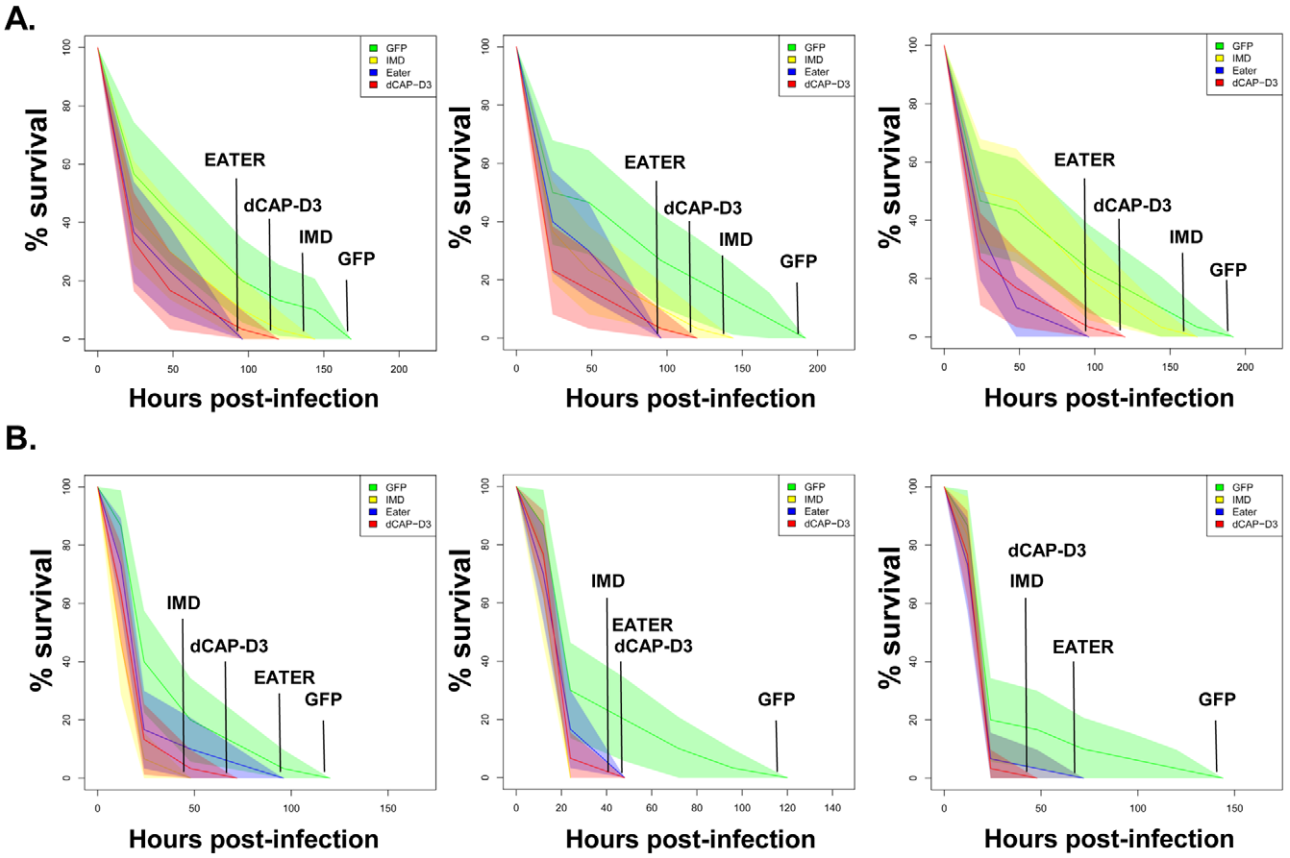

Figure 7. dCAP-D3 is necessary for a proper immune response to bacterial infection. Adult female flies expressing dCAP-D3 (red) dsRNAs under the control of *yolk-GAL4* were infected with the Gram positive bacterium, *Staphylococcus aureus* (A) or the Gram negative bacterium, *Pseudomonas aeruginosa* (B). Flies expressing GFP dsRNAs under the control of *yolk-GAL4* (green) were used as "wild-type" controls. Eater mutants which are defective in phagocytosis (blue) or flies expressing IMD dsRNAs which are compromised in a major innate immune signaling pathway (yellow) were used as positive controls. Results demonstrate that flies expressing reduced levels of dCAP-D3 in the fat body cells are more susceptible to either type of infection than wild type controls. Three independent experiments are depicted with results of each experiment shown as the average of three sets of 10 infected adults per genotype. These experiments were also performed using a sterile needle dipped in PBS to rule out death as a result of wounding and survival curves matched those of yolk-GAL4 expressing flies (data not shown). Results are presented as cox regression models with statistical significance ($p \leq 0.05$) represented as shaded areas above and below the curves.
doi:10.1371/journal.pgen.1002618.g007

dCAP-D3 regulated genes is that they do not seem to be the classically repressed genes with functions in cell cycle progression, DNA damage and DNA replication. Instead, many RBF1/dCAP-D3-dependent genes are classified as being involved in cell-type specific functions and include genes that are involved in enzymatic cascades, organ development and cell fate commitment.

The idea that dCAP-D3 and RBF1 could cooperate to promote tissue development and differentiation is supported by the fact that both proteins are most highly expressed in the late stages of the fly life cycle, and accumulate at high levels in the nuclei of specific cell types in adult tissues. As an illustration of the cell-type specific nature of RBF1/dCAP-D3-regulation we show that dCAP-D3 and RBF1 are both required for the constituitive expression of a large set of AMP genes in fat body cells. The loss of this regulation compromises pathogen-induction of gene expression and has functional consequences for innate immunity. Interestingly, different sets of RBF1/dCAP-D3-dependent genes were evident in the gene expression profiles of mutant larvae and adults. Given this, and the fact that the gene ontology classification revealed multiple groups of genes, we suggest that the targets of RBF1/dCAP-D3-regulation do not represent a single transcriptional program, but diverse sets of cell-type specific programs that need to be activated (or repressed) in specific developmental contexts.

The changes in gene expression seen in the mutant flies suggest that RBF1 has a significant impact on the expression of nearly half of the dCAP-D3-dependent genes. This fraction is consistent with our previous data showing partial overlap between RBF1 and dCAP-D3 banding patterns on polytene chromatin, and the finding that chromatin-association by dCAP-D3 is reduced, but not eliminated, in *rbf1* mutant animals and RBF1-depeleted cells. Although we have previously shown that RBF1 and dCAP-D3 physically associate with one another [11], and our current studies illustrate the fact that they each bind to similar sites at a direct target, the molecular events that mediate the co-operation between RBF1 and dCAP-D3 remain unknown.

These results represent the first published ChIP data for the CAP-D3 protein in any organism. Although we have only examined a small number of targets it is interesting to note that the dCAP-D3 binding patterns are different for activated and repressed genes (compare Figure 5 and Figure S5). More specifically, dCAP-D3 binds to an area within the open reading frame of a gene which it represses (Figure S5C and S5D). However, dCAP-D3 binds to regions which flank a cluster of genes that it activates (Figure 5). Whether or not this difference in binding is true for all dCAP-D3 regulated genes will require a more global analysis.

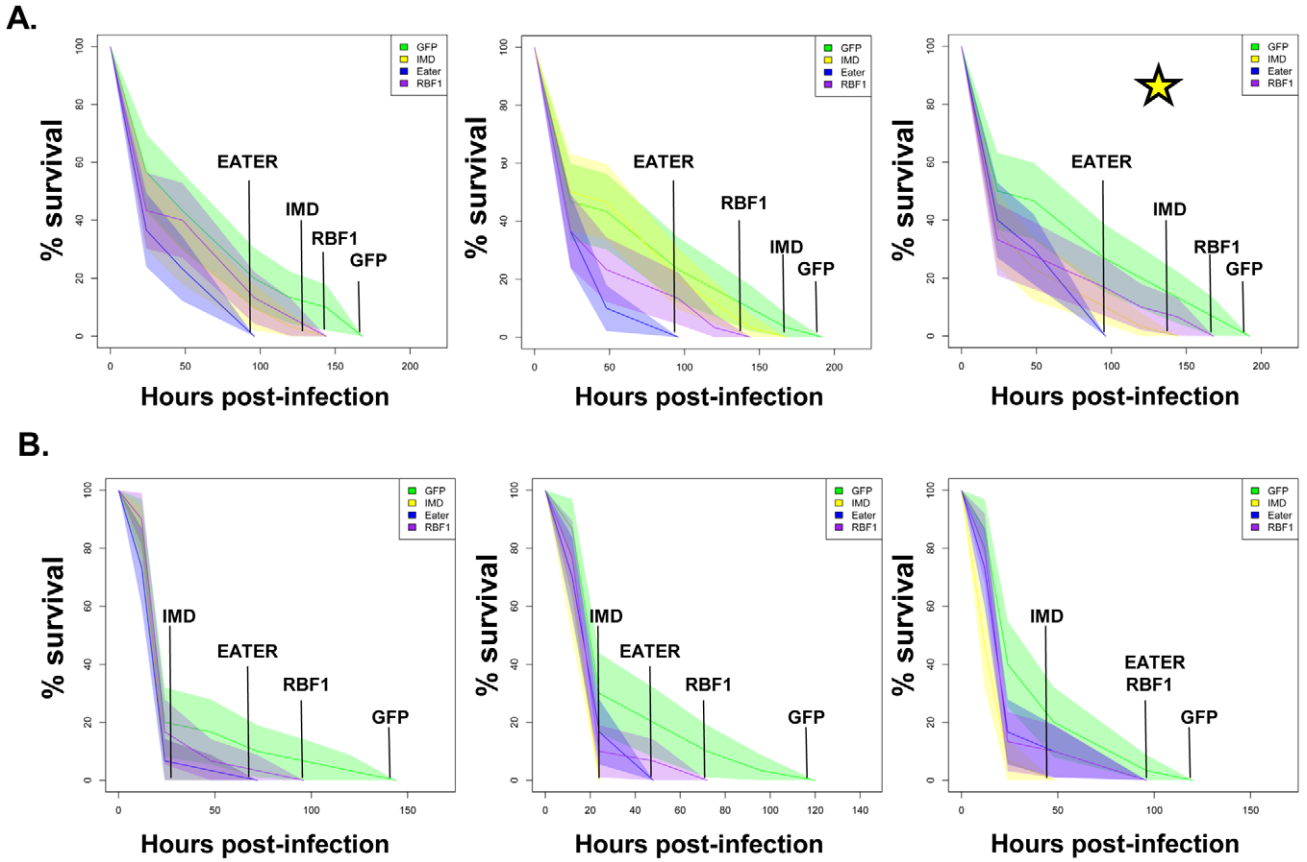

Figure 8. RBF1 is necessary for a proper immune response to Gram positive bacterial infection. Adult female flies expressing RBF1 (purple) dsRNAs under the control of *yolk-GAL4* were infected with the Gram positive bacterium, *Staphylococcus aureus* (A) or the Gram negative bacterium, *Pseudomonas aeruginosa* (B). Flies expressing GFP dsRNAs under the control of *yolk-GAL4* (green) were used as "wild-type" controls. Eater mutants which are defective in phagocytosis (blue) or flies expressing IMD dsRNAs which are compromised in a major innate immune signaling pathway (yellow) were used as positive controls. Results demonstrate that flies expressing reduced levels of RBF1 in the fat body cells are more susceptible to infection with Gram positive bacteria (A) than wild type controls. Three independent experiments are depicted with results of each experiment shown as the average of three sets of 10 infected adults per genotype. Results are presented as cox regression models with statistical significance ($p \leq 0.05$) represented as shaded areas above and below the curves. In the third experiment in (A), which is highlighted by a star, the survival endpoint becomes significant when the confidence level is changed to 90% ($p \leq 0.10$) instead of 95% ($p \leq 0.05$). These experiments were also performed using a sterile needle dipped in PBS to rule out death as a result of wounding and survival curves matched those of yolk-GAL4 expressing flies (data not shown).
doi:10.1371/journal.pgen.1002618.g008

Human Condensin non-SMC subunits are capable of forming subcomplexes *in vitro* that are separate from the SMC protein-containing holocomplex [59], but currently, the extent to which dCAP-D3 relies on the other members of the Condensin II complex remains unclear. We note that fat body cells contain polytene chromatin. Condensin II subunits have been shown to play a role in the organization of polytene chromatin in *Drosophila* nurse cells [60]. Given that RB proteins physically interact with other members of the Condensin II complex [11], it is possible that RBF1 and the entire Condensin II complex, including dCAP-D3, may be especially important for the regulation of transcription on this type of chromatin template.

A potentially significant insight is that the genes that are deregulated in both *rbf1* and *dCap-D3* mutants tend to be present in clusters located within 10 kb of one another. This clustering effect seems to be a more general feature of regulation by dCAP-D3, which is enhanced by RBF1, since clustering was far more prevalent in the list of dCAP-D3 target genes than in the list of RBF1 target genes.

We chose to focus our studies on one of the most functionally related families of clustered target genes that were co-dependent on RBF1/dCAP-D3 for activation in the adult fly: the AMP family of genes. AMP loci represent 20% of the gene clusters regulated by RBF1 and dCAP-D3 in adults. ChIP analysis of one such region, a cluster of AMP genes at the *diptericin* locus, showed this locus to be directly regulated by RBF1 and dCAP-D3 in the fat body and revealed a pattern of RBF1 and dCAP-D3-binding that was very different from the binding sites typically mapped at E2F targets. Unlike the promoter-proximal binding sites typically mapped at E2F-regulated promoters, RBF1 and dCAP-D3 bound to two distant regions, one upstream of the promoter and one downstream of the *diptericin B* translation termination codon, a pattern that is suggestive of an insulator function. We hypothesize that RBF1 and dCAP-D3 act to keep the region surrounding AMP loci insulated from chromatin modifiers and accessible to transcription factors needed for basal levels of transcription. The modEncode database shows binding sites for multiple insulator proteins, as well as GATA factor binding sites, at these regions. GATA has been previously implicated in transcriptional regulation of AMPs in the fly [61], and future studies of dCAP-D3 binding partners in *Drosophila* fat body tissue may uncover other essential activators. Additionally, the chromatin regulating com-

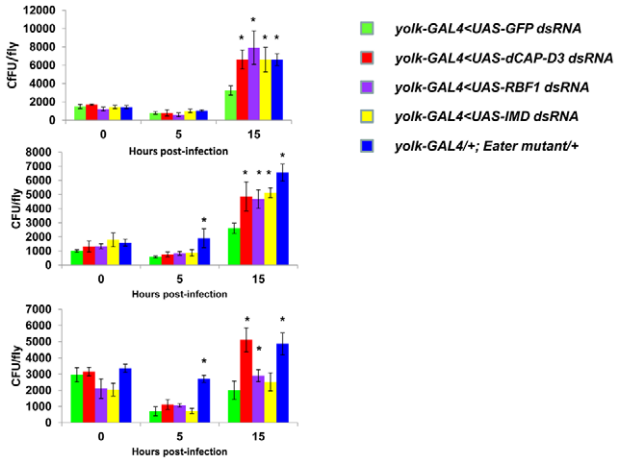

Figure 9. RBF1 and dCAP-D3 are necessary for the ability to clear bacteria *in vivo*. Adult female flies expressing RBF1 (purple) or dCAP-D3 (red) dsRNAs under the control of *yolk-GAL4* were infected with the Gram positive bacterium, *Staphylococcus aureus*. Flies expressing GFP dsRNAs under the control of *yolk-GAL4* (green) were used as "wild-type" controls. Eater mutants which are defective in phagocytosis (blue) or flies expressing IMD dsRNAs which are compromised in a major innate immune signaling pathway (yellow) were used as positive controls. Results demonstrate that at 15 hours following infection, flies expressing reduced levels of dCAP-D3 or RBF1 in the fat body cells exhibit increased numbers of bacteria in comparison to wild type controls. Three independent experiments are shown and results for each experiment are the average of three sets of three infected adults, per genotype, per timepoint. Asterisks emphasize statistical significance ($p \leq 0.05$) as determined by a students paired t-test.
doi:10.1371/journal.pgen.1002618.g009

plex, Cohesin, which exhibits an almost identical structure to Condensin [62–64], has been shown to promote looping of chromatin and to bind proteins with insulator functions [65,66]. Therefore, it remains a possibility that Condensin II, dCAP-D3 may actually possess insulator function, itself. We would like to propose that dCAP-D3 may be functioning as an insulator protein, both insulating regions of DNA containing clusters of genes from the spread of histone marks and possibly looping these regions away from the rest of the body of chromatin. This would serve to keep the region in a "poised state" available for transcription factor binding following exposure to stimuli that would induce activation. In the case of AMP genes, which are made constituitively in specific organs at low levels [37,67,68], dCAP-D3 would bind to regions flanking a cluster, and loop the cluster away from the body of chromatin. Upon systemic infection, these clusters would be more easily accessible to transcription factors like NF-κB. If dCAP-D3 is involved in looping of AMP clusters, then it may also regulate interchromosomal looping which could bring AMP clusters on different chromosomes closer together in 3D space, allowing for a faster and more coordinated activation of all AMPs.

AMP expression is essential for the ability of the fly to recover from bacterial infection. Experiments with bacterial pathogens show that RBF1 and dCAP-D3 are both necessary for induction and maintenance of the AMP gene, *drosomycin* following infection, but only dCAP-D3 is necessary for the induction of the *diptericin* AMP gene. Similarly, survival curves indicate, that while dCAP-D3 deficient flies die more quickly in response to both Gram positive and Gram negative bacterial infection, RBF1 deficient flies only die faster in response to Gram positive bacterial infection. The differences seen between RBF1 and dCAP-D3 deficient flies in diptericin induction cannot be attributed to functional compensation by the other *Drosophila* RB protein family member, RBF2, since results show that loss of RBF2 or both RBF2 and RBF1 do not decrease AMP levels following infection. Since results demonstrate that RBF1 binds most strongly to an AMP cluster prior to infection and regulates basal levels of almost all AMPs tested, we hypothesize that RBF1 (and possibly RBF2) may be more important for cooperating with dCAP-D3 to regulate basal levels of AMPs. Reports have shown that basal expression levels of various AMPs are regulated in a gene-, sex-, and tissue-specific manner, and it is thought that constituitive AMP expression may help to maintain a proper balance of microbial flora and/or help to prevent the onset of infections [37,68,69]. In support of this idea, one study in *Drosophila* which characterized loss of function mutants for a gene called *caspar*, showed that *caspar* mutants increased constituitive transcript levels of diptericin but not transcript levels following infection. This correlated with increased resistance to septic infection with Gram negative bacteria [70], proving that changes in basal levels of AMPs do have significant effects on the survival of infected flies. Additionally, disruption of Caudal expression, a protein which suppresses NF-κB mediated AMP expression following exposure to commensal bacteria, causes severe defects in the mutualistic interaction between gut and commensal bacteria [71]. It is therefore possible that RBF1 and dCAP-D3 may help to maintain the balance of microbial flora in specific organs of the adult fly and/or be involved in a surveillance-type mechanism to prevent the start of infection. RBF1 deficient flies also exhibit defects in *Drosomycin* induction following Gram positive bacterial infection. Mutation to Drosophila GNBP-1, an immune recognition protein required to activate the Toll pathway in response to infection with Gram positive bacteria has been show to result in decreased *Drosomycin* induction and decreased survival rates, without affecting expression of *Diptericin* [72,73]. Therefore, it is possible that inefficient levels of *Drosomycin*, a major downstream effector of the Toll receptor pathway, combined with decreased basal transcription levels of a majority of the other AMPs, would cause RBF1 deficient flies to die faster following infection with Gram positive *S. aureus* but not Gram negative *P. aeruginosa*.

Some dCAP-D3 remains localized to DNA in RBF1 deficient flies [11] and it is also possible that other proteins may help to promote the localization of dCAP-D3 to AMP gene clusters following infection. Given that dCAP-D3 regulates many AMPs including some that do not also depend on RBF1 for activation, and given that dCAP-D3 binding to an AMP locus increases with time after infection whereas RBF1 binding is at its highest levels at the start of infection, it may not be too surprising that dCAP-D3 showed a more pronounced biological role in pathogen assays involving two different species of bacteria.

Remarkably, and perhaps unexpectedly, the levels of both RBF1 and dCAP-D3 impact the basal levels of human AMP transcripts, as well. This indicates that the mechanism of RBF1/dCAP-D3 regulation may not be unique to *Drosophila*. It is striking that many of the human AMP genes (namely, the defensins) are clustered together in a region that spans approximately 1 Mb of DNA. It seems telling that both the clustering of these genes, and a dependence on pRB and CAP-D3, is apparently conserved from flies to humans. The fact that dCAP-D3 and RBF1 dependent activation of *Drosomycin* was necessary for resistance to Gram positive bacterial infection in flies suggests the same could also be true for the human orthologs in human cells. Human AMPs expressed by epithelial cells, phagocytes and neutrophils are an important component of the human innate immune system.

Human AMPs are often downregulated by various microbial pathogenicity mechanisms upon infection [58,74–76]. They have also been reported to play roles in the suppression of various diseases and maladies including cancer and Inflammatory Bowel Disease [77]. We note that the chronic or acute loss of Rb expression from MEFs resulted in an unexplained decrease in the expression of a large number of genes that are involved in the innate immune system [78]. In humans, the bacterium, *Shigella flexneri* was recently shown to down regulate the host innate immune response by specifically binding to the LXCXE cleft of pRB, the same site that we had previously shown to be necessary for CAP-D3 binding [11,79]. An improved understanding of how RB and CAP-D3 regulate AMPs in human cells may provide insight into how these proteins are able to regulate clusters of genes, and may also open up new avenues for therapeutic targeting of infection and disease. Further studies of in differentiated human cells may identify additional sets of genes that are regulated by pRB and CAP-D3.

Materials and Methods

Fly strains

W^{1118} flies were used as "wild type" controls for microarray experiments. Unless otherwise noted, the genotype of RBF mutants was a transheterozygous combination of $rbf1^{\Delta 14}/rbf1^{120a}$ which was obtained by mating $rbf1^{\Delta 14}/FM7$, *GFP* virgins to $rbf1^{120a}/FM7$, *GFP* males at 18°C. Similarly, the genotype of CAP-D3 mutants was a transheterozygous combination of $dCAP\text{-}D3^{\Delta 25}/dCAP\text{-}D3^{c07081}$ which was obtained by mating $dCAP\text{-}D3^{\Delta 25}/CyO$, *GFP* virgins to $dCAP\text{-}D3^{c07081}/CyO$, *GFP* males at 23°C. *yolk-GAL4/FM7c* flies were a kind gift of M. Birnbaum and the timing of expression driven by *yolk-GAL4* has been previously characterized in [40]. The RBF1, dCAP-D3, RBF2, and IMD dsRNA expressing strains were obtained from the VDRC and their transformant IDs were 10696, 29657, 100635, and 101834 respectively. UASt-FLAG-HA tagged strains were created by first amplifying the ORF from either the CAP-D3 RE18364 cDNA clone (DGRC) or the RBF1 LD02906 cDNA clone (DGRC) using Pfx polymerase (Invitrogen). The pENTR/D-TOPO Cloning Kit (Invitrogen) was used to clone the ORF into a Gateway entry vector as described in the manufacturer's protocol and at http://www.ciwemb.edu/labs/murphy/Gateway%20vectors.html. The LR Clonase kit (Invitrogen) was then used to recombine the ORF into the pUASt-FHW vector (DGRC) described in detail at the website mentioned above. pUASt-FLAG-HA-RBF1 and pUASt-FLAG-HA-dCAP-D3 vectors were then injected into embryos to create transgenic fly lines expressing the tagged proteins. Mutant flies used as positive controls in infection experiments included the Imd^1 strain which was a generous gift from L. Stuart and the *Eater* mutant strain [51]. All flies were maintained at 25°C and placed in vials containing standard dextrose medium.

Cell culture and RNAi

hTERT-RPE-1 cells were grown in Dulbecco'sModified Essential Medium (DMEM) supplemented with 10% fetal bovine serum (FBS) and 1% penicillin/streptomycin. RNAimax (Invitrogen) was used, according to manufacturer's protocol, to transfect non-targeting, RB, and CAP-D3 specific siRNAs (described in [12]) at final concentrations of 100 nM. Total RNA was harvested 48 hours post transfection and reverse transcribed into cDNA, as described below.

qRT–PCR

TRIzol (Invitrogen) was used to harvest total RNA from whole flies/specific tissues according to the manufacturer's protocol. After RNA was purified using the Qiagen RNAeasy kit, the Taqman Reverse Transcription kit (Applied Biosystems) was used to reverse transcribe 1.5 µg of RNA into cDNA. qRT-PCR was performed using the Roche Lightcycler 480 to amplify 15 µL reactions containing .5 µL of cDNA, .5 µL of a 10 µM primer mix and 7.5 µL of SYBR Green Master Mix (Roche). All qRT-PCR experiments were performed using three groups of 5 flies per genotype and three independent experiments were performed. Primer sequences are as follows: Rbf1qPCR F1-CTGCAGGGCTACGAGACGTAC, Rbf1qPCR R1 GTGTGCTGGTTCTTCGGCAGG, Rbf2qPCR R1-CTCCCAGTGCTTCTAGCACGC, Rbf2qPCR F1-CGTGAACGCCTTAGAGGTGCC, dCAP-D3 qPCR F3-CGTGCTGTTGCTTTACTTCGGCC, dCAP-D3 qPCR R3- GGCGCATGATGAAGAGCATATCCTG, AttAqPCR F1-GTGGTCCAGTCACAACTGGCG, AttAqPCR R1- CTTGGCATCCAGATTGTGTCTGCC, DroqPCR F1-CACCATCGTTTTCCTGCTGCTTGC, DroqPCR R1-GGTGATCCTCGATGGCCAGTG, AttBqPCR F1- CTCAAAGCGGTCCAGTCACAACTG, AttBqPCR R1- GAATAAATTGGCATGGGCCTCCTGC, Dro4qPCR F1- GTTTGCTCTCCTCGCTGTGGTG, Dro4qPCR R1-GCCCAGCAAGGACCACTGAATC, Dro3qPCR F1- GGCCAACACTGTTTTGGCACGTG, Dro3qPCR R1- GTCCCTCCTCAATGCAGAGACG, Dro2qPCR F1- GTTGTCCTGGCCGCCAATATGG, Dro2qPCR R1- GGACTGCAGTGGCCACTGATATG, DptBqPCR F1- GGACTGGCTTGTGCCTTCTCG, DptBqPCR R1- CAGGGGCACATCAAAATTGGGAGC, DrsqPCR F1-GTACTTGTTCGCCCTCTTCGCTG, DrsqPCR R1- CAGGTCTCGTTGTCCCAGACG, DptqPCR F1- GCTTATCCGATGCCCGACGAC, DptqPCR R1-GTGACCCTGGACTGCAAAGCC, DefqPCR F1- CAAACGCAGACGGCCTTGTCG, DefqPCR R1- AAGCGAGCCACATGCGACCTAC, Dro5qPCR F1- CAAGTTCCTGTACCTCTTCCTGGC, Dro5qPCR R1- CAGGGTCCTCCGTATCTTCCAG, Dro6qPCR F1-CTTCGCACCAGCATTGCAGCC, Dro6qPCR R1-GAAGGTACAGACCTCCCTGTGC, Dro7qPCR F1- GGCTGCAGTGTCCACTGGTTC, Dro7qPCR R1- CACATGCCGACTGCCTTTCCG, MtkqPCR F1- GATTTTTCTGGCCCTGCTGGGTG, MtkqPCR R1- GGTTGGTTAGGATTGAAGGGCGAC, rp49qPCR F1- TACAGGCCCAAGATCGTGAAG, rp49qPCR R1- GACGCACTCTGTTGTCGATACC, CecCqPCR F1-CAATCGGAAGCCGGTTGGCTG, CecqPCR R1-GCGCAATTCCCAGTCCTTGAATGG, AndqPCR F1- CATTTTGGCCATCAGCGTGGGTC, AndqPCR R1- GGGCTTAGCAAAGCCAATTCCCAC, AttCqPCR F1- GTACTTGGCTCCCTTGCGGTG, AttCqPCR R1- CTTAGGTCCAATCGGGCATCGG, AttDqPCR F1- CCAAGGGAGTTTATGGAGCGGTC, AttDqPCR R1- GCTCTGGAAGAGATTGGCTTGGG, CecA1qPCR F1- CAATCGGAAGCTGGGTGGCTG, CecA1qPCR R1- GGCGGCTTGTTGAGCGATTCC, CecA2qPCR F1- GGACAATCGGAAGCTGGTTGGC, CecA2qPCR R1- GGCCTGTTGAGCGATTCCCAG, CecBqPCR F1- GATTCCGAGGACCTGGATTGAGG, CecBqPCR R1-GGCCATCAGCCTGGGAAACTC, tub84BqPCR F1- GGCAAGGAGATCGTCGATCTGG, tub84BqPCR R1- GACGCTCCATCAGCAGCGAG, hCAP-D3qPCR F1- TCCGGAAGCAGGCCCTCCAG, hCAP-D3qPCR R1- GGACCTGGCTGTCGTCCCCA, hRBqPCR F1- AGCTGTGGGACAGGGTTGTGTC, hRBqPCR R1- CAACCTCAAGAGCGCACGCC, eaterqPCR F1: CTCGTATCGGCTCAGATCTGCAC, eaterqPCR R1: CATCTGAGTGCGGAGCTCCTTAC, IMDqPCR F1- CGAATCCACTGGAGCAACAGCTG, IMDqPCR R1-GTTTCCACGCACTTGGGCGAG, hGAPDHqPCR F1- AGCCTCCCGCTTCGCTCTCT, hGAPDHqPCR R1- CCAGGCGCCCAATACGACCA, orc1qPCR F1- CATCATCCTCAAA-

CACGCGCTGC, orc1qPCR R1- CCCTCGACGAGGCGTAAAAGC, cg5250qPCR F1- GACATTGCCGGAGGTGAAGAGC, cg5250qPCR R1- CTATTCGACTATGTGGTGGGCCTG, dupqPCR F1- GGGTGGCGGTATTTTTGTGGGAG, dupqPCR R1- CAACAGGAAACTCCGCGACGC, mus209qPCR F1- CTTGTCGAAGCCATCGGAACGC, mus209qPCR R1- GGGTCAAGCCACCATCCTGAAG, dnkqPCR F1- CCGCCCCAACCAACAAGAAGC, dnkqPCR R1- CCTCCAGCGTATTGTACATGCCC, RnrSqPCR F1- GAAGAAGGCAAGCACGTGCGAG, RnrSqPCR R1- CCAGTACCACGACATCTGGCAG, dnapoldeltaqPCR F1- CCATCGCCCATTAGCAGAGTCTG, dnapoldeltaqPCR R1- GGAACCTCCAATGGACATGCCAAG, mcm7qPCR F1- CATTGAGCACCGCCTGATGATGG, mcm7qPCR R1- GAGTGCGCCTTCTCTGTGGAC, mcm3qPCR F1- CGAGGTGATGGAACAGGGTCG, mcm3qPCR R1- GAAAGCAGCGAATCCTGCAGTCC, mcm2qPCR F1- GAGATCCCGCAGGACTTGTTGC, mcm2qPCR R1- CAAAAGACTCCTGTCGCAGCTGG, mcm5qPCR F1- CTGGTCTCACGGCTTCGGTTATG, mcm5qPCR R1- GCCACACGATCATCCTCTCGC, dnapolalpha50qPCR F1- CCTTCTACCGTTGGCTATCGTATGG, dnapolalpha50qPCR R1- CAGCTTGGGTATCAAAGCAGAGG, DEFA-1qPCR F1- TGCCCTCTCTGGTCACCCTGC, DEFA-1qPCR R1- GCCTGGAGTGGCTCAGCCTG, DEFB-3qPCR F1- GCGTGGGGTGAAGCCTAGCA, DEFB-3qPCR R1- AGCTGAGCACAGCACACCGG.

Generation of anti–dCAP-D3 antibody

The rabbit anti–dCAP-D3 YZ834 antibody was generated by Yenzyme Corporation. The antibody was purified using the BIO-RAD Affi-Gel 10 Gel according to manufacturer's protocol.

Immunofluorescence analysis of cryosections

Adult female flies were cryosectioned (10 μm) and stained as previously described [80]. Primary antibodies included RBF1 (DX2), dCAP-D3 (YZ384), and anti-GFP (Jackson Immunoresearch). Images were obtained using a Zeiss LSM510 Confocal microscope.

Preprocessing of array data

Nimblegen microarray data were pretreated according to the manufacturer's recommendation and replicate probes were averaged. Affymetrix microarray data was downloaded from array express as raw .CEL files and normalized by robust multi array averaging (RMA)[RMS] before further analysis [81]. The entire set of microarray data can be found in Table S1.

Hypothesis testing

Differentially expressed genes were identified using a linear model with a moderated T-test [82]. P values were corrected for multiple testing by calculating false discovery rates using the method of Benjamini and Hochberg [83]. Genes with a false discovery rate (FDR)<0.15 and a log2 fold change >0.1 were taken as significant. Gene ontology (GO) annotations were downloaded from FLYBASE [84], and gene ontology terms overrepresented on the lists of differentially expressed genes were identified using a hypergeometric test. P-values from the hypergeometric test were corrected for multiple testing using the same method as for the individual genes and GO-categories with FDR<0.05 were taken as significant.

Gene clustering analysis

Chromosomal positions of transcription start and stop sites for all genes on the chip were taken from FLYBASE. Genes were counted as clustered if they overlapped, or if the genes lay within 10 000 base pairs of each other. Overall chromosomal clustering for a list of genes was quantified as the number of genes that co-localize according to this criterion. Significance of co-localization was evaluated by comparing to lists of randomly selected genes from the same chip.

Infection of flies with pathogenic bacteria

S. aureus and *P. aeruginosa* bacteria were gifts from L. Stuart. *S. aureus* was grown in a shaking incubator at 37°C, in DIFCO Columbia broth (BD Biosciences) supplemented with 2% NaCl and *P. aeruginosa* was grown in a shaking incubator at 37°C in DIFCO Luria broth (BD Biosciences). Bacteria were inoculated in 10 mL cultures grown overnight. 10^{-4} bacterial cells were then inoculated into a new 10 mL culture and this was grown to an $OD_{600\ nm}$ of 0.5. These cultures were then centrifuged at 3000 rpm in a 1.5 mL eppendorf tube for 5 minutes at 4°C and subsequently washed twice with PBS. After a third centrifugation, PBS wash was removed from the pellet and 25 μL of new PBS was used to resuspend the pellet. Infections were performed as previously described [85]. Specifically, a .25 mm diameter straight stainless steel needle and pin vise (Ted Pella Inc, Redding, CA) were used to infect adult flies. The needle was dipped into the resuspended bacterial pellet and used to prick the thorax of a CO_2-anesthetized adult fly in a region just underneath where the wing connects to the thorax. Flies were then separated from the needle using a brush and put into fresh vials containing standard dextrose medium with no more than 10 flies per vial.

Chromatin immunoprecipitation

40 flies per IP were used in all ChIP experiments. Flies were homogenized with a KONTES pellet pestle grinder (Kimble Chase) in 1 mL of buffer A (60 mM KCl, 15 mM NaCl, 4 mM MgCl2, 15 mM HEPES pH 7.6, .5% Triton X-100, .5 mM DTT, EDTA-free protease inhibitors cocktail (Roche)) containing 1.8% formaldehyde. Homogenized flies were incubated at RT for 15 minutes, at which point glycine was added to a concentration of 225 mM. 2–4 mLs of homogenized flies were transferred to 15 mL conical tubes and centrifuged at 4°C for 5 min at 4000 g. Supernatant was discarded and pellets were washed with 3 mL of buffer A. Tubes were centrifuged as described above, supernatant was discarded, and pellets were washed with 3 mL of buffer B (140 mM NaCl, 15 mM HEPES pH 7.6, 1 mM EDTA, .5 mM EGTA, 1% Triton, .5 mM DTT, .1% sodium deoxycholate, EDTA free protease inhibitors cocktail). Tubes were centrifuged as described above, supernatant was discarded, and 500 μL of buffer B+1% SDS per IP was added to each tube. Tubes were rotated at 4°C for 20 min. Samples were then sonicated using the Branson sonifier at a setting of 3, with 8 sonication intervals of 20 seconds interspersed by 10 second breaks. Tubes were centrifuged at 4°C for 5 min at 2000 RPM and 500 μL supernatant was used for each IP. 50 μL of Dynal Protein A beads (Invitrogen) per IP were prepared according to the manufacturer's recommendations. Beads were incubated with anti-FLAG M2 antibody (Sigma) or dCAP-D3 antibody (YZ384) for 2 hours at RT with rotation. Beads were washed according to manufacturer's protocol and added to the diluted chromatin samples which were then incubated at 4°C overnight, with rotation. Samples were centrifuged at 3000 RPM, 4°C for 1 min and washed three times with buffer B+.05% SDS and once with TE. Bound protein was eluted by adding 125 μL of Buffer C (1%SDS, .2% NaCl, TE) to the beads for 30 min at 65°C. Samples were again centrifuged and eluates were harvested and incubated for 4 hours at 65°C to reverse crosslinks. Samples were digested with Proteinase K and RNase A (Sigma), phenol-chloroform

extracted, and ethanol precipitated. DNA pellets were dissolved in 105 µL of ddH2O and .5 µL was used per qRT-PCR reaction.

Survival curves

Flies were collected approximately 5–8 days after eclosure and were infected as described above. Following infection, each group of flies was placed in a new vial of food and monitored for the number of surviving flies at each timepoint. Three experiments were performed, with each experiment including 3 groups of 10 flies per genotype per timepoint. Survival statistics were calculated using a cox proportional hazard model, and hazard ratios with a two sided p-value less than 0.05 were taken as significant.

Bacterial clearance assays

Flies were anestitized by CO2 inhalation and infected as described above. Following infection, flies were dipped in 95% Ethanol, air dried, and placed into 1.5 mL Eppendorf tubes containing 500 µL of PBS. Flies were homogenized with a Kontes battery powered homogenizer and plastic pestle (USA scientific). The tubes were centrifuged for 2 min at 3000 rpm. Various dilutions were plated onto Columbia CNA with 5% Sheep's Blood Agar (Becton Dickinson and Company). This type of agar contains antibiotics to inhibit growth of organisms other than *Staphylococcus aureus*.

Supporting Information

Figure S1 dCAP-D3 and RBF1 mutants expressing a transheterozygous combination of alleles retain approximately 15% of wild type protein expression. qRT-PCR (A) and Immunoblots (B) for *rbf1* transcript levels/protein levels and *dCap-D3* transcript levels/protein in wild type (w^{1118}) and dCAP-D3 transheterozygous mutant ($dCAP\text{-}D3^{c07081/\Delta 25}$) or RBF1 transheterozygous mutant ($rbf1^{120a/\Delta 14}$) female flies indicates that mutants retain 10–15% of wild-type protein expression levels. Transcript levels were normalized to *tubulin 84B* mRNA levels and α-tubulin was used as a loading control in B.
(TIF)

Figure S2 RBF1 regulates E2F targets in specific tissues of the adult fly. Ovaries were dissected from female adult flies and cDNA was made from either carcass or ovaries. Top table: qRT-PCR analyses performed on cDNA from ovaries shows that decreased RBF1 expression results in the upregulation of a few E2F targets while decreased dCAP-D3 expression largely has no effect. Bottom table: qRT-PCR analyses performed on cDNA from carcass without ovaries shows that decreased RBF1 expression in the carcass does result in upregulation of many E2F targets, however, dCAP-D3 does not share regulation of these genes with RBF1. Transcript levels were normalized to *tubulin 84B* mRNA levels. All results were significant with p-values≤0.05.
(TIF)

Figure S3 RBF1 and dCAP-D3 antibodies are specific. Immunostaining for dCAP-D3 (A) and RBF1 (B) in cryosections of abdomens of adult female flies expressing dCAP-D3 (A) or RBF1 (B) dsRNA in combination with GFP protein in fat body cells shows the antibodies recognize protein where dsRNAs are not expressed. Flies used in A were of the genotype *yolk-GAL4, UAS-GFP/+;+;UAS-dCAP-D3 dsRNA*, and flies used in B were of the genotype *yolk-GAL4, UAS-GFP/+;+;UAS-RBF1 dsRNA*.
(TIF)

Figure S4 qRT–PCR analysis of genes adjacent to the *diptericin* locus. qRT–PCR analysis of cDNA from 1) flies expressing driver alone (*yolk-GAL4/+;+;+*), 2) flies expressing *rbf1 dsRNA (yolk-GAL4;+;UAS-rbf1 dsRNA)* in the fat body cells and 3) flies expressing *dCAP-D3 dsRNA (yolk-GAL4;+;UAS-dCAP-D3 dsRNA)* in the fat body cells demonstrates that *CG43070* is also activated by RBF1 and dCAP-D3.
(TIF)

Figure S5 Endogenous dCAP-D3 binds to *CG5250* in a similar pattern as FLAG-HA-dCAP-D3. A) qRT-PCR was performed on cDNA generated from whole female flies (1) expressing yolk-GAL4 driver alone (*yolk-GAL4/+; +;+*) or (2) exhibiting acute, fat body specific knockdown of dCAP-D3 (*yolk-GAL4/+; +/UAS-dCAP-D3 dsRNA/+*). Transcript levels for genes surrounding *CG5250* indicate that *CG5250* is the only gene in the locus that is significantly regulated by dCAP-D3. B) Graphic representation of the *CG5250* locus on which ChIP for dCAP-D3 in both the whole adult and the adult fat body was performed. Relative positions of primer sets used are listed under the diagram of the locus. *CG5250* is highlighted in red since it is repressed by dCAP-D3 in the whole adult fly. C) Chromatin immunoprecipitation for FLAG protein in female adult flies expressing FLAG-HA-dCAP-D3 in the fat body (*yolk-GAL4/+; +; UAS-FLAG-HA-dCap-D3/+*) shows that the *CG5250* locus is a direct target of dCAP-D3. ChIP signal corresponding to FLAG-HA-dCAP-D3 binding in the absence of *Staphylococcus aureus* infection is colored in burgundy. ChIP signal corresponding to FLAG-HA-dCAP-D3 binding two and four hours after *S. aureus* infection is colored in blue and yellow, respectively. D) ChIP for endogenous dCAP-D3 in whole adult flies at the *CG5250* locus demonstrates the dCAP-D3 binding pattern is identical to the pattern exhibited specifically in the fat body.
(TIF)

Figure S6 Confirmation of rbf1 and rbf2 transcript knockdown in flies expressing RBF2 or RBF1 and RBF2 dsRNAs. qRT-PCR was performed on cDNAs from flies deficient for RBF2 alone or deficient for a combination of both RBF1 and RBF2.
(TIF)

Figure S7 RBF2 does not regulate AMP induction following bacterial infection. Adult female flies expressing RBF2 (turquoise) or a combination of RBF1 and RBF2 (black) dsRNAs under the control of *yolk-GAL4* were infected with the Gram positive bacteria, *Staphylococcus aureus*. A) qRT-PCR analyses for transcript levels of the *Drosomycin* AMP gene in these flies show that control flies expressing GFP dsRNAs under the control of *yolk-GAL4* (green) undergo a large induction of AMPs at 8–24 hours post-infection. Flies expressing RBF2 dsRNA or a combination of RBF1 and RBF2 dsRNAs show no significant, repeated changes in transcript levels upon comparison to control flies. B) qRT-PCR analyses for transcript levels of the *Diptericin* AMP gene in these flies show that control flies expressing GFP dsRNAs under the control of *yolk-GAL4* (green) undergo a large induction of AMPs at 8–24 hours post-infection. Flies expressing RBF2 dsRNA or a combination of RBF1 and RBF2 dsRNAs exhibit a significant decrease in basal transcript levels in the majority of experiments, but do not exhibit significant changes in transcript levels following infection. Three independent experiments are shown and results for each experiment are the average of three sets of five infected adults. The inset boxes in the upper right corner of each graph are a larger representation of the 0 hour timepoint and therefore depict basal transcription levels. Asterisks emphasize statistical significance (p≤0.05) as determined by a students paired t-test.
(TIF)

Figure S8 RBF2 deficiency in the fat body does not significantly affect survival following bacterial infection. Adult female flies expressing RBF2 (turquoise) dsRNAs or a combination of RBF1 and RBF2 dsRNAs (black) under the control of *yolk-GAL4* were infected with the Gram positive bacterium, *Staphylococcus aureus* (A) or

the Gram negative bacterium, *Pseudomonas aeruginosa* (B). Flies expressing GFP dsRNAs under the control of *yolk-GAL4* (green) were used as "wild-type" controls. Eater mutants which are defective in phagocytosis (blue) or flies expressing IMD dsRNAs which are compromised in the Gram negative arm of the innate immune signaling pathway (yellow) were used as positive controls. Results demonstrate that flies expressing reduced levels of RBF2 or reduced levels of both RBF1 and RBF2 in the fat body cells do not significantly and repeatedly affect survival times in response to either type of infection upon comparison to wild type controls. Three independent experiments are depicted with results of each experiment shown as the average of three sets of 10 infected adults per genotype. Results are presented as cox regression models with statistical significance ($p \leq 0.05$) represented as shaded areas above and below the curves. These experiments were also performed using a sterile needle dipped in PBS to rule out death as a result of wounding and survival curves matched those of yolk-GAL4 expressing flies (data not shown).
(TIF)

Figure S9 Regulation of AMP genes by RB and CAP-D3 is conserved in human cells. A) RPE-1 cells were transfected with (1) non-targeting Control siRNA, (2) pRB siRNA or (3)CAP-D3 siRNAs. qRT-PCR analyses were performed on cDNAs generated from cellular RNA collected 48 hours post transfection and results show that RB and CAP-D3 are significantly decreased. B) qRT-PCR for AMPs in cells described in A shows that pRB or dCAP-D3 deficiency results in significant decreases in basal levels of two human AMP genes.
(TIF)

Table S1 Microarray data from multiple samples of wild type cDNA, dCAP-D3 mutant cDNA, and RBF1 mutant cDNA. Experiments were performed using Nimblegen 385 k whole genome arrays. A detailed description of the information found in each column is provided to the right of the table.
(XLS)

Table S2 Analysis of clustering frequencies among dCAP-D3 and/or RBF1 regulated target genes. A detailed description of the information found in each column is provided to the right of the table. Numbers within individual columns are arbitrary and designate genes present within the same cluster; they do not indicate any information about the strength of their misregulation in mutant flies.
(XLS)

Table S3 List of significant Gene Ontology categories represented by the total number of shared RBF1/dCAP-D3 target genes in the adult fly. Column C lists the Gene Ontology (GO) term. Column D lists the term name associated with the GO category. Column E lists the total number of significant genes found in this GO category. Column F lists the total number of genes found in this GO category. Column G lists the P values associated with the GO category. Column H lists the actual Flybase Gene Numbers associated with the microarray genes found in the GO category.
(XLS)

Table S4 dCAP-D3/RBF1 do not regulate the majority of genes previously reported to be involved in phagocytosis. Microarray data from dCAP-D3 mutant adult flies vs. wild type flies (Table S1) was analyzed for changes to transcript levels of 19 genes previously reported to be involved in phagocytosis (Column A). Only two genes were shown to be misregulated in the mutant flies (Columns B and C).
(XLS)

Table S5 dCAP-D3/RBF1 do not regulate the majority of genes previously reported to be involved in coagulation and melanization. Microarray data from dCAP-D3 mutant adult flies vs. wild type flies (Table S1) was analyzed for changes to transcript levels of 18 genes previously reported to be involved in coagulation and melanization (Column A). Only one gene was shown to be misregulated in the mutant flies (Columns B and C).
(XLS)

Acknowledgments

We thank Morris Birnbaum, Lynda Stuart, Christine Kocks, and Neal Silverman for reagents used in this paper. We thank Spiros Artavanis-Tsakonas and the Harvard/Exelixis Collection for the use of multiple *Drosophila* stocks. We thank Andrea Livey in the Pathology Core at the M.G.H. Cancer Center for cryosectioning of flies. We would also like to thank Nicholas Paquette, Lynda Stuart, and the members of the Dyson lab for advice and technical assistance.

Author Contributions

Conceived and designed the experiments: MSL JAW EA NJD. Performed the experiments: MSL JAW. Analyzed the data: MSL EA NJD. Contributed reagents/materials/analysis tools: N-SM MMSH AG SR. Wrote the paper: MSL NJD.

References

1. Hanahan D, Weinberg RA (2000) The hallmarks of cancer. Cell 100: 57–70.
2. Sherr CJ, McCormick F (2002) The RB and p53 pathways in cancer. Cancer Cell 2: 103–112.
3. Trimarchi JM, Lees JA (2002) Sibling rivalry in the E2F family. Nat Rev Mol Cell Biol 3: 11–20.
4. Thomas DM, Carty SA, Piscopo DM, Lee JS, Wang WF, et al. (2001) The retinoblastoma protein acts as a transcriptional coactivator required for osteogenic differentiation. Mol Cell 8: 303–316.
5. Schneider J, Gu W, Zhu L, Mahdavi V, Nadal-Ginard B (1994) Reversal of terminal differentiation mediated by p107 in Rb-/- muscle cells 10.1126/science.8197461. Science 264: 1467–1471.
6. Novitch B, Mulligan G, Jacks T, Lassar A (1996) Skeletal muscle cells lacking the retinoblastoma protein display defects in muscle gene expression and accumulate in S and G2 phases of the cell cycle 10.1083/jcb.135.2.441. J Cell Biol 135: 441–456.
7. Zacksenhaus E, Jiang Z, Chung D, Marth JD, Phillips RA, et al. (1996) pRb controls proliferation, differentiation, and death of skeletal muscle cells and other lineages during embryogenesis. Genes Dev 10: 3051–3064.
8. Nicolay BN, Bayarmagnai B, Moon NS, Benevolenskaya EV, Frolov MV (2010) Combined inactivation of pRB and hippo pathways induces dedifferentiation in the Drosophila retina. PLoS Genet 6: e1000918. doi:10.1371/journal.pgen.1000918.
9. Longworth MS, Dyson NJ (2010) pRb, a local chromatin organizer with global possibilities. Chromosoma 119: 1–11.
10. Isaac CE, Francis SM, Martens AL, Julian LM, Seifried LA, et al. (2006) The retinoblastoma protein regulates pericentric heterochromatin. Mol Cell Biol 26: 3659–3671.
11. Longworth MS, Herr A, Ji JY, Dyson NJ (2008) RBF1 promotes chromatin condensation through a conserved interaction with the Condensin II protein dCAP-D3. Genes Dev 22: 1011–1024.
12. Manning AL, Longworth MS, Dyson NJ (2010) Loss of pRB causes centromere dysfunction and chromosomal instability. Genes Dev 24: 1364–1376.
13. Gerlich D, Hirota T, Koch B, Peters JM, Ellenberg J (2006) Condensin I stabilizes chromosomes mechanically through a dynamic interaction in live cells. Curr Biol 16: 333–344.
14. Ono T, Losada A, Hirano M, Myers MP, Neuwald AF, et al. (2003) Differential contributions of condensin I and condensin II to mitotic chromosome architecture in vertebrate cells. Cell 115: 109–121.
15. Steffensen S, Coelho PA, Cobbe N, Vass S, Costa M, et al. (2001) A role for Drosophila SMC4 in the resolution of sister chromatids in mitosis. Curr Biol 11: 295–307.
16. Hirota T, Gerlich D, Koch B, Ellenberg J, Peters JM (2004) Distinct functions of condensin I and II in mitotic chromosome assembly. J Cell Sci 117: 6435–6445.
17. Bazett-Jones DP, Kimura K, Hirano T (2002) Efficient supercoiling of DNA by a single condensin complex as revealed by electron spectroscopic imaging. Mol Cell 9: 1183–1190.
18. Strick TR, Kawaguchi T, Hirano T (2004) Real-time detection of single-molecule DNA compaction by condensin I. Curr Biol 14: 874–880.

19. Ono T, Fang Y, Spector DL, Hirano T (2004) Spatial and temporal regulation of Condensins I and II in mitotic chromosome assembly in human cells. Mol Biol Cell 15: 3296–3308.
20. Kimura K, Cuvier O, Hirano T (2001) Chromosome condensation by a human condensin complex in Xenopus egg extracts. J Biol Chem 276: 5417–5420.
21. Gosling KM, Makaroff LE, Theodoratos A, Kim YH, Whittle B, et al. (2007) A mutation in a chromosome condensin II subunit, kleisin beta, specifically disrupts T cell development. Proc Natl Acad Sci U S A 104: 12445–12450.
22. Xu Y, Leung CG, Lee DC, Kennedy BK, Crispino JD (2006) MTB, the murine homolog of condensin II subunit CAP-G2, represses transcription and promotes erythroid cell differentiation. Leukemia 20: 1261–1269.
23. Cobbe N, Savvidou E, Heck MM (2006) Diverse mitotic and interphase functions of condensins in Drosophila. Genetics 172: 991–1008.
24. Dej KJ, Ahn C, Orr-Weaver TL (2004) Mutations in the Drosophila condensin subunit dCAP-G: defining the role of condensin for chromosome condensation in mitosis and gene expression in interphase. Genetics 168: 895–906.
25. Lemaitre B, Hoffmann J (2007) The host defense of Drosophila melanogaster. Annu Rev Immunol 25: 697–743.
26. Dimova DK, Stevaux O, Frolov MV, Dyson NJ (2003) Cell cycle-dependent and cell cycle-independent control of transcription by the Drosophila E2F/RB pathway. Genes Dev 17: 2308–2320.
27. Kwon SY, Xiao H, Glover BP, Tjian R, Wu C, et al. (2008) The nucleosome remodeling factor (NURF) regulates genes involved in Drosophila innate immunity. Dev Biol 316: 538–547.
28. Meister M (2004) Blood cells of Drosophila: cell lineages and role in host defence. Curr Opin Immunol 16: 10–15.
29. Kurucz E, Markus R, Zsamboki J, Folkl-Medzihradszky K, Darula Z, et al. (2007) Nimrod, a putative phagocytosis receptor with EGF repeats in Drosophila plasmatocytes. Curr Biol 17: 649–654.
30. Lebestky T, Chang T, Hartenstein V, Banerjee U (2000) Specification of Drosophila hematopoietic lineage by conserved transcription factors. Science 288: 146–149.
31. Alfonso TB, Jones BW (2002) gcm2 promotes glial cell differentiation and is required with glial cells missing for macrophage development in Drosophila. Dev Biol 248: 369–383.
32. Lanot R, Zachary D, Holder F, Meister M (2001) Postembryonic hematopoiesis in Drosophila. Dev Biol 230: 243–257.
33. Elrod-Erickson M, Mishra S, Schneider D (2000) Interactions between the cellular and humoral immune responses in Drosophila. Curr Biol 10: 781–784.
34. Nappi AJ, Ottaviani E (2000) Cytotoxicity and cytotoxic molecules in invertebrates. Bioessays 22: 469–480.
35. Irving P, Ubeda JM, Doucet D, Troxler L, Lagueux M, et al. (2005) New insights into Drosophila larval haemocyte functions through genome-wide analysis. Cell Microbiol 7: 335–350.
36. Wertheim B, Kraaijeveld AR, Schuster E, Blanc E, Hopkins M, et al. (2005) Genome-wide gene expression in response to parasitoid attack in Drosophila. Genome Biol 6: R94.
37. Uvell H, Engstrom Y (2007) A multilayered defense against infection: combinatorial control of insect immune genes. Trends Genet 23: 342–349.
38. Brennan CA, Anderson KV (2004) Drosophila: the genetics of innate immune recognition and response. Annu Rev Immunol 22: 457–483.
39. Imler JL, Bulet P (2005) Antimicrobial peptides in Drosophila: structures, activities and gene regulation. Chem Immunol Allergy 86: 1–21.
40. DiAngelo JR, Birnbaum MJ (2009) Regulation of fat cell mass by insulin in Drosophila melanogaster. Mol Cell Biol 29: 6341–6352.
41. Aggarwal K, Silverman N (2008) Positive and negative regulation of the Drosophila immune response. BMB Rep 41: 267–277.
42. Ferrandon D, Imler JL, Hetru C, Hoffmann JA (2007) The Drosophila systemic immune response: sensing and signalling during bacterial and fungal infections. Nat Rev Immunol 7: 862–874.
43. Senger K, Harris K, Levine M (2006) GATA factors participate in tissue-specific immune responses in Drosophila larvae. Proc Natl Acad Sci U S A 103: 15957–15962.
44. Tanji T, Yun EY, Ip YT (2010) Heterodimers of NF-kappaB transcription factors DIF and Relish regulate antimicrobial peptide genes in Drosophila. Proc Natl Acad Sci U S A 107: 14715–14720.
45. Meister M, Braun A, Kappler C, Reichhart JM, Hoffmann JA (1994) Insect immunity. A transgenic analysis in Drosophila defines several functional domains in the diptericin promoter. Embo J 13: 5958–5966.
46. Georgel P, Meister M, Kappler C, Lemaitre B, Reichhart JM, et al. (1993) Insect immunity: the diptericin promoter contains multiple functional regulatory sequences homologous to mammalian acute-phase response elements. Biochem Biophys Res Commun 197: 508–517.
47. Kappler C, Meister M, Lagueux M, Gateff E, Hoffmann JA, et al. (1993) Insect immunity. Two 17 bp repeats nesting a kappa B-related sequence confer inducibility to the diptericin gene and bind a polypeptide in bacteria-challenged Drosophila. Embo J 12: 1561–1568.
48. Valanne S, Myllymaki H, Kallio J, Schmid MR, Kleino A, et al. (2010) Genome-wide RNA interference in Drosophila cells identifies G protein-coupled receptor kinase 2 as a conserved regulator of NF-kappaB signaling. J Immunol 184: 6188–6198.
49. Meng X, Khanuja BS, Ip YT (1999) Toll receptor-mediated Drosophila immune response requires Dif, an NF-kappaB factor. Genes Dev 13: 792–797.
50. Kaneko T, Silverman N (2005) Bacterial recognition and signalling by the Drosophila IMD pathway. Cell Microbiol 7: 461–469.
51. Kocks C, Cho JH, Nehme N, Ulvila J, Pearson AM, et al. (2005) Eater, a transmembrane protein mediating phagocytosis of bacterial pathogens in Drosophila. Cell 123: 335–346.
52. Ayres JS, Freitag N, Schneider DS (2008) Identification of Drosophila mutants altering defense of and endurance to Listeria monocytogenes infection. Genetics 178: 1807–1815.
53. Ayres JS, Schneider DS (2008) A signaling protease required for melanization in Drosophila affects resistance and tolerance of infections. PLoS Biol 6: e305. doi:10.1371/journal.pbio.0060305.
54. Dionne MS, Pham LN, Shirasu-Hiza M, Schneider DS (2006) Akt and FOXO dysregulation contribute to infection-induced wasting in Drosophila. Curr Biol 16: 1977–1985.
55. Schneider DS, Ayres JS (2008) Two ways to survive infection: what resistance and tolerance can teach us about treating infectious diseases. Nat Rev Immunol 8: 889–895.
56. Korenjak M, Taylor-Harding B, Binne UK, Satterlee JS, Stevaux O, et al. (2004) Native E2F/RBF complexes contain Myb-interacting proteins and repress transcription of developmentally controlled E2F target genes. Cell 119: 181–193.
57. Lewis PW, Beall EL, Fleischer TC, Georlette D, Link AJ, et al. (2004) Identification of a Drosophila Myb-E2F2/RBF transcriptional repressor complex. Genes Dev 18: 2929–2940.
58. Diamond G, Beckloff N, Weinberg A, Kisich KO (2009) The roles of antimicrobial peptides in innate host defense. Curr Pharm Des 15: 2377–2392.
59. Kimura K, Hirano T (2000) Dual roles of the 11S regulatory subcomplex in condensin functions. Proc Natl Acad Sci U S A 97: 11972–11977.
60. Hartl TA, Smith HF, Bosco G (2008) Chromosome alignment and transvection are antagonized by condensin II. Science 322: 1384–1387.
61. Petersen UM, Kadalayil L, Rehorn KP, Hoshizaki DK, Reuter R, et al. (1999) Serpent regulates Drosophila immunity genes in the larval fat body through an essential GATA motif. Embo J 18: 4013–4022.
62. Hirano T (2006) At the heart of the chromosome: SMC proteins in action. Nat Rev Mol Cell Biol 7: 311–322.
63. Nasmyth K, Haering CH (2005) The structure and function of SMC and kleisin complexes. Annu Rev Biochem 74: 595–648.
64. Hirano T (2005) SMC proteins and chromosome mechanics: from bacteria to humans. Philos Trans R Soc Lond B Biol Sci 360: 507–514.
65. Nativio R, Wendt KS, Ito Y, Huddleston JE, Uribe-Lewis S, et al. (2009) Cohesin is required for higher-order chromatin conformation at the imprinted IGF2-H19 locus. PLoS Genet 5: e1000739. doi:10.1371/journal.pgen.1000739.
66. Wendt KS, Yoshida K, Itoh T, Bando M, Koch B, et al. (2008) Cohesin mediates transcriptional insulation by CCCTC-binding factor. Nature 451: 796–801.
67. Ferrandon D, Jung AC, Criqui M, Lemaitre B, Uttenweiler-Joseph S, et al. (1998) A drosomycin-GFP reporter transgene reveals a local immune response in Drosophila that is not dependent on the Toll pathway. Embo J 17: 1217–1227.
68. Ryu JH, Nam KB, Oh CT, Nam HJ, Kim SH, et al. (2004) The homeobox gene Caudal regulates constitutive local expression of antimicrobial peptide genes in Drosophila epithelia. Mol Cell Biol 24: 172–185.
69. Tzou P, Ohresser S, Ferrandon D, Capovilla M, Reichhart JM, et al. (2000) Tissue-specific inducible expression of antimicrobial peptide genes in Drosophila surface epithelia. Immunity 13: 737–748.
70. Kim M, Lee JH, Lee SY, Kim E, Chung J (2006) Caspar, a suppressor of antibacterial immunity in Drosophila. Proc Natl Acad Sci U S A 103: 16358–16363.
71. Ryu JH, Kim SH, Lee HY, Bai JY, Nam YD, et al. (2008) Innate immune homeostasis by the homeobox gene caudal and commensal-gut mutualism in Drosophila. Science 319: 777–782.
72. Gobert V, Gottar M, Matskevich AA, Rutschmann S, Royet J, et al. (2003) Dual activation of the Drosophila toll pathway by two pattern recognition receptors. Science 302: 2126–2130.
73. Pili-Floury S, Leulier F, Takahashi K, Saigo K, Samain E, et al. (2004) In vivo RNA interference analysis reveals an unexpected role for GNBP1 in the defense against Gram-positive bacterial infection in Drosophila adults. J Biol Chem 279: 12848–12853.
74. Bergman P, Johansson L, Asp V, Plant L, Gudmundsson GH, et al. (2005) Neisseria gonorrhoeae downregulates expression of the human antimicrobial peptide LL-37. Cell Microbiol 7: 1009–1017.
75. Chakraborty K, Ghosh S, Koley H, Mukhopadhyay AK, Ramamurthy T, et al. (2008) Bacterial exotoxins downregulate cathelicidin (hCAP-18/LL-37) and human beta-defensin 1 (HBD-1) expression in the intestinal epithelial cells. Cell Microbiol 10: 2520–2537.
76. Sperandio B, Regnault B, Guo J, Zhang Z, Stanley SL, Jr., et al. (2008) Virulent Shigella flexneri subverts the host innate immune response through manipulation of antimicrobial peptide gene expression. J Exp Med 205: 1121–1132.
77. Wehkamp J, Salzman NH, Porter E, Nuding S, Weichenthal M, et al. (2005) Reduced Paneth cell alpha-defensins in ileal Crohn's disease. Proc Natl Acad Sci U S A 102: 18129–18134.
78. Markey MP, Bergseid J, Bosco EE, Stengel K, Xu H, et al. (2007) Loss of the retinoblastoma tumor suppressor: differential action on transcriptional programs related to cell cycle control and immune function. Oncogene 26: 6307–6318.

79. Zurawski DV, Mumy KL, Faherty CS, McCormick BA, Maurelli AT (2009) Shigella flexneri type III secretion system effectors OspB and OspF target the nucleus to downregulate the host inflammatory response via interactions with retinoblastoma protein. Mol Microbiol 71: 350–368.
80. Tsichritzis T, Gaentzsch PC, Kosmidis S, Brown AE, Skoulakis EM, et al. (2007) A Drosophila ortholog of the human cylindromatosis tumor suppressor gene regulates triglyceride content and antibacterial defense. Development 134: 2605–2614.
81. Bolstad BM, Irizarry RA, Astrand M, Speed TP (2003) A comparison of normalization methods for high density oligonucleotide array data based on variance and bias. Bioinformatics 19: 185–193.
82. Smyth GK (2004) Linear models and empirical bayes methods for assessing differential expression in microarray experiments. Stat Appl Genet Mol Biol 3: Article3.
83. Benjamini Y, Hochberg Y (1995) Controlling the false discovery rate: a practical and powerful approach to multiple testing. Journal of the Royal Statistical Society Series 57: 289–300.
84. Tweedie S, Ashburner M, Falls K, Leyland P, McQuilton P, et al. (2009) FlyBase: enhancing Drosophila Gene Ontology annotations. Nucleic Acids Res 37: D555–559.
85. Romeo Y, Lemaitre B (2008) Drosophila immunity: methods for monitoring the activity of Toll and Imd signaling pathways. Methods Mol Biol 415: 379–394.

Human Molecular Genetics, 2012, Vol. 21, No. 24 ***5239–5245***
doi:10.1093/hmg/dds370
Advance Access published on September 4, 2012

Expression of *SMARCB1 (INI1)* mutations in familial schwannomatosis

Miriam J. Smith[1,†], James A. Walker[1,2,3], Yiping Shen[3], Anat Stemmer-Rachamimov[4], James F. Gusella[3] and Scott R. Plotkin[1,5,*]

[1]Department of Neurology, [2]Massachusetts General Hospital Center for Cancer Research, [3]Center for Human Genetic Research, [4]Division of Neuropathology, [5]Pappas Center for Neuro-oncology, Massachusetts General Hospital, Boston, MA 02114, USA

Received June 21, 2012; Revised August 10, 2012; Accepted August 28, 2012

Genetic changes in the *SMARCB1* tumor suppressor gene have recently been reported in tumors and blood from families with schwannomatosis. Exon scanning of all nine *SMARCB1* exons in genomic DNA from our cohort of families meeting the criteria for 'definite' or 'presumptive' schwannomatosis previously revealed constitutional alterations in 13 of 19 families (68%). Screening of four new familial schwannomatosis probands identified one additional constitutional alteration. We confirmed the presence of mRNA transcripts for two missense alterations, four mutations of conserved splice motifs and two additional mutations, in less conserved sequences, which also affect splicing. Furthermore, we found that transcripts for a rare 3′-untranslated region (c.*82C > T) alteration shared by four unrelated families did not produce splice variants but did show unequal allelic expression, suggesting that the alteration is either causative itself or linked to an unidentified causative mutation. Overexpression studies in cells lacking SMARCB1 suggest that mutant SMARCB1 proteins, like wild-type SMARCB1 protein, retain the ability to suppress cyclin D1 activity. These data, together with the expression of SMARCB1 protein in a proportion of cells from schwannomatosis-related schwannomas, suggest that these tumors develop through a mechanism that is distinct from that of rhabdoid tumors in which SMARCB1 protein is completely absent in tumor cells.

INTRODUCTION

Schwannomatosis (MIM#162091) is a third major form of neurofibromatosis, that is clinically and genetically distinct from NF1 (MIM#162200) and NF2 (MIM#101000) (1). The most common clinical symptom of schwannomatosis is intractable pain, although the mechanism by which this occurs is not well understood. Tumors from familial schwannomatosis patients frequently harbor somatic truncating mutations at the *NF2* (MIM#607379) gene on the long arm of chromosome 22 and loss of the wild-type *NF2* allele. However, they do not carry germline *NF2* mutations (2). Recently, a number of constitutional alterations have been reported in familial and some sporadic schwannomatosis patients in the *SMARCB1* (MIM#601607) gene (3–6), which is situated 5.8 Mb proximal to *NF2*.

Loss of *SMARCB1* has been linked previously to development of rhabdoid tumors (RTPS1; MIM#609322) (7). Rhabdoid tumors are highly malignant, appear in the first few years after birth, and are almost always lethal. Several RTPS1 families have been described (8) to include family members who are constitutional carriers of a *SMARCB1* mutation, but who never develop schwannomas. Recently, a multigenerational family was described with multiple members affected by either malignant rhabdoid tumors or by schwannomatosis, all of whom share a common germline *SMARCB1* exon 6 duplication mutation (9). A second family affected by RTPS1 and schwannoma has also been described with a c.472C > T *SMARCB1* mutation (10).

The existence of adult mutation carriers in RTPS1 families has led to the hypothesis that the risk of rhabdoid tumor development from these mutations is time dependent (6,11), in

*To whom correspondence should be addressed at: Massachusetts General Hospital, 55 Fruit St, Yawkey 9E, Boston, MA 02114, USA. Tel: +1 6177263650; Fax: +1 6176432591; Email: splotkin@partners.org
†Present address: St Mary's Hospital, University of Manchester, Manchester, M13 9WL, UK.

which case the development of schwannomas later in life becomes feasible. However, the majority of RTPS1 and schwannomatosis families remain distinct, making it more likely that the type or location of the mutation determines the resulting disease status.

Almost all of the constitutional *SMARCB1* alterations found in familial schwannomatosis patients are predicted to be non-truncating. In contrast, the mutations found in RTPS1 are mainly truncating mutations and large deletions, which lead to a complete loss of SMARCB1 protein. This difference in mutation type may underlie the difference in phenotype presented by these two conditions.

To address this issue, we have carried out analysis of *SMARCB1* transcripts from 14 schwannomatosis families, shown to harbor constitutional alterations (6), in order to verify expression of the non-truncated products predicted from each mutation.

RESULTS

Immunohistochemistry of schwannomas reveals mosaic pattern of SMARCB1 expression

Immunostaining for schwannomas from families 1, 5 and 10 which harbor the c.*82C > T mutation and family 11 harboring the c.364G > T mutation have been published previously (12) and show a mosaic pattern of staining for SMARCB1 protein, consistent with loss of expression in a subset of tumor cells. Tumor sections from families 9 and 19 were subsequently analyzed by immunostaining for SMARCB1 and also revealed a mosaic pattern of mixed positive and negative nuclei in all four schwannomas from a member of family 19 (c.795 + 1G > T) and a single schwannoma from family 9 (c.158G > T). Representative staining is shown for a tumor from family 19 in Figure 1. No tumors were available for testing from other families in this study.

cDNA analysis of familial schwannomatosis samples

To confirm the predicted effects of constitutional mutations identified previously (6), we analyzed cDNA derived from mRNA of lymphoblastoid cell lines carrying each of the 10 germline alterations found in 14 families. The results are summarized in Table 1. Representative chromatograms of the sequencing results for each of the seven mutant transcripts predicted to produce a viable protein and the three predicted to undergo nonsense-mediated decay are shown in Figure 2A–J.

Missense mutations

Each of the missense alterations, c.41C > A (p.Pro14His) and c.158G > T (p. Arg53Leu), found in family 4, and families 9 and PA-3, respectively, was detected in the cDNA transcript generated from its corresponding lymphoblast cell line (Fig. 2A and B), indicating that the mutant allele for both of these alterations is expressed at the mRNA level.

Splicing alterations

Four mutations were detected in conserved splice sites in four kindreds. An intron 3 mutation (c.362 + 1G > A) amplified a faint band containing a splice variant that results in an in-frame deletion of the last 45 bp of exon 3 (Fig. 2C). An exon 4 alteration, c.364G > T, caused skipping of exon 4, without changing the reading frame (Fig. 2D). Another mutation at the ultimate base of exon 4, c.500G > A, produced altered splicing that resulted in the in-frame loss of the last 111 bp of the exon (c.390_500del, Fig. 2E). The intron 6 change, c.795 + 1G > T produced two alternative splice variants. The first involved the in-frame inclusion of the first 45 bp of intron 6 (Fig. 2F) while the second, which was much less abundant, involved skipping of exon 6, with the resulting frame-shift predicted to lead to a premature stop codon and mRNA decay (Fig. 2G).

Sequence analysis of lymphocyte DNA from family 23 [family 07-367 in Eaton *et al*., (10)] identified the nonsense mutation c.472C > T in exon 4. We isolated three alternately spliced cDNA amplicons derived from the corresponding lymphoblast cell line RNA for this family. First, amplification of exons 3–6 detected two different deletions: complete exon 4 loss (c.363_500del) and partial exon 4 deletion (c.390_500del). Amplicons for exons 5–9 then detected a deletion of the whole of exon 7 (Fig. 1H). The exon 4 changes in the transcript were the same as those found in other families and have the potential to produce non-truncated protein. However, the presence of the exon 7 deletion would lead to a premature stop codon and destabilize these mutant transcripts; therefore, they are predicted to undergo nonsense-mediated decay.

Two additional potential splice site alterations were identified further from the consensus splice sequence the intron 4 change, c.500 + 5G > T, and the intron 5 change, c.629-5T > G. Interestingly, the former leads to the same splicing alteration as the c.500G > A mutation, five bases away (Fig. 2E). The intron 5 alteration, c.629-5T > G, in family P/Qu, seems to disrupt the exon 6 splice acceptor sequence, leading to the insertion of 145 bp of the 3′ end of intron 5 (Fig. 2I), using a cryptic splice acceptor, ag/TTT. This alteration results in a premature stop codon within the intronic sequence and is predicted to lead to mRNA decay.

Variants of uncertain significance

Four unrelated families contained the same alteration, c.*82C > T, within their 3′UTR (Fig. 2J). This alteration was not found in an unaffected panel of 100 alleles and is not recorded in the dbSNP database (6,13). None of the four families produced splice variants in the cDNA analysis screen, but the alteration was observed in the transcript.

Allelic expression analysis of the c.*82C > T alteration

Allelic expression analysis has previously been used to quantify under- or overexpression of mutant *NF2* transcripts from NF2 patient-derived lymphoblast cell RNAs (14). We used this technique to measure expression levels of the c.*82C > T alteration.

The full-length *SMARCB1* transcripts were amplified, sequenced and the level of expression of the mutant 'T' allele in cDNA was calculated, relative to the genomic sequence, using the Mutation Surveyor DNA analysis program (SoftGenetics, State College, PA, USA). The results revealed unequal allelic expression, with a decreased expression of

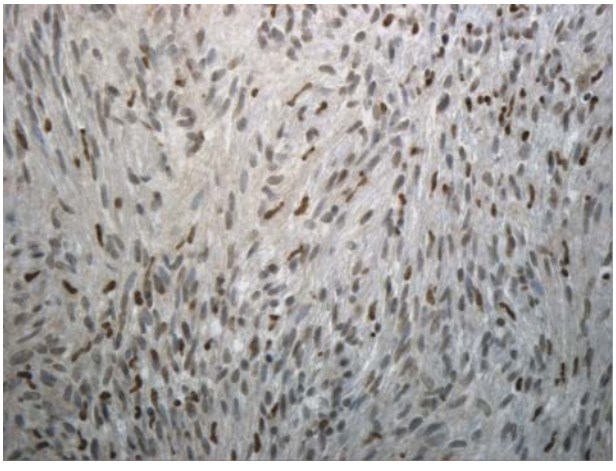

Figure 1. Immunostaining for SMARCB1 shows a mosaic pattern of SMARCB1 expression in a schwannoma from family 19 with a mixture of positive (brown) and negative (blue) nuclei in cells.

Table 1. Germline mutations found in familial schwannomatosis kindreds and the effects observed in mRNA (family 23 has both schwannomatosis and RTPS1)

Family ID	Exon	Germline mutation	Mutant amplicons identified
4	1	c.41C > A	r.41C > A
9	2	c.158G > T	r.158G > U
PA-1	2	c.158G > T	r.158G > U
E	3	c.362 + 1G > A	r.318_362del
11	4	c.364G > T	r.363_500del
23	4	c.472C > T	r.363_500del, r.390_500del, r.796_986del
PA-3	4	c.500G > A	r.390_500del
V	4	c.500 + 5G > T	r.390_500del
P/Qu	6	c.629-5T > G	r.500ins501-145_501-1
19	6	c.795 + 1G > T	r.795_796ins795 + 1_795 + 45ins, r.628_795del
1	9	c.*82C > T	r.*82C > U
3	9	c.*82C > T	r.*82C > U
5	9	c.*82C > T	r.*82C > U
10	9	c.*82C > T	r.*82C > U

the mutant allele by ~27% compared with the wild-type. To ensure that differences in expression for the c.*82C > T change were not due to differential expression in lymphoblastoid cells, two known SNPs (rs34399789 and rs2229354), identified on an unaffected allele in two families, were tested for unequal expression in unaffected family members. These polymorphisms both showed equal expression in full-length *SMARCB1* cDNA. The results suggest that the c.*82C > T alteration is associated with reduced expression and is either causative or linked to a causative mutation.

The *SMARCB1* mutant 3′UTR alters mRNA stability

To substantiate the effect of the mutant *SMARCB1* 3′UTR on RNA expression levels, we transfected HEK293T cells with a pGL3-promoter luciferase vector containing a wild-type *SMARCB1* 3′UTR, or a c.*82C > T mutant 3′UTR. Forty-eight hours after transfection, the level of luciferase expression was significantly reduced under the regulation of the c.*82C > T mutant 3′UTR compared with the wild-type 3′UTR (Fig. 3A). To distinguish between the possibilities of the c.*82C > T mutation affecting either translational efficiency or stability of the mRNA, we performed qRT–PCR on RNA extracted from HEK293T cells transfected with luciferase constructs bearing the wild-type or the c.*82C > T 3′UTRs, at 48 and 96 h post-transfection. At 48 and 96 h, the c.*82C > T mutant mRNA levels were reduced by ~20 and ~45%, respectively, compared with the wild-type (Fig. 3B). Together, these results suggest that the c.*82C > T mutant 3′UTR leads to a reduced expression of the *SMARCB1* transcript, possibly by destabilizing the mRNA.

Cyclin D1 reporter activity is appropriately suppressed by mutant SMARCB1

To begin to elucidate the mechanism by which mutations in *SMARCB1* affect its normal function in cells, we created expression constructs for three of the mutant *SMARCB1* transcripts found in our cohort, predicted to result in altered protein sequence. The exon 1 missense, c.41C > A, and exon 2 missense, c.158G > T, mutations were created by site-directed mutagenesis. The splice mutant lacking exon 4 was isolated from full-length cDNA derived from mRNA from a lymphoblastoid cell line with the c.364G > T mutation. These expression constructs were used to determine whether mutant SMARCB1 proteins are able to suppress elevated cyclin D1 expression, as has been shown previously for wild-type SMARCB1 (15). A luciferase reporter construct containing the cyclin D1 promoter region −1745 to +35 was used to transfect MON cells, which lack endogenous SMARCB1 and have elevated levels of cyclin D1 (15). This construct was co-transfected with either a wild-type SMARCB1 construct or a mutant transcript construct. When wild-type SMARCB1 was reintroduced into MON cells, luciferase expression was suppressed by ~60% (Fig. 4) similar to previous reports (15). Similarly, when MON cells were transfected with mutant *SMARCB1* constructs, luciferase expression was suppressed by 53% (exon 1 missense), 74% (exon 2 missense) or 65% (exon 4 deletion). The results show that these schwannomatosis-related mutant SMARCB1 proteins retain the ability to repress cyclin D1 transcription.

DISCUSSION

Exon scanning analysis of *SMARCB1* in our cohort of familial schwannomatosis patients has now identified a total of 14/23 (61%) probands with a germline point mutation. The majority of these mutations are predicted to be non-truncating. This contrasts with the mutational spectrum of RTPS1 in which mutations are predicted to be truncating (7,16). We analyzed cDNA from this select group of familial schwannomatosis patients to confirm the predicted effects of constitutional mutations identified during initial *SMARCB1* exon scanning and found that almost all of the constitutional alterations in the *SMARCB1* gene produced a mutant transcript that is likely to produce a non-truncated protein.

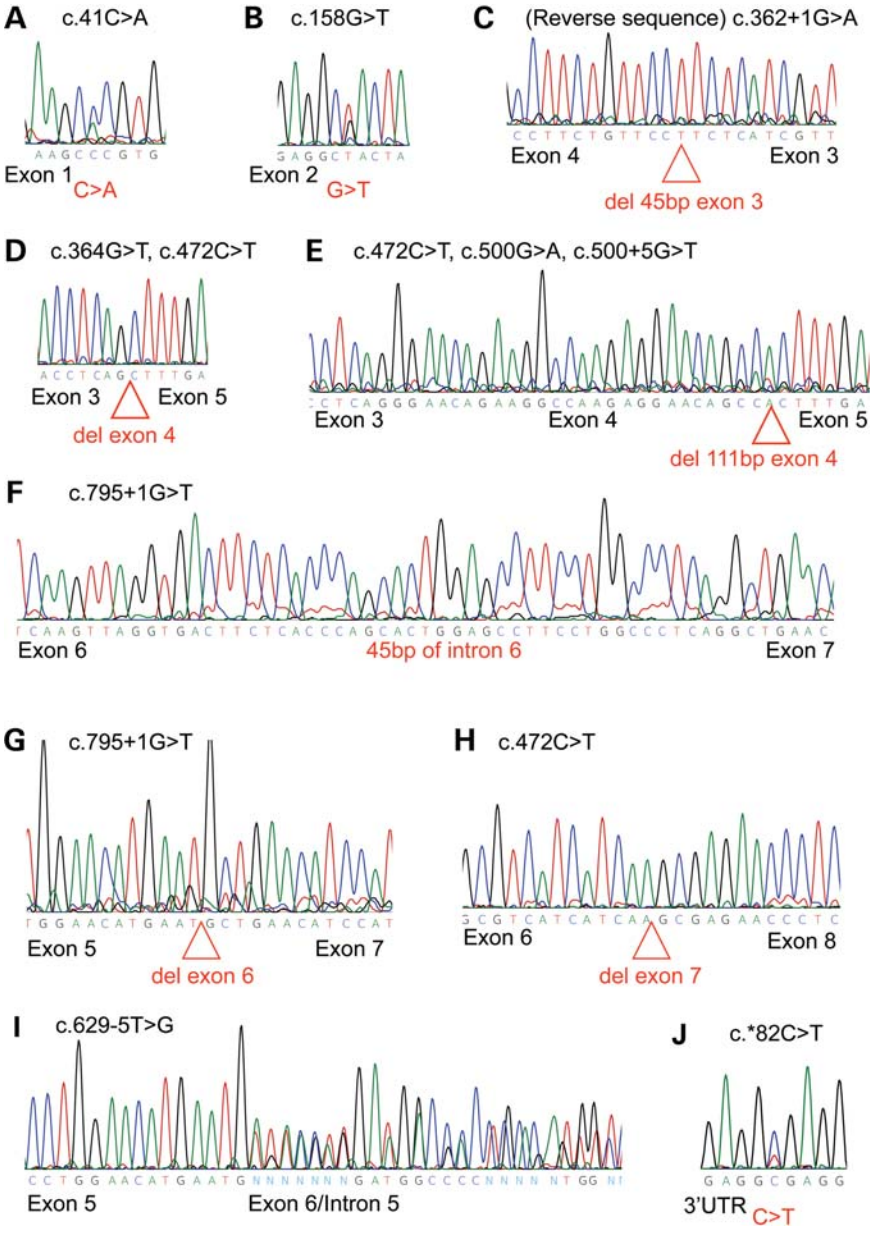

Figure 2. Chromatograms showing *SMARCB1* mutant transcripts identified in the study. (**A**) Exon 1 missense mutation; (**B**) exon 2 missense mutation found in families 9 and PA1; (**C**) exon 3 splice mutation that removes the first 45 bp of exon 3; (**D**) in-frame deletion of the entire exon 4 sequence found in families 11 and 23;(**E**) exon 4 splice mutation leading to the deletion of the last 111 bp of exon 4 in families PA-3, V and 23; (**F**) exon 6 splice mutation causing inclusion of the first 45 bp of intron 6; (**G**) family 19 transcript deleting exon 6, predicted to cause nonsense-mediated decay; (**H**) family 23 deletion of exon 7, predicted to cause nonsense-mediated decay; (**I**) family P/Qu mutant transcript including 145 bp of intron 5, predicted to cause nonsense-mediated decay; (**J**) 3′UTR change found in families 1, 3, 5 and 10.

Families P/Qu and 23 both produced mutant transcripts that are likely to be degraded by nonsense-mediated decay. Family 23 has a family history of both schwannomatosis and RTPS1 and, in addition to the truncating mutation, also has a somatic deletion of the wild-type *SMARCB1* allele in a tumor (10). The c.472C > T nonsense mutation is known to predispose to RTPS1, but it is unclear why some members of the same family developed schwannomas rather than rhabdoid tumors. It is possible that a modifier gene is involved. It is also unclear how the mutation, which occurs in exon 4, causes a deletion of exon 7. It is possible that a second, unidentified, mutation exists within intron 6, leading to skipping of exon 7.

The only mutant transcript detected in family P/Qu contained an insertion of the last 145 bp of intron 5, which leads to a stop codon 26 codons into the insertion. This is predicted to lead to mRNA decay and no expression of the mutant copy of *SMARCB1*. This family did not show loss of heterozygosity (LOH) by microsatellite marker analysis at the *SMARCB1* locus, suggesting that the wild-type copy of *SMARCB1* is still present in tumors, although it remains

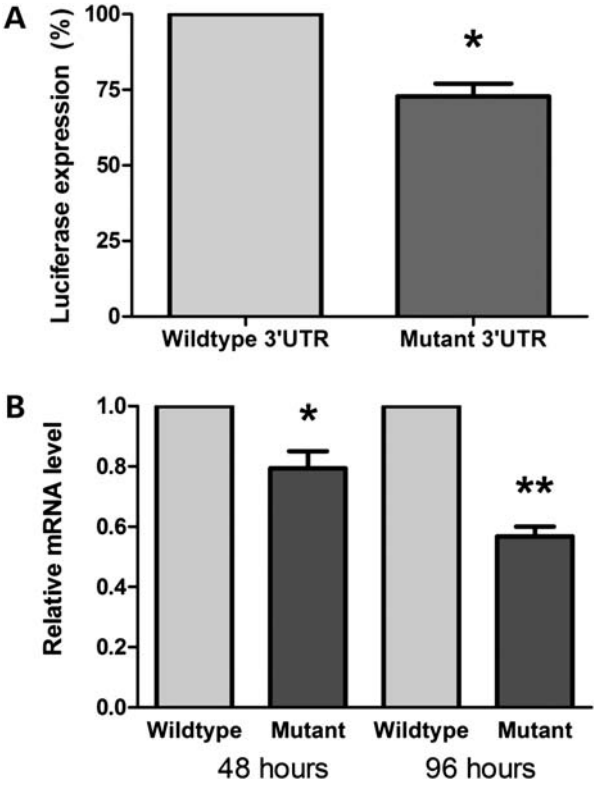

Figure 3. The *SMARCB1* mutant 3′UTR alters mRNA stability. Relative mRNA expression levels of wild-type and mutant *SMARCB1* 3′untranslated regions in HEK293T cells. (**A**) Luciferase levels indicate the relative expression under the control of wild-type and c.*82C > T mutated *SMARCB1* 3′UTRs, normalized to transfection efficiency by GFP fluorescence $^{*}P < 0.01$. (**B**) qRT–PCR of wild-type and mutant *SMARCB1* 3′UTR expression levels at 48 and 96 h post-transfection normalized to both GFP and GAPDH $^{*}P < 0.015$; $^{**}P < 0.001$.

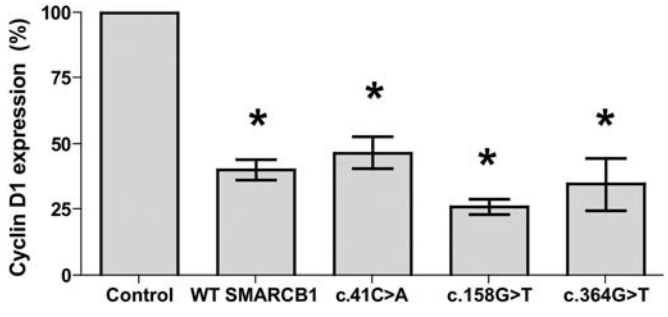

Figure 4. Cyclin D1 activity is appropriately suppressed by both wild-type and mutant SMARCB1 proteins. Introduction of both wild-type and mutant *SMARCB1* transcripts (c.41C > A missense, c.158G > T missense or c.364G > T splice mutant) into MON cells which lack endogenous SMARCB1 leads to suppression of luciferase reporter activity under the control of the cyclin D1 promoter. Normalized to transfection efficiency by GFP fluorescence $^{*}P < 0.05$.

possible that other mechanisms may affect this remaining allele. LOH was, however, seen at the *NF2* locus—downstream of *SMARCB1*—in a tumor from family P/Qu, supporting the theory that co-mutation of these two genes is involved in schwannoma formation (4–6). Unfortunately, no tumor material was available for immunohistochemical analysis.

Tumors from schwannomatosis kindreds frequently carry *SMARCB1* alterations in conjunction with loss of the wild-type allele. The combination of a constitutional *SMARCB1* mutation with a somatically acquired truncating mutation in the *NF2* gene and loss of the wild-type copies of both genes indicates cross-talk between tumorigenic pathways and a complex mechanism of schwannoma formation in this disorder. Indeed, a multi-hit hypothesis has been suggested (3–6).

The alteration, c.*82C > T, found in the 3′ UTR of four unrelated kindreds (13) in our cohort, showed no splice variants, but was detected by sequencing of the full-length transcript from lymphoblast cell lines, suggesting that the mutant mRNA is expressed. Allelic expression analysis, and qRT–PCR on cells transfected with wild-type and mutant 3′UTRs, showed unequal expression with decreased levels of the mutant allele in comparison with the wild-type. Families 3 and 5, for which tumor DNA was available, showed LOH for both the *SMARCB1* and *NF2* loci and showed somatic mutation of the remaining *NF2* allele (6). These results, together with the frequency of this alteration in unrelated families, support a pathogenic status for the c.*82C > T mutation and implicate it in the occurrence of schwannomatosis disease.

SMARCB1 regulation of cyclin D1

Loss of SMARCB1 in RTPS1 leads to upregulation of cyclin D1 and progression into the cell cycle. A cyclin D1 repression assay showed that schwannomatosis-related missense and splice mutants are capable of suppressing cyclin D1 activity in a similar way to that shown for the wild-type SMARCB1 protein. This finding suggests that the downstream effects of *SMARCB1* alterations are different in schwannomatosis compared with RTPS1, with cyclin D1 and related cell cycle processes being affected primarily in the RTPS1 tumors.

Immunohistochemistry for SMARCB1 revealed a mosaic pattern of mixed positive and negative nuclei in all tumor specimens. In a previous report, this finding was interpreted as loss of protein expression in a subset of tumor cells resulting in a mosaic of null and haploinsufficient cells (12). This could be as a result of transient or unstable expression. However, further work would be required to determine this. It is also unclear why the exon 2 mutation, which appears to produce a more highly expressed transcript, also leads to a mosaic pattern of protein production. It could be that the mutant DNA is transcribed normally, while the mutant mRNA is mis-folded, causing a reduction in translation efficiency.

This data, in conjunction with the different spectrum of mutations in comparison with that seen in RTPS1, suggests that in familial schwannomatosis kindreds, almost all constitutional alterations in the *SMARCB1* gene are capable of producing mutant, but viable transcripts, that yield SMARCB1 protein with altered levels of functionality in schwannoma tumor cells. Further work is required to determine the precise mechanism by which mutant SMARCB1 protein can promote the pathogenesis of schwannomas.

MATERIALS AND METHODS

Patient material

We studied 13 of 19 carefully characterized schwannomatosis kindreds described previously (6) and four additional familial probands. Lymphoblastoid cell lines were established from peripheral blood samples as described previously (17). High-molecular-weight DNA was extracted from peripheral blood leukocytes, cultured lymphoblasts, frozen pulverized tumor, cultured tumor and normal tissues obtained at autopsy using a PureGene DNA isolation kit (Gentra Systems, Minneapolis, MN, USA). This study was approved by the Institutional Review Board of Partners HealthCare and informed consent was obtained from the patients participating in the study. For patients who had died, an autopsy permit was used as consent.

Multiplex ligation-dependent probe amplification

Multiplex ligation-dependent probe amplification was carried out as described by Boyd *et al*. (6), using a SALSA multiplex ligation-dependent probe amplification P258 SMARCB1 kit (MRC-Holland, Amsterdam, the Netherlands). Briefly, 20–500 ng DNA were used for hybridization, ligation and amplification of the *SMARCB1* exon probes according to the manufacturer's instructions. The amplification products were analyzed using an ABI 3730 DNA Analyzer, with Biomek FX robotics and with GeneScan 500 LIZ (Applied Biosystems, Foster City, CA, USA) as the internal size standard. Relative probe signals were calculated by dividing each measured peak by the sum of all peak areas for that sample. DNA from four unaffected individuals was used for control samples.

cDNA analysis

mRNA was extracted from frozen cell pellets of established lymphoblastoid cell lines for each kindred, using the PolyA-Tract mRNA extraction kit (Promega, Madison, WI, USA). Poly(A)+ mRNA was reverse transcribed to cDNA with oligo(d)T primers, using the Superscript III cDNA first strand synthesis kit (Invitrogen, Carlesbad, CA, USA). Full-length *SMARCB1* and three overlapping fragments of the *SMARCB1* transcript were PCR amplified from the cDNAs using nested primers. For the full-length transcript, the primers 5′-CAGCCCTCCTGATCCCT-3′ and 5′-CCCAAT CTTCTGAGATGCTC-3′ were used. The reverse primer 5′-ACAAATGGAATGTGTGCCGG-3′ was used when the 3′UTR SNPs were amplified. Exons 1 through 4 were amplified with primers 5′-CAGCCCTCCTGATCCCT-3′ and 5′-TCACAGCTGGGTCATGGTC-3′, exons 3–6 were amplified by 5′-CACGGATACACGACTCTAGC-3′ and 5′-CACT CAAACTGGTCCACC-3′ and for exons 5–9, 5′-CCATG CTCCACAACCATC-3′ and 5′-CCCAATCTTCTGAGATGC TC-3′were used. PCR products were electrophoresed on 2% agarose gels, with a normal control. Aberrantly sized fragments were excised and analyzed by direct sequencing on an ABI Prism 3730 DNA analyzer.

Quantitative analysis of the c.*82C > T mutation (previously denoted c.1240C > T) was carried out using the Mutation Surveyor program v3.20 (Softgenetics LLC, State College, PA, USA) by comparison of relative levels of C and T alleles in cDNA with reference to levels in genomic DNA.

Construction of wild-type and mutant *SMARCB1* expression vectors

Mutagenic primers were designed to introduce the c.41C > A and c.158G > T point mutations identified in our cohort into the wild-type human *SMARCB1* sequence obtained from Origene (Rockville, MD, USA). Site-directed mutagenesis was carried out using the Quick-change site-directed mutagenesis kits (Stratagene, Carlesbad, CA, USA). Mutagenic primers for c.41C > A were GACCTTCGGGCAGAAG CACGTGAAGTTCCAGCTGG and CCAGCTGGAACTTCA CGTGCTTCTGCCCGAAGGTC. Mutagenic primers used for c.158G > T were CCCTCACTCTGGAGGCTACTAGCCAC TGTGGAAG and CTTCCACAGTGGCTAGTAGCCTCCA GAGTGAGGG.

The splice mutant lacking exon 4 was obtained by PCR amplification of full-length cDNA generated from mRNA of a lymphoblastoid cell line from family 11, using a forward primer containing an *Nhe*I restriction site, GCATGCTAG CATGATGATGATGGCGCTGAGC, and a reverse primer containing a *Hin*dIII restriction site, TTTAAGCTTCCA GGCCGGGGCCGTGTT. Each mutant transcript was subcloned into a pcDNA plasmid, containing a C-terminal GFP tag.

For the cyclin D1 repression experiment, the cyclin D1 promoter region −1745 to +35 was sub-cloned into the pGL3-basic plasmid, which contains a luciferase reporter gene (Promega, Madison, WI, USA).

For the 3′UTR experiment, site-directed mutagenesis was used to generate the c.*82C > T mutant, with primers TGGCAAGGACAGAGGTGAGGGGACAGCCCA and TGG GCTGTCCCCTCACCTCTGTCCTTGCCA. cDNAs representing the wild-type and c.*82C > T mutant 3′UTRs were each sub-cloned into the pGL3-promoter vector, downstream of the luciferase coding region.

Cell lines

HEK293T cells were purchased from ATCC (Manassas, VA , USA). MON tumor cells were obtained from the laboratory of Dr Olivier Delattre.

Luciferase reporter assays

For experiments investigating *SMARCB1* 3′UTR regulation, using a luciferase reporter, HEK293T cells were co-transfected with the pGL3-promoter vector construct with either a wild-type or mutant *SMARCB1* 3′UTR and an eGFP vector, using Lipofectamine transfection reagent (Invitrogen, Carlesbad, CA, USA). Cells were harvested after 48 h and luciferase activity was measured using One-glow luciferase reagent (Promega, Madison, WI, USA).

For experiments investigating the regulation of cyclin D1, the wild-type *SMARCB1* transcript and three mutant transcripts [containing the exon 1 missense mutation (c.41C > A), the exon 2 missense mutation (c.158G > T) or the deletion of exon 4], were subcloned into the pcDNA vector with a

C-terminal GFP tag. The cyclin D1 luciferase vector was transfected into MON cells which lack endogenous SMARCB1 along with each of the *SMARCB1* constructs, or an empty GFP control vector. Cells were harvested after 48 h and luciferase activity was measured using One-glow luciferase reagent (Promega, Madison, WI, USA). Luciferase levels were normalized to transfection efficiency using GFP fluorescence.

qRT–PCR analysis of luciferase-3′UTR reporters

Total RNA was extracted from transfected cells using the RNeasy kit (Qiagen, Valencia, CA, USA) and treated with DNase (Ambion, Foster City, CA, USA). First-strand cDNA synthesis was performed using random hexamers (GE Healthcare, Piscataway, NJ, USA). Subsequently, mRNA expression levels of luciferase-3′ UTR reporters were assessed using 1 μl of the appropriate cDNA for real-time qRT–PCR using FastStart Universal SyberGreen and a LightCycler 480 machine (Roche, Indianapolis, IN, USA). The forward oligonucleotide primer (5′-GGTCTTACCGGAAAACTCGAC-3′) corresponds to a sequence at the 3′ end of the luciferase cDNA; the reverse primer (5′-CTCTGTCCTTGCCAGAAGATG-3′) is within the 3′UTR of *SMARCB1*. The results were analyzed using the comparative Ct method (ΔΔCt) and normalized to GAPDH and eGFP expression levels to ensure equal loading and transfection efficiencies.

Immunohistochemistry

Formalin-fixed, paraffin-embedded tissue sections from four schwannomas resected from member of family 19 (c.795 + 1G > T) and a single schwannoma from family 9 were immunostained using a commercial SMARCB1 antibody (BD Transduction Laboratories, Franklin Lakes, NJ, USA) along with appropriate positive (normal cortex) and negative controls (RTPS1). Antigen retrieval was achieved by microwaving in a Borg Decloaker RTU for 45 min (primary antibody concentration 1:50).

ACKNOWLEDGEMENTS

We would like to thank Dr Olivier Delattre for the generous gift of MON cells and Dr Ganjam Kalpana for reagents and technical assistance with the luciferase assays. We would also like to thank Robert Maher for help with formatting of the figures.

Conflict of Interest statement. None declared.

FUNDING

This work was supported in part by NINDS grant NS24279 and by the Harvard Medical School Center for Neurofibromatosis and Allied Disorders. J.A.W. is supported by the DOD (W81XWH-09-1-0487). M.J.S. is currently supported by the Children's Tumor Foundation and the Association for International Cancer Research.

REFERENCES

1. MacCollin, M., Chiocca, E.A., Evans, D.G., Friedman, J.M., Horvitz, R., Jaramillo, D., Lev, M., Mautner, V.F., Niimura, M., Plotkin, S.R. *et al.* (2005) Diagnostic criteria for schwannomatosis. *Neurology*, **64**, 1838–1845.
2. MacCollin, M., Willett, C., Heinrich, B., Jacoby, L.B., Acierno, J.S. Jr, Perry, A. and Louis, D.N. (2003) Familial schwannomatosis: exclusion of the NF2 locus as the germline event. *Neurology*, **60**, 1968–1974.
3. Hulsebos, T.J., Plomp, A.S., Wolterman, R.A., Robanus-Maandag, E.C., Baas, F. and Wesseling, P. (2007) Germline mutation of INI1/SMARCB1 in familial schwannomatosis. *Am. J. Hum. Genet.*, **80**, 805–810.
4. Sestini, R., Bacci, C., Provenzano, A., Genuardi, M. and Papi, L. (2008) Evidence of a four-hit mechanism involving SMARCB1 and NF2 in schwannomatosis-associated schwannomas. *Hum. Mutat.*, **29**, 227–231.
5. Hadfield, K.D., Newman, W.G., Bowers, N.L., Wallace, A., Bolger, C., Colley, A., McCann, E., Trump, D., Prescott, T. and Evans, D.G. (2008) Molecular characterisation of SMARCB1 and NF2 in familial and sporadic schwannomatosis. *J. Med. Genet.*, **45**, 332–339.
6. Boyd, C., Smith, M.J., Kluwe, L., Balogh, A., Maccollin, M. and Plotkin, S.R. (2008) Alterations in the SMARCB1 (INI1) tumor suppressor gene in familial schwannomatosis. *Clin. Genet.*, **74**, 358–366.
7. Versteege, I., Sevenet, N., Lange, J., Rousseau-Merck, M.F., Ambros, P., Handgretinger, R., Aurias, A. and Delattre, O. (1998) Truncating mutations of hSNF5/INI1 in aggressive paediatric cancer. *Nature*, **394**, 203–206.
8. Sevenet, N., Sheridan, E., Amram, D., Schneider, P., Handgretinger, R. and Delattre, O. (1999) Constitutional mutations of the hSNF5/INI1 gene predispose to a variety of cancers. *Am. J. Hum. Genet.*, **65**, 1342–1348.
9. Swensen, J.J., Keyser, J., Coffin, C.M., Biegel, J.A., Viskochil, D.H. and Williams, M.S. (2009) Familial occurrence of schwannomas and malignant rhabdoid tumour associated with a duplication in SMARCB1. *J. Med. Genet.*, **46**, 68–72.
10. Eaton, K.W., Tooke, L.S., Wainwright, L.M., Judkins, A.R. and Biegel, J.A. (2011) Spectrum of SMARCB1/INI1 mutations in familial and sporadic rhabdoid tumors. *Pediatr. Blood Cancer*, **56**, 7–15.
11. Janson, K., Nedzi, L.A., David, O., Schorin, M., Walsh, J.W., Bhattacharjee, M., Pridjian, G., Tan, L., Judkins, A.R. and Biegel, J.A. (2006) Predisposition to atypical teratoid/rhabdoid tumor due to an inherited INI1 mutation. *Pediatr. Blood Cancer*, **47**, 279–284.
12. Patil, S., Perry, A., Maccollin, M., Dong, S., Betensky, R.A., Yeh, T.H., Gutmann, D.H. and Stemmer-Rachamimov, A.O. (2008) Immunohistochemical analysis supports a role for INI1/SMARCB1 in hereditary forms of schwannomas, but not in solitary, sporadic schwannomas. *Brain Pathol. (Zurich, Switzerland)*, **18**, 517–519.
13. Smith, M.J., Boyd, C.D., MacCollin, M.M. and Plotkin, S.R. (2009) Identity analysis of schwannomatosis kindreds with recurrent constitutional SMARCB1 (INI1) alterations. *Clin. Genet.*, **75**, 501–502.
14. Jacoby, L.B., MacCollin, M., Parry, D.M., Kluwe, L., Lynch, J., Jones, D. and Gusella, J.F. (1999) Allelic expression of the NF2 gene in neurofibromatosis 2 and schwannomatosis. *Neurogenetics*, **2**, 101–108.
15. Zhang, Z.K., Davies, K.P., Allen, J., Zhu, L., Pestell, R.G., Zagzag, D. and Kalpana, G.V. (2002) Cell cycle arrest and repression of cyclin D1 transcription by INI1/hSNF5. *Mol. Cell. Biol.*, **22**, 5975–5988.
16. Biegel, J.A., Zhou, J.Y., Rorke, L.B., Stenstrom, C., Wainwright, L.M. and Fogelgren, B. (1999) Germ-line and acquired mutations of INI1 in atypical teratoid and rhabdoid tumors. *Cancer Res.*, **59**, 74–79.
17. Anderson, M.A. and Gusella, J.F. (1984) Use of cyclosporin A in establishing Epstein-Barr virus-transformed human lymphoblastoid cell lines. *In Vitro*, **20**, 856–858.